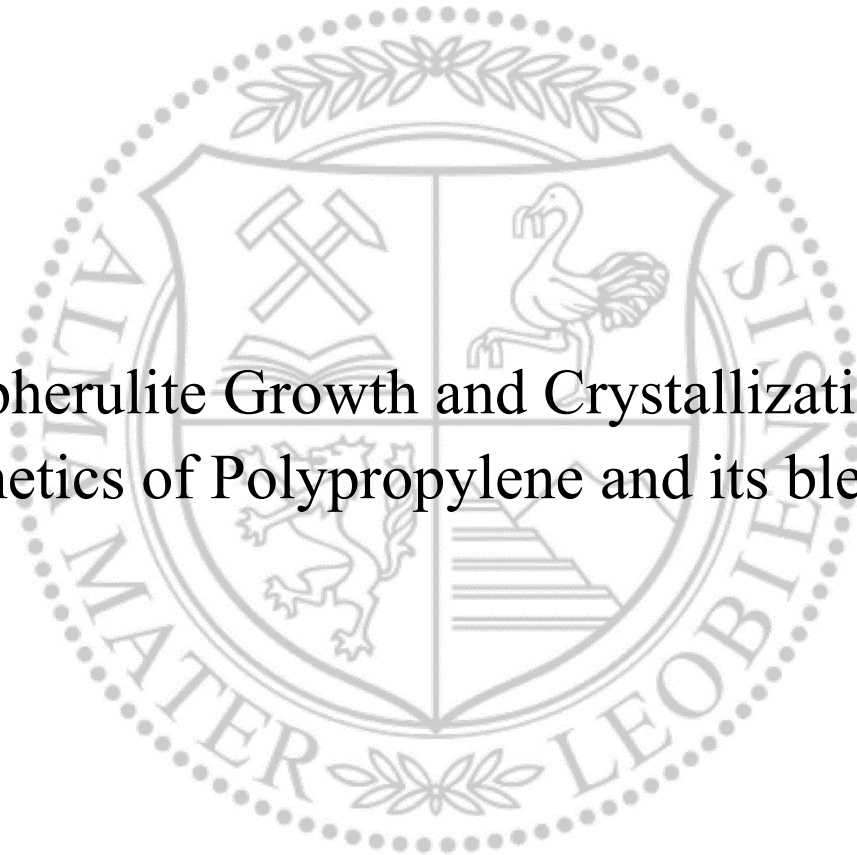Chair of Materials Science and Testing of Polymers

Master's Thesis

Spherulite Growth and Crystallization Kinetics of Polypropylene and its blends

Anna Baaba Jacobs

September 2024

MONTANUNIVERSITÄT LEOBEN
www.unileoben.ac.at

AFFIDAVIT

I declare on oath that I wrote this thesis independently, did not use any sources and aids other than those specified, have fully and truthfully reported the use of generative methods and models of artificial intelligence, and did not otherwise use any other unauthorized aids.

I declare that I have read, understood and complied with the "Good Scientific Practice" of the Montanuniversität Leoben.

Furthermore, I declare that the electronic and printed versions of the submitted thesis are identical in form and content.

Date 26.08.2024

Signature Author
Anna Baaba Jacobs

ACKNOWLEDGEMENT

KURZFASSUNG

Die Kristallisationskinetik in Polymeren ist ein sehr wichtiges Thema im Bereich der Kunststofftechnik, da die Kristallisation mit den Eigenschaften von Polymeren korreliert. Die Kristallisation befasst sich mit der Ausrichtung und Anordnung der Polymerkristalle in ihrer Mikrostruktur, was wiederum den Grad der Kristallinität des Polymers bestimmt, der sich auf die thermischen, optischen und mechanischen Eigenschaften sowie auf die allgemeine Anwendung der Polymere auswirkt. In Bezug auf die Anwendungen ist Polypropylen (PP) eines der am häufigsten verwendeten Polymere in der Kunststoffindustrie, weshalb es unbedingt erforderlich ist, es zu recyceln und im Kreislauf der Wirtschaft zu halten. Das Mischen von Polypropylen ist eine nachhaltige und materialeffiziente Art des Polymerrecyclings. Um erfolgreich gemischtes recyceltes PP zu entwickeln, ist es wichtig, die Kristallisationskinetik der einzelnen Polypropylentypen und ihrer Mischungen zu verstehen. In dieser Arbeit wurde die Kinetik des Kristallisationswachstums der verschiedenen Polypropylentypen und ihrer Mischungen auf zwei verschiedenen Wegen mittels isothermischer Analyse untersucht. Sowohl die Differential Scanning Calorimetry als auch die optische Mikroskopie mit polarisiertem Licht unter Verwendung eines Heiztisches bei verschiedenen isothermen Kristallisationstemperaturen wurden eingesetzt, um die Keimbildungsrate, die Wachstumsrate und die allgemeine Kristallisationskinetik von Polypropylen und seinen Blends zu untersuchen. Bei der Analyse der aus den Experimenten gewonnenen Ergebnisse wurde das Avrami-Gesetz, das die Grundlage für das Verständnis der Kristallisationskinetik von Polymeren bildet, zur Bewertung der Wachstumsrate von Polypropylen Homo, Polypropylen Block und Polypropylen Random sowie von Mischungen, die aus den Typen Polypropylen Random und Block, Polypropylen Homo und Random und Polypropylen Homo und Block bestehen, verwendet. Dies geschah, um die Auswirkungen der Proben aufeinander in Bezug auf die Kristallisationskinetik zu untersuchen und zu verstehen. Die Avrami-Zahlen und Exponentiale wurden für die Vorhersage der Keimbildungsrate und der Kristallgeometrie von PP und seinen Blends verwendet. Die erhaltenen Werte lagen zwischen 2 und 4, was bedeutet, dass die Geometrie kugel- oder scheibenförmig ist. Die Keimbildungskonstanten und präexponentiellen Konstanten, die aus der Lauritzen-

Hoffman-Analyse unter Verwendung von PLOM und DSC gewonnen wurden, wurden miteinander und mit Literaturwerten verglichen, um die Ähnlichkeiten und Unterschiede zwischen ihnen zu ermitteln. Auf der Grundlage der Ergebnisse können verschiedene PP-Typen, insbesondere Polypropylen-Blockcopolymere und Polypropylen-Homopolymere, gemischt werden, um eine einzige interpenetrierende Phase ohne offensichtliche Trennung zu erhalten, die während der Verarbeitung für das Recycling ko-kristallisiert werden kann.

ABSTRACT

Crystallization kinetics in polymers is a very important topic in the field of plastics technology since crystallization is correlated with the properties of polymers. Crystallization deals with the orientation and arrangement of polymer crystals in their microstructure and this in turn dictates the degree of crystallinity of polymer affecting their thermal properties, optical properties, mechanical properties and the general application of polymers. In terms of applications, polypropylene (PP) is one of the most utilized polymers in the plastic industry hence it is imperative to recycle them and maintain them in the circular economy loop. Blending of Polypropylene is a sustainable and material efficient way of polymer recycling and to successfully engineer blended recycled PP, it is important to understand the crystallization kinetics of individual types of polypropylene and their blends. In this work, crystallization growth kinetics of the different types of polypropylenes and their blends were investigated via two distinct routes using isothermal analysis. Both Differential Scanning Calorimetry and Polarized Light Optical Microscopy using a Heating stage at various isothermal crystallization temperatures were employed to investigate the nucleation rate, growth rate and overall crystallization kinetics of polypropylene and its blends. In analysis the results gained from the experiments, the Avrami´s Law which is the basis for understanding crystallization kinetics of polymers was used in evaluating the growth rate of Polypropylene Homo, Polypropylene Block, and Polypropylene Random polymers, as well as blends consisting of Polypropylene Random and Block, Polypropylene Homo and Random and Polypropylene Homo and Block types. This was done to investigate and understand the effects the samples had on each other in terms of crystallization kinetics. The Avrami numbers and exponentials were used in the prediction of nucleation rate and crystal geometry of PP and its blends. The obtained values were between 2 and 4 which meant the geometry was spheres or disc-like. The nucleation constants and pre-exponential constants obtained from Lauritzen-Hoffman analysis using both PLOM and DSC were compared to each other and with literature values to help identify the similarities and differences between them. Based on the results, different types of PP especially Polypropylene Block copolymer and Polypropylene Homopolymer can be

blended to obtain a single interpenetrating phase with no obvious separation and may undergo co-crystallization during processing for recycling.

TABLE OF CONTENTS

SYMBOLS AND ABBREVIATIONS

Ø   diameter of spherulite

b   stem's width

I*   Nucleation rate

Q   Heat energy

r   radius of nucleus

Tm^o equilibrium melting temperature

Tm   Melting temperature

U*   Energy molecules transportation in the melt

Xt   Degree of relative crystallinity

β   Kinetic free factor

μ   chemical potential of spherulite

σ   Interfacial tension

t   time

ΔS   Change in entropy in the crystallization system

α   fraction of melt crystallized with respect to time

A(T)   work per gram molecule required for forming a growth nucleus at temperature

aPP   atactic Polypropylene

d V   The volume of the new phase per unit

DIC   Differential Inference Contrast

DSC   Differential Scanning Calorimetry

EbP   ethylene-propylene block copolymers

f   correction factor

G   Gibb's Free energy

g   spreading rate

h   heat of fusion

H   enthalpy of reaction

ICPP   Impact Copolymer PP

iPP   Isotactic Polypropylene

k   Avrami constant

kb   Boltzmann constant

K_G Nucleation Constant

L   effective growth length

l   length

LH   Lauritzen Hoffman

n   Avrami exponent

N   Number of uncrystallized elements

n(T)   Probability of a nuclei transforming

nr   radial direction

nt   tangential direction refractive

ω   volume fractions

PLOM   Polarized Light Optical Microscope

PP   Polypropylene

PP-B   Polypropylene Block Copolymer

PP-BR   Polypropylene Block Random Blend

PP-H   Polypropylene Homopolymer

PP-HB   Polypropylene HomoBlock Blend

PP-HR   Polypropylene Homo Random Blend

PP-R   Polypropylene Random

PP-R-CT   Polypropylene random modified with crystallinity and Temperature

R   Universal Gas Constant

SPE   Solid Plastic Electrolytes

sPP   syndiotactic Polypropylene

T   Temperature

Tc   Crystallization Temperature

V(τ)   The volume of transformed nuclei at time, t.

W*   Energy Barrier

τ   crystallization time

$\varkappa 12$ Florry-Huggins Interaction parameter

IMAGE DIRECTORY

1   INTRODUCTION AND SCOPE

Until the early 1950s, polypropylene (PP) in its oligomeric and polymeric forms were known to be amorphous because of their low molecular sources (B. Malpass and Band, 2012). The production of PP is mainly done by polymerization and oligomerization depending on the choice of PP. Polymerization and oligomerization depend on the processing conditions, mainly on the types of free radical initiators, types of catalysts, pressure and temperature. These conditions affect the final properties of the polypropylene resulting in the production of amorphous polypropylene (B. Malpass and Band, 2012). The discovery of polypropylene was made by Paul Hogan and Robert Banks accidentally while working at Phillips Petroleum Company due to a gas leakage (Tanvir and Abdus, 2024). Afterwards scientists, specifically Giulio Natta, researched on improving the stereoregularity of polypropylene to influence its crystallinity (B. Malpass and Band, 2012; Busico, 2001).

The stereoregularity and unique molecular arrangement of polypropylene introduces versatility in its properties and subsequent applications. Polypropylene used for commercial purposes has a linear configuration, inducing a high crystallinity, chemical resistance, low density and good mechanical properties (Tanvir and Abdus, 2024). The selection of polypropylene for commercial applications is based on the type and degree of crystallinity of PP. Due to the versatility of PPs, they are used for generalized commercial applications and specialized advanced applications. In the area of water filtration, air filtration and biomedicine, electro spun PP fibers mostly nanosized or micro sized are applicable due to their robust mechanical property, chemical resistance, thermal stability and low price (Tanvir and Abdus, 2024). Moreover, PP fibers are easy to spin and have a large specific surface area (Tanvir and Abdus, 2024). Polypropylene is also used in composite manufacturing mostly as matrix of the system due to its low weight, formability, chemical resistance and toughness. Generally, PP is used in food packaging and beverage packaging, automotive industry for production of different vehicle parts such as bumpers, door rims, battery parts, medical industry, fashion industry. In the plumbing industry PP is utilized for transportation of potable water, irrigation for farming and sewage wastewater.

Commercially, polypropylene can be produced into two main types: homopolymers and copolymers, whereby the copolymers are subdivided into random copolymers and block copolymers.

Due to its high demand in the plastic industry, it is imperative to find a front of pipe sustainable method of recycling PP and to maintain it in a circular economic loop to reduce PP waste in the environment, reduce carbon footprint of PP in the environment and decrease production costs. The use of different types of PP for different applications introduces complexity in recycling of polymers since different PPs have different properties. Hence during recycling the crystallization, spherulite growth, mechanical properties and crystallization kinetics of the PP when blended have to be investigated to ascertain their behavior when blended and if blends can be reused for commercial applications after recycling.

This research work delves intensively into the different types of polypropylenes precisely homopolymer, polymer random (PP-R), block copolymer (PP-B) and the blends of these three types of polypropylenes. Polypropylene properties are affected by chemical structures, polymerization conditions, and crystallinity. Crystallinity in polypropylene is affected by crystallization kinetics, that involves the orderly alignment of molecules under pressure, temperature, and nucleating agents. The desired properties of plastics can be manipulated during parts manufacturing if the engineers know about the crystallization kinetics of the plastics.

Chapter two of this thesis consists of the state of the art of the research necessary for the current work. Here, the focal point is the models for describing semi crystalline polymers, types of PP and classification of PP according to stereoregularity. Again, studies will be done on the kinetics of crystallization of polymers and their blends with a focus on the kinetics of crystallization of PP and its blends while briefly discussing the thermodynamics of crystallization. The models for describing crystallization will be discussed with much attention on the Lauritzen-Hoffman Secondary Nucleation Theory.

In Chapter three, the methodology and materials used for the study of crystallization kinetics and growth of spherulites of PP will be presented; experimental methods used for this study are the DSC and PLOM with a heating stage which will be utilized to isothermally

analyze the overall crystallization kinetics of the polypropylene at specific temperatures. Chapter four delves into the analysis and explanation of the results obtained using different models, precisely Avrami´s theory and Lauritzen-Hoffman's theory whilst comparing the results to a similar body of research. Finally, in chapter five, there is a conclusive explanation of the results and discussion. Furthermore, recommendations for further investigations are given.

The objective of this thesis is to study the crystallization kinetics of polypropylene and its blends and compare the results from each polypropylene to understand how PP and their blends crystallize isothermally. Additionally, the spherulite growth rate and its morphology were investigated to analyze the relationship between spherulite growth rates, spherulite morphology in the different types of PP and their blends, and the evolution of the spherulites concerning crystallization temperatures.

2 STATE OF THE ART

2.1 Semicrystalline Polymers

Semi-crystalline polymers as the name depicts, are a combination of both amorphous and crystalline parts in their morphological structure. The crystalline part of semicrystalline polymers consists of highly ordered chains which are stacked and mostly long-range order (Shrivastava, 2018). However, in the amorphous region, the chains are disordered, have high entanglement, and exhibit glassy-like nature (Shrivastava, 2018). Figure 2.1 shows a schematic representation of a typical semicrystalline polymer having crystalline and amorphous regions.
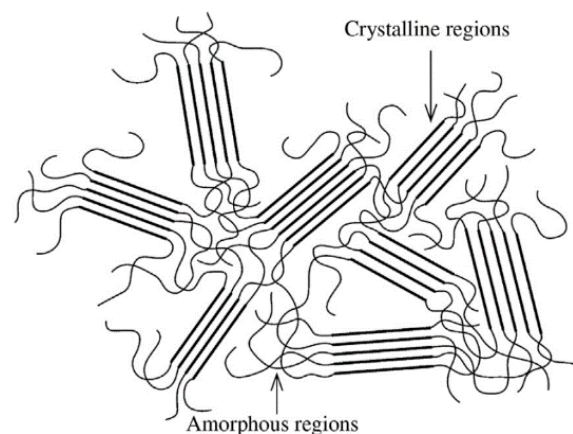
Fig. 2.1: Structure of Semi-Crystalline Polymer (Shrivastava, 2018)

From figure 2.1, the crystalline part has chains that are packed parallel to each other and forms a lamellar structure with a size of a few nanometers in a unit cell and the amorphous region is shaped helical, disordered, and embedded in the crystalline part (Li, 2020; Murmu et al., 2021). The orientation and formation of these regions are influenced by the polymer's molecular structure and the conditions under which crystallization takes place during processing (Murmu et al., 2021). Crystallinity in polymers is very important because of its direct effect on mechanical properties, optical properties, electrical properties, and thermodynamic properties. Other crystallinity-related factors, distribution of crystallites and crystallites size in the polymer play a major factor in the overall properties of polymers.

The mechanical behavior of semi-crystalline polymers is dictated mostly by the crystalline part of the polymers. The polymeric chains´ strength in a semi-crystalline polymer system is mainly dependent on the -(C-C)- bonds between the molecules (Galeski, 2003). The bonding and orientation of the polymer chains are the purpose of withstanding shear stresses upon application of external loads. High strengths in polymers can be achieved by the perfect orientation of polymer chains parallel to each other, the strength in the axial direction of this perfect crystalline system will be higher than that of the parallel direction (Murmu et al., 2021). However, due to anisotropy in the polymers, the lateral strength of crystalline polymers is very minimal. S. Humbert et. al. (Humbert et al., 2011) investigated the relationship between Elastic Modulus and Crystallinity. Four Polyethylene samples (branched and linear) were subjected to either quenching, annealing, or isothermal heating. Tensile Testing, Dynamic Mechanical, and DSC analysis were performed on these samples to ascertain their Elastic Modulus, loss Modulus, and degree of crystallinity respectively. From the results, it was concluded that there is a linear correlation between elastic modulus and degree of crystallinity in linear polymers. Although this observation is the same for branched polymers, the degree of crystallinity is not the only deciding factor for strength (Humbert et al., 2011).

The applications of semicrystalline polymers are driven by the properties which are also affected by polymer crystallinity. In biomedical applications, the morphology and crystalline structure influence the biodegradability and biocompatibility properties. A highly crystalline polymer will have a slower degradation rate whereas a polymer with low crystallinity will possess a faster degradation rate. In electrolytes, polyethylene oxide is mostly utilized as solid plastic electrolytes (SPE) in Lithium batteries but due to its high crystallinity, there is an undesired effect on ion conductivity. Nevertheless, the crystalline areas are important because they are responsible for the strength of the SPEs (Li, 2020). Hence studies are being conducted to improve the ion conductivity properties of PEO whilst maintaining its mechanical properties (Li, 2020).

2.1.1 Polypropylene

Polypropylene is a vinyl polymer that belongs to the polyolefins family, having a linear hydrocarbon structure containing a small amount or absence of unsaturation, with an attachment of a methyl (CH_3) group to its backbone, as shown in Figure 2.2 (Ariff et al., 2012).

The arrangement of the methyl group on the backbone of PP has effects on the properties of the PP, mostly enhancing the thermal and mechanical properties of PP whilst reducing the chemical resistance. (Ariff et al., 2012).

Polypropylene is a stereotactic polymer and depending on the placement of the methyl groups they have three different molecular structures namely atactic, syndiotactic and isotactic PP. The tacticity of atactic PP (aPP) is characterized by the randomness of the positioning of the pendant methyl groups on the carbon backbone of the chain. The atacticity of this kind of PP makes aPP an amorphous thermoplastic material and increases its solubility with chloroform, diethyl ether, toluene, THF, methylene chloride, heptane and hexane and including mixtures polar and non-polar solvent mixtures even at room temperature (Karger-Kocsis, 1999). It has high chemical resistance against acids hence does not degrade upon acid exposure. This type of aPP can be used as additives in rubber production, adhesives and modifiers in adhesives, and chemical foaming agents in PVC through chemical modifications (Meng-Heng Wu et al., 2020; Šimoník and Drexler, 1979).

The CH_3 methyl groups in syndiotactic PP (sPP) are arranged in a regular alternating pattern along the molecular chain. Due to this arrangement of the methyl side chains, sPP has higher impact strength, enhanced ductility, and decreased crystallinity compared to aPP. It also has good mechanical and electrical performance (Javier Arranz-Andrés et al., 2005). They are mostly used in the insulation of cables due to their good electrical properties. Isotactic Polypropylene (iPP) is the most used and researched among the three kinds of PP. The production of this PP is usually in the presence of Ziegler-Natta catalysts and the addition of a head-tail configuration of polypropylene monomer to produce stereospecific PP. The arrangement of the methyl side group of the iPP is on one side of the main chain. The positioning of the side group favors the formation of helical chains rather than a zigzag shape, which would have a negative impact on the overall properties (Ariff et al., 2012). iPP is commercially used for various applications ranging from packaging to medical applications, to automotive applications. Figure 2.2 shows the different stereoregularities of PP.

$$CH_3 \quad CH_3 \quad CH_3$$
$$- C - CH_2 - C - CH_2 - C - CH_2 -$$
$$H \quad\quad H \quad\quad H$$

$$CH_3 \quad H \quad CH_3$$
$$- C - CH_2 - C - CH_2 - C - CH_2 -$$
$$H \quad CH_3 \quad H$$

$$CH_3 \quad CH_3 \quad H \quad CH_3$$
$$C - CH_2 - C - CH_2 - C - CH_2 - C - CH_2$$
$$H \quad\quad H \quad CH_3 \quad H$$
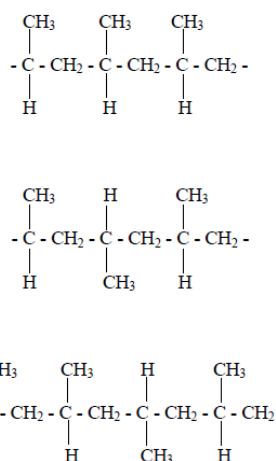
Fig. 2.2: Different Tacticity of PP (Ariff et al., 2012)

2.1.2 Commercially Produced Polypropylene Types

2.1.2.1 Polypropylene Homopolymer

This PP Homopolymer is the pure form of Polypropylene (not copolymerized with other olefins), and the most widely utilized in terms of commercial applications. The investigation of the creep properties by Kurt and Kagoz conveys that because of the high crystallinity of PP-H, PP homopolymer, it has a better creep resistance in comparison with other polyolefins (Kurt and Kasgoz, 2021). Kurt and Kasgoz also proved that molecular weights of PP influence the mechanical properties of PP homopolymers. An increase in molecular weight resulted in increased maximum creep strain and viscosity (Kurt and Kasgoz, 2021).

Food packaging, healthcare and medical items, textiles, electrical components, toys, and sports equipment are just a few of the industries that use PP-H extensively. It is the optimal option for these applications because of its resilience to chemicals, greases, and food oils. It is appropriate for syringes, surgical instruments, medical devices, and other supplies due to its exceptional strength, toughness, and biocompatibility. Because of its low weight, it is a desirable option for gasoline tanks and car interiors. In addition, toys, sports equipment, fabrics, and electrical components all contain homopolymer polypropylene. Both producers and consumers choose it due to its cost-effectiveness and favorable environmental impact. Its resilience to heat and chemicals, robustness, and affordability make it the perfect option for demanding applications.

2.1.2.2 Polypropylene Random Copolymers

The outstanding and versatile nature of Polypropylene random (PP-R) has attracted a lot of attention from scientists and researchers. PP-R has a relatively high percentage of the amorphous region in comparison with its crystalline part. PP-R is copolymerized with about 0.2 to 7 mol% of α-olefins (butene, ethylene, hexane etc.) by the random insertion of the olefins. The addition of these olefins mostly butene and ethylene disrupt the sequential order of the polypropylene leading to a decrease in crystallinity, rigidity, melting temperature, glass transition temperature and nucleation energy barriers (Benarab et al., 2021). In comparison to PP-H, PP-R has greater ductility, high impact strength at minimal temperature, resistance to stress-induced cracks, corrosion resistance, and good sealing properties. However, due to its random configuration, this PP has low strength (Benarab et al., 2021) but has good transparency with light (Wu et al., 2024).

Commercially, PP-R is mostly used in the plumbing industry for the fabrication of hot water pipes due to its high thermal and mechanical properties, corrosion resistance and durability (Benarab et al., 2021). Polypropylene random modified with crystallinity and Temperature (PP-R-CT) is an improved version of PP-R which is desirable for many applications due to the advancement in its crystallinity, thermal properties, mechanical properties, energy efficiency, chemical compatibility, and resistance to abrasion. They can be used in residential and commercial plumbing systems, agricultural and irrigation systems, heating and air conditioning networks, industrial refrigeration systems, and water treatment installations.

2.1.2.3 Polypropylene Block Copolymer

Impact Copolymer PP (ICPP), which is another name for polypropylene block polymer (PP-B), is a heterophasic copolymer which is a mechanical and physical compatibilization of ethylene Polypropylene random, a range of PP homopolymer and ethylene-propylene block copolymers with varying sequence lengths (EbP) (Chen et al., 2015; Gahleitner et al., 2013; J. Jancar and J. Tochacek, 2011). The heterogeneous phase is made up of amorphous rubbery inclusions and a semicrystalline polyethylene phase (Chen et al., 2015). Using Fourier Transform Infrared Spectroscopy and ^{13}C nuclear magnetic resonance characterization technique, Hongjun et al. (Hongjun et al., 1999) fractionated the individual components of ICPP. The amorphous rubbery inclusions contribute to high impact resistance whereas the

semicrystalline phase is responsible for the strength of the PP (Chen et al., 2015). Due to it being a multiphase polymer system (Hongjun et al., 1999), it possesses great mechanical properties, especially under impact conditions (Feng Luo et al., 2012; Shijie Song et al., 2009; Shijie Song et al., 2010). Studies by Chen et al. show the relationship between the composition of ICPP individual components on the overall properties (Chen et al., 2015). Their results show that an increase in the rubber size of the polymer system improves the impact properties of the polymer, however at lower temperatures rubber size does not affect polymer impact properties (Chen et al., 2015). ICPP are primarily used in automotive applications, hence necessitating recycling regulations, requiring an understanding of changes in structure and properties due to thermomechanical shocks during multiple extrusions (J. Jancar and J. Tochacek, 2011). Injection molding and cast or blown film technologies are critical to the packaging industry. Because of its high stiffness and impact strength, block copolymers are used in this area as well (Gahleitner et al., 2013).

2.2   Models for Describing Semicrystalline Polymers

In terms of describing the structure of semicrystalline polymers, there have been different theories from different polymer scientists based on their scientific works. Models such as the Lamellar Folding model, the interlamellar amorphous models, and the Fringed Cell model have been some of the most researched models in the field of polymer science. This section will highlight the three main models of describing the molecular chains of polymers, make comparisons with these models, and how they differ from one another. Additionally, other models will be briefly touched on, and explained how these models have a connection with the current thesis. The three main models discussed in this thesis are:

A. Fringed Cell Model

B. Lamellar Model

C. Interlamellar Amorphous Model

2.2.1   Fringed Cell Model

The fringed cell model was amongst the first models proposed in the description of polymer chains in semi-crystalline polymers which was first brought about by Hermann et al (Herrmann et al., 1930). This model assumes that the long linear macromolecules have a

random arrangement and regions of sufficient alignment which can form crystal lattices existing in a non-stationary binary phase (Peterlin, 1965). This model is graphically represented below in Figure 2.3.

The Fringed cell model suggests that polymers such as rubber are amorphous at room temperature however shows crystallinity upon application of tensile stress (stretching) (Keller, 1959). Studies on the fringed cell model were usually conducted by Xray Diffractometer (XRD), the production of XRD reflections which were well defined suggested an ordered lattice although these reflections are independent of the molecular length (Keller, 1959). There was the observation of broad halos in the XRD patterns that showed the presence of amorphous regions whereas the broad reflections suggested the small sizes of the crystallites (Keller, 1959). Although this model had been widely used in the early discovery of polymer morphology to describe the toughness and strength of polymers via chain crosslinking (Opperlander, 1968), it was an oversimplified model and did not account for structural observations in addition to the exhibition of broad range mechanical properties by a polymer.

Fig. 2.3: The Fringed Cell Model (Keller, 1959)

2.2.2   Lamellar Model

During crystallization, the type of polymer, the conditions of processing, and most importantly the crystallization process affect the morphology of the polymer. One of the most basic structures a polymer can form into, especially in diluted solutions, mostly as isolated sole entities, is the lamellar structure (Xu, 1987). Apart from diluted solutions, lamellas can exist in melt solutions. This is uncommon since the process for the preparation of the samples

is very elaborate and time-consuming (Keller and Goldbeck-Wood, 1996). Lamellar morphology is a layered structure having stacks of ordered patterns (Matyjakszewski and Möller, 2012). Micelles that occur in the nanoscale are packed in a regular manner per stack in the lamellar to form microlattices. The stacks can exist in different structures and do not have constant spatial orientations (Rabiej and Rabiej, 2011). Two kinds of layers can be used to describe the stacks in polymers; the "decorated" layer and the "undecorated" layer (Matyjakszewski and Möller, 2012). They are categorized according to the stacking disorders in the layers, undecorated layers have a 1D translational in the normal axis. Decorated layers contain 2D-dimensional patterns that exhibit translation distortions or defects in the oblique direction, rotational disorders, and stacking faults (Matyjakszewski and Möller, 2012). The lamellar model is represented in figure 2.4.
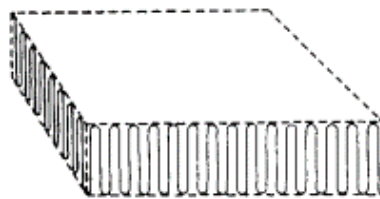
Fig. 2.4: The Lamellar Model (Rabiej and Rabiej, 2011)

2.2.3   Interlamellar Model

The interlamellar model was suggested by Opperlander, in his review work (Opperlander, 1968). He stated that a semicrystalline polymer, whether it is described by the chain folding model, adjacent re-entry, or the fringed cell model, so far as the semi-crystalline polymer had amorphous interfaces separating and connecting the crystalline regions, can be described as an interlamellar model (Opperlander, 1968). This model is very similar to the fringed cell model due to the amorphous part in the polymer. Opperlander stated in his review that this model cannot be used for all crystalline polymers since polymers can crystallize in different conditions leading to different molecular structures. In Peterlin's work (Peterlin, 1965) the importance of the amorphous phase in the lamellae during re-entry of the chains was highlighted although he did not emphatically back this model. Research works performed by Sedighiamiri et al. (Sedighiamiri et al., 2010), Viana and Cunha (Viana and Cunha, 2006), Sauer and Hsiao (Bryan B. Sauer and Benjamin S. Hsiao, 1995) go further to support this

interlamellar model even as far as treating the semi-crystalline polymer as a three-phase system with sandwiching of the amorphous region between a rigid phase and crystalline phase.
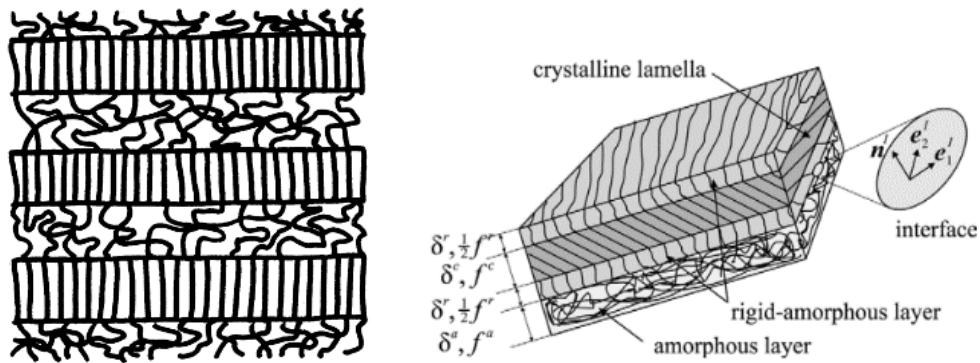
Fig. 2.5: Interlamellar Three phase Models (Opperlander, 1968; Sedighiamiri et al., 2010)

2.3   Spherulite Growth from Polymer Melt

Spherulites are grown from a polymer melt during crystallization of the melt. They first gained recognition as spherulites by Bunn and Alcock (Bunn and Alcock, 1945) for branched polyethylene in as much as the phenomena of spherulites in other materials such as silicate were known before this recognition. Apart from polymers, a wide range of metallurgical alloys, metals, minerals, rocks, liquid crystals and a variety of biomolecules are associated with and   contain spherulites (Gránásy et al., 2005). In polycrystalline polymers, the structure of spherulites consists of lamellae having their basal surfaces with an alignment parallel to the direction radial of the spherulites. The formation of the symmetrical spherulites is characterized by branching and splitting, including hedrite or axialite forms (Tien et al., 2015). The spherulites can exist in different morphologies and forms and are mainly characterized into two categories as illustrated in fig.2.6. To retain their space-filling quality, Category 1 spherulites branch sporadically as they expand radially from the nucleation site. On the other hand, category 2 spherulites begin as fibers that resemble threads and then expand into new grains at the growth front (Gránásy et al., 2005).
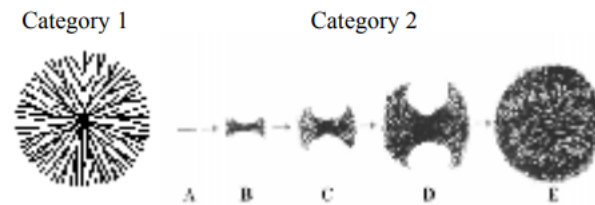
Fig. 2.6: The two main categories of spherulite (Gránásy et al., 2005)

Depending on the polymer melt type, spherulites exhibit diverse morphologies and patterns and they are represented in the picture below. Mostly these spherulites exhibit regular Maltese patterns or ring-banded patterns. Figure 2.7 shows the different morphologies that spherulites can possibly exhibit depending on the conditions of crystallization and the type of polymer. Figure 2.7(a) is a densely branched spherulite, (b) is a spiky spherulite, (c) is an arboresque spherulite, (d) and (e) are quadrites, (f) is a spherulite from Se, (g) is a crystal sheaf, (h) is a category 2 spherulite, (i) is a multi-sheave or early spherulite and (j) shows an arboresque growth.
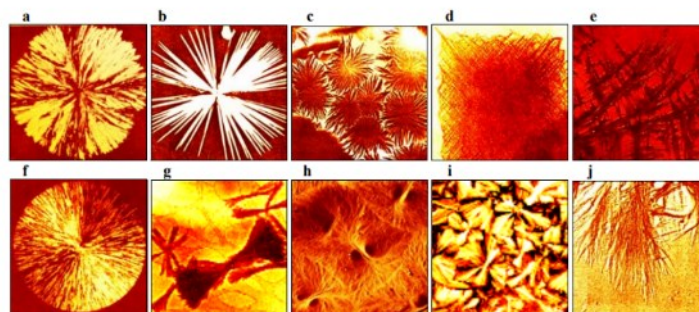
Fig. 2.7: Pictorial illustrations of the different spherulite morphologies of polymers (Gránásy et al., 2005)

The morphology of spherulites can be characterized by Transmission Electron Microscopy, Xray Computerized Tomography and Polarized Light Microscopy. A polymer spherulite interaction with visible light shows an optical birefringent with two refractive indices in the radial direction (n_r) and tangential direction (n_t) (Lugito and Woo, 2013). The birefringence classifies the spherulites into positive spherulites, negative spherulites, and zero birefringence spherulites depending on which refractive index is greater on interaction with the spherulites.

2.3.1 Positive Spherulites

Positive spherulites possess a refractive index that is higher in the radial direction than the tangential direction ($n_r > n_t$) (Lugito and Woo, 2013). Morphologically, they can be ringed or fibrillar and have more optical polarizability along the radial direction in comparison with the average of the other perpendicular indicatrices (Magill, 2001). Polymers containing strong dipole bonds, mostly H-bonds exhibit this kind of birefringence in their backbone chains at large angles and exhibit chain titling and twisting. An example for this would be polyamide (Magill, 2001). In terms of color from the visible light, the first and fourth quadrants of the spherulite (upper right section and lower left section) display the blue hue, while the second and third quadrants display the yellow color.

2.3.2 Negative Birefringence Spherulite

This kind of birefringence is very common in synthetic polymers having fibrillar or banded ring patterns (Magill, 2001). In negative birefringence, the radial direction refractive index is smaller than tangential direction refractive index (nr<nt). The blue color appears in the upper left and lower right quadrants (second and third quadrants) of the spherulite, whereas the upper right and lower left quadrants (first and fourth quadrants) show the yellow color. Despite having regularly recurring concentric rings, high-density PE is an example of a negative spherulite. Between the ring spacing and the radial growth phase, the lamellae periodically twist (Handbook of Polymer Crystallization, 2013).

Spherulites have a relationship with the properties of polymers, mostly mechanical properties. Starkweather and Brooks (Starkweather Jr. and Brooks, 1959) studied how spherulites affected the mechanical behavior of nylon 66. The observation made was that as the spherulite size reduces (causing an increase in spherulite number) there is an increase in the yield point and high flexural strength of the nylon, whereas the ultimate elongation decreases leading to low ductility (Starkweather Jr. and Brooks, 1959). Studies on the effect of spherulite size on the mechanical properties of polymers have shown that a decrease in spherulite size causes an increase in the strength of the polymer due to the presence of several grain boundaries that serve as load arresters.

2.4   Nucleation

Based on the assumptions that the density fluctuations during supercooling of polymer melt help to overcome the nucleation barrier, the classical nucleation theory was formed by Gibbs (Gibbs and Bumstead, 1906) and Kossel (Kossel, 1927). The Boltzmann Law describes the possibility of the existence of a nucleus at a specific volume and energy. This law is a function of entropy change related to $\exp(\Delta S/k_b)$. The probability of finding a nucleus with a specific size is in relation to $\exp(\Delta G/RT)$. According to Turnbull and Fisher (Turnbull and Fisher, 1949), the rate of nucleation can be expressed as:

$$I^* = \left(\frac{NKT}{h}\right) \exp\left(-\Delta G^* + \Delta G\eta\right)/kT \tag{2.1}$$

The number of uncrystallized elements 'N' that can take part in the nucleation of a nucleus with critical radius is known as the nucleation rate, and it is expressed in nuclei per second.
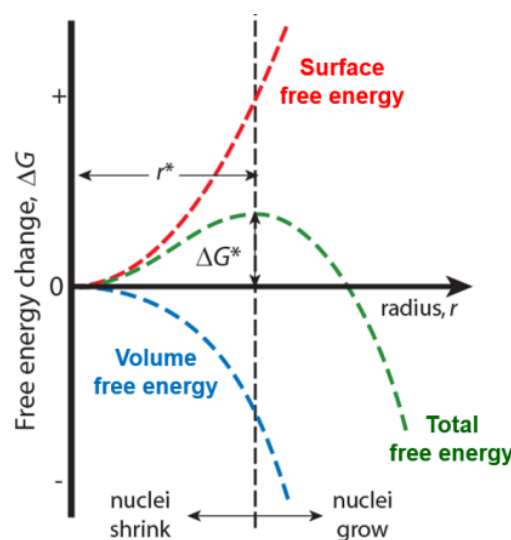
Fig. 2.8: Diagrammatic illustration of the nucleation process showing how ΔG changes with crystalline aggregate size (Muthukumar, 2003)

The nucleation path affects the overall properties of a polymer (Xu et al., 2021) and it is also the rate-determining step. Nucleation is the first step during polymer crystallization and for a polymer to crystallize successfully it must be able to overcome its nucleation energy barrier. Nucleation is because of fluctuation in the density of fluids and quenching of fluids to temperatures below their melting point (Muthukumar, 2003). Thermodynamically, the stabilization of the nuclei formed is achieved by reducing the free energy used to form stabilized crystalline phase and destabilization occurs when the free energy is increased

(Muthukumar, 2003). The free energy needed for a spherulite nuclei to form crystals is given as:

$$\Delta G = -\frac{4}{3}\pi r3\Delta\mu + 4\pi r^2\sigma \tag{2.2}$$

Given that at the nucleus' spherical surface, σ represents the interfacial tension and

$$\Delta\mu = \Delta h\Delta TTm \tag{2.3}$$

For $\Delta T = T^o{}_m - T > 0$, $\Delta\mu$ becomes positive. At critical radius, $(\frac{d\Delta G}{dr})_{r=rc} = 0$.

$$\text{Making } r_c = \frac{2\sigma}{\Delta\mu} = 2oT^o m\Delta h\Delta T \tag{2.4}$$

As the degree of supercooling increases, the critical radius shows an inverse divergent property. This process can be a time and energy-consuming process due to the nature of the connection between large molecules, however, strategies such as the addition of nucleating agents, blending polymers with amorphous blends, and optimization of external conditions have been employed to enhance nucleation rates. Nucleation is classified into two, namely primary nucleation and secondary nucleation.

2.4.1 Primary Nucleation

Primary nucleation happens when a nucleus is formed from a new liquid phase whereas secondary nucleation is the nucleation of a growing interface. With regards to energy barrier, primary nucleation has a higher energy barrier than secondary nucleation due to the presence of foreign materials in melts of secondary nucleation, reducing the T_g of the melts and hence decreasing the energy barrier (Zhang et al., 2021).

Primary nucleation is further grouped into heterogeneous and homogeneous nucleation (Mercier, 1990). Homogeneous nucleation occurs randomly in the melt due to fluctuations in the temperature whilst heterogeneous nucleation is an instantaneous process caused by random dispersions of insoluble particles (Mercier, 1990). The topics involving primary nucleation such as self-seeding, epitaxy, and chemical have been extensively by Wittmann and Lotz (Wittmann and Lotz, 1985), Blundell, Keller and Kovacs (Mercier, 1990) however, the

lower density of nuclei from primary nucleation makes it complicated to study. Hence, secondary nucleation will be discussed in detail in this session.

2.4.2 Secondary Nucleation and Theories for Describing Secondary Nucleation

Secondary nucleation can be best understood through the study of radial growth rate, lamellar thickness, and the morphology of the polymer (Burnett and McDevit, 1957; Phillips and Tseng, 1989). This process is an important step in the prediction of the overall crystallization kinetics and most importantly controlling the crystallization process (C. Virone et al., 2005). Polymer scientists in crystallization have researched and proposed various theories in describing secondary nucleation. The focus will be on the Lauritzen-Hoffman (LH) theory since this theory will be used in the experimental part of this thesis. Nevertheless, other important theories are summarized in the subsequent chapter.

2.4.2.1 Lauritzen-Hoffman Theory: Stem by Stem Nucleation

Six decades ago, Lauritzen and Hoffman discovered the theory of chain folding in dilute solution (Hoffman et al., 1975; Hoffman et al., 1976; Lauritzen, JR and Hoffman, 1960) (Hoffman et al., 1976). This theory was the basis of their works on secondary nucleation. Their work on 'the Growth Rate of Spherulites and Axialites from the Melt in Polyethylene Fractions: Regime I and Regime II Crystallization' (Hoffman et al., 1975), described the mechanism of secondary nucleation in detail and gave birth to Lauritzen-Hoffman secondary nucleation theory. This theory is a simplistic one because it connects microscopic parameters to macroscopic quantities by ignoring complex molecular details of chains bringing them into a common mean field (Zhang et al., 2017). This theory has become the standardized theory for secondary nucleation, although most scientists argue that it has been oversimplified. Nevertheless, this theory is the basis of other secondary nucleation theories. The assumptions in this theory are listed below:

1. The critical nucleus is assumed to be a single stem. Molecules randomly fluctuating in and out of the embryo occur till a critical nucleus with specific dimensions (bigger than the minimum lamellar thickness) is formed and stability of the nuclei is established (Cox et al., 2015; Lupi et al., 2014). This model is known as the coarse-graining model, and the steps involved are intricate. The opposite is the fine-graining model whereby the steps taken are in sequence. In the paper of Frank and Tosi (Frank and Tosi, 1961),

it was proven that the same outcome is obtained when both models are used for a system in equilibrium. Additionally, this research proposed that chain folding ends before the cumulative length of molecules reaches the lamellar thickness and that molecular fluctuation occurs along the lamellar direction. Point made modifications to the model by including the probability of occurrence of chain folding in the lamellar (Point, 1979a; Point, 1979b).

2. The polymer remaining after the nucleus is initially deposited onto the crystal surface undergoes adsorption and has the same length as the original lamellar (Zhang et al., 2017). This stem length is also subjected to a certain level of thermally influenced fluctuation (δl) which is approximated to zero by Hoffman's treatment (Zhang et al., 2017). The fluctuation-dissipation theorem shows that there is an interconnection between the fluctuation lamellar thickness and the corresponding dissipation since the thermal driving force ($k_b T$) is shared between the two. T is the absolute temperature and k_b is the Boltzmann constant (R Kubo, 1966).

This can be represented as:

$$\sigma b \delta l = k_b T \tag{2.5}$$

$$\text{Hence } \delta l = k_b T / \sigma b \tag{2.6}$$

where b is the stem's width

3. Upon the formation of a nucleus, lateral growth will occur in the whole chain in the system. Chain growth will be in a sequential order, i.e. the growth of a new chain can be possible only if an old chain in the process of growth has finished its growth process (Zhang et al., 2017). This can be possible in a diluted solution. However, in a concentrated solution or melts new chains can emanate from the melt whilst growth is still happening in old chains. This results in a 'cilia' morphology which can pass through various lamella when it has a maximum length (DiMarzio, 1967).

4. The most important assumption is the smooth surface nucleation whereby the pre-existing surface is atomically smooth (few 'vacancies') leading to the creation of a new surface in each deposition (Zhang et al., 2017).

From the above assumptions, the Lauritzen-Hoffman theory is said to be an 'enthalpy barrier' model which involves two major steps. The first is the creation of new nucleus subjected to

random fluctuations and the other growth of the molecules to a length greater than the lamellar width causing lateral growth. According to this theory, two important parameters are used to describe crystallization kinetics: nucleation rate i, and spreading rate g. There are three regimes used in describing the parameters. The nucleation stages according to Lauritzen Hoffman Theory is represented in figure 2.9 below.
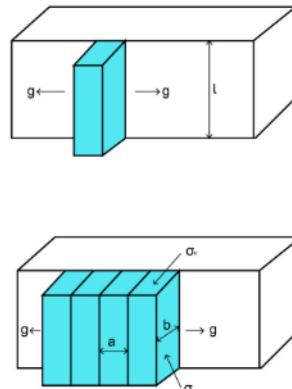
Fig. 2.9: Stages involved in Nucleation According to Lauritzen Hoffman Theory (Zhang et al., 2017)

Regime I

In this regime, i<<g and this occurs at very high temperatures. Following nucleation, lateral growth will quickly expand a layer before waiting for the subsequent nucleation to begin. To calculate for crystal growth rate in this regime,

$$G=ibL \qquad (2.7)$$

Where L is the crystal size making iL the nucleation rate, i is the nucleation rate per unit length, and ibL the growth rate. From the above equation, the growth rate is linearly related to the crystal size which is inconsistent with experimental data since slow growth rate increases crystal size. Therefore, L is redefined as the 'effective' growth length or persistent growth length (Lauritzen, JR and Passaglia, 1967; Point et al., 1986) and considerably narrower than the crystal growth face's width (Zhang et al., 2017).

$G_I = biL_I$

(2.8)

2. Regime II

i=g in this regime, it occurs at moderate temperature rate and there is a competition between the two parameters of nucleation rate and spreading rate.

$$G_{II=} b\sqrt{i}g \tag{2.9}$$

3.   Regime III

In this regime, $i >> g$, this occurs at low temperatures and nucleation is faster than lateral growth rate. The behavior of this regime is like that of region I since there is constant mean spacing between adjacent nuclei making the lateral spreading rate negligible (Guerin et al., 2021; John D. Hoffman, 1983).

$$G_{III=} biL_{III} \tag{2.10}$$

According to Lauritzen Hoffman, the formation and spread of nucleus are due to steady state approximation in detailed balancing connects the addition and removal of sequential stems and the probabilities between the addition and removal of the stems (Zhang et al., 2017). During the nucleation process, the first step of addition does not lead to surface folding yet solely two new lateral surfaces are produced due to the lateral spreading process (Zhang et al., 2017). Every polymer molecule starts at the growth surface, where the lateral dimension is expressed as Lp. This is where the first stem is positioned. This phase is thought to be related to nucleation. The secondary nucleus then continues to grow laterally at a pace of g. The stem grows at a growth rate of G and has thickness in both the lateral and growth directions. This is represented by the equation:

$$\Delta G = -abL\Delta\mu + 2bL\sigma_l \tag{2.11}$$

There is an alternation between the formation of lateral and folded surfaces; if lateral surfaces are formed, folded surfaces cease to form, and vice versa. Hence each process i.e. addition and removal process have specified free energies.

Hoffman also proposed that the surface free energy used serves as a barrier that the nucleus must overcome to lay the stems which can be represented by the probabilities of adding a stem (nucleation barrier). Nonetheless, there is an addition of free energy during the deposition of the stem which helps minimize the barrier leading to the determination of the net free energy by factor. This is graphically represented below in Fig 2.10.
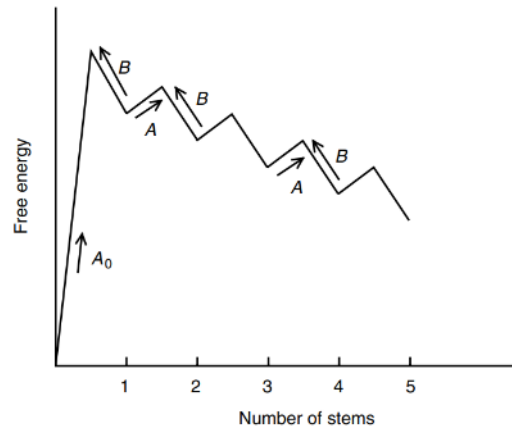
Fig. 2.10: Lauritzen Hoffman Free Energy Landscape (Kundagrami and Muthukumar, 2007)

In connecting the macroscopic quantities, the LH theory can be expressed and simplified mathematically in the following equations:

Average lamellar thickness:

$$< l >_{av} = 2\sigma_e /_{\Delta F} + \delta l \tag{2.12}$$

$$\delta l = (K_b T/2b\sigma\ 2 + (1-2\omega)\ a\Delta F/2\omega)/(1-a\Delta F\omega/2\omega)\ (1+a\Delta F(1-\omega/2a)) \tag{2.13}$$

Fluctuation lamellar thickness

$$(<l-<l>_{av})^2 = \frac{(KT)^2}{(2bo-ab\Delta F\omega)^2} + \frac{(KT)^2}{(2bo-(1-\omega)ab\Delta F\omega)^2}\ \frac{1}{2}\left(\frac{K}{bo}\right)^2 \tag{2.14}$$

Growth Rates

$$G_I = \frac{b}{a}\beta Lp\exp\left(\frac{2ab\sigma_e\omega}{KT}\right)\exp\left(\frac{-2bo\sigma_e}{\Delta FKT}\right) \tag{2.15}$$

$$G_{II} = b\beta\exp\left(\frac{-ab\sigma_e\omega}{KT}\right)\exp\left(\frac{-ab\sigma_{e(1-\omega)}}{KT}\right)\exp\left(\frac{-2bo\sigma_e}{\Delta FKT}\right) \tag{2.16}$$

$$G_{III} = \frac{b}{a}\beta L'p\exp\left(\frac{2ab\sigma_e\omega}{KT}\right)\exp\left(\frac{-4bo\sigma_e}{\Delta FKT}\right) \tag{2.17}$$

where the kinetic prefactor is denoted by β. Based on these findings, it may be concluded that, in general, the main experimental findings can be quantitatively or semi-quantitatively replicated via LH theory. This shows the theory's viability because, even with such basic assumptions, it can accurately forecast most experimental outcomes (Zhang et al., 2017).

2.4.3   Other Models

Apart from the Lauritzen-Hofmann model, other models have been used in the description of secondary nucleation and growth. These models are used either in modification of the

Lauritzen Hoffman or for multiphase polymer systems. These models are, namely, the Sadler-Gilmer Model, Wunderlich Molecular Theory, Hu Intramolecular Models, Mutukumar's Continuum Theory and Strobl Model. The Sadler-Gilmer Model is a theoretical entropical barrier model based on the modification of the LH theory (Zhang et al., 2017; Zhang et al., 2021). This model is typically used for short chain crystal systems due to consideration of nearest neighboring interactions and potential molecular adsorption and desorption issues (Zhang et al., 2017). The Wunderlich Molecular Theory is applied in a polymer system of a combination of two bimodal polymers with different molecular masses (Zhang et al., 2017). This model is qualitatively based on molecular segregation of the two bimodal polymers as crystal growth occurs and shows the effect of molecular weight on crystallization. An improvement of the Wunderlich Molecular Model is the Hu Intramolecular Model. It was formulated by Hu et al. (Zhang et al., 2017) to quantitatively explain the dependence of molecular weight on molecular chain segregation using a single chain model. It showed that an increase in molecular weight increases the melting barrier, although the nucleation barrier remains constant irrespective of molecular weight. Muthukumar et al. (Kundagrami and Muthukumar, 2007) developed a model that combines two distinct physical processes into a single formalism. The first process is dominated by nucleation control in solution-grown crystals, while the second is diffusion-controlled in solution-grown crystals. The model uses an entropic barrier theory to explain polymer chain accumulation, accounting for concentration, molecular weight, and long-chain polymer properties. Inspired by the polyethylene research of Keller et al., Strobl's multistage crystallization model proposes a third stage of growth. A model was put out to explain why random copolymers of sPP exhibit lamellar thicknesses that are comparable to those of homopolymers at higher equilibrium melting temperature (Zhang et al., 2021).

2.5   Thermodynamics of Polymer Crystallization and Melting

Crystallization refers to a first-order irreversible process that involves transitioning of phase from the amorphous phase to the crystalline phase at a specific temperature namely equilibrium crystallization temperature (Guo, 2016). Since crystallization is an irreversible reaction, the process from a crystalline to amorphous phase is melting and this also occurs at a specific temperature called equilibrium melting temperature. To thermodynamically

investigate a polymeric melting system, the system must be in equilibrium and when this happens the free energy state becomes null. This is represented by:

$$\triangle Gm = \triangle Qm - Tm \triangle Sm \qquad (2.18)$$

At equilibrium

$$\triangle Gm = 0 \qquad (2.19)$$

Hence

$$Tm = \triangle Qm / \triangle Sm \qquad (2.20)$$

The enthalpy of fusion of polymers is low due to weak Van der Waals bonds between chains whilst having high entropy. Hence, highly crystalline polymers have higher melting points than the flow temperature of amorphous polymers due to their low disorderliness (entropy) and high heat of fusion. The Gibb's-Thomson equation which takes into consideration the lamellar thickness of the polymer chains modifies the above equation to:

$$Tm = Tmi - 2\sigma eTm/l\Delta h \qquad (2.21)$$

where l is the lamellar thickness, σe is the fold-end surface free energy density and Δh is the heat of fusion. From the equation, the distribution of lamellar thickness affects the melting point, a wide distribution of lamellar thickness shows a broad peak on the DSC melting curve (Guo, 2016).

Polymer crystallization follows the law of thermodynamics, which determines whether a crystallization reaction should occur under specific conditions (Raka and Bogoeva-Gaceva, 2008). Gibb's Free energy determines whether a reaction would occur or not under specific conditions and it is determined by both enthalpy and entropy. For a crystallization reaction to occur under certain conditions the value of Gibb's Free energy must be negative.

The Gibb's Free energy can be expressed as:

$$G = H - TS \qquad (2.21a)$$

In terms of crystallization, the Gibb's Free energy will be at its minimum (G=0) when the system is in equilibrium (Raka and Bogoeva-Gaceva, 2008). Comparing melting to crystallization, a polymer melt will have a high entropy due to its randomly entangled and coiled chains leading to the system having a negative and lower G compared to a crystallized

polymer which has a lower entropy. This random coil model was first discovered by Kuhn (Werner Kuhn, 1934) together with Guth and Mark (Guth and Mark, 1934) for the prediction of the entropic elasticity of polymers. It should be noted that if the magnitude of enthalpy change H is greater than the product of the TS, then G is negative and crystallization will occur (Raka and Bogoeva-Gaceva, 2008).

The development of statistical thermodynamics in blends of polymers was formulated by Flory and Huggins (Polypropylene handbook, 2019). The number of possible configurations for the molecules on a lattice is counted to determine the entropy of mixing, or $\triangle S_{mix}$, which is computed under the assumption that it is solely combinatorial. If the interaction energy is temperature independent, the difference between like and unlike pairings can be summed up into a single term, the Flory-Huggins interaction parameter, $\varkappa$, which varies linearly with inverse temperature. The van der Waals energy of contact is what is known as the enthalpy, or $\triangle Hmix$. (Polypropylene handbook, 2019).

The Flory-Huggins equation is stated as follows:

$$\triangle \frac{Gmix}{RT} = \omega_1 \ln(\omega_1)/N_1 + \omega_2 \ln(\omega_2)/N_2 + \varkappa_{12}\, \omega_1\, \omega_2 \qquad (2.22)$$

where ω_1 and ω_2 are the volume fractions, N1 and N2 are the segment numbers of the two blend components, respectively, $\varkappa_{12}$ is the Flory–Huggins interaction parameter, and $\triangle G_{mix}$ is the change in free energy when mixing two polymers (Polypropylene handbook, 2019). The blending of two high molecular weight polymers results in a small gain in entropy, $\omega_1 \ln(\omega_1)/N_1 + \omega_2 \ln(\omega_2)/N_2$ which leads to $\triangle G_{mix}$ becoming negative or small (Polypropylene handbook, 2019)

2.6   Crystallization Kinetics of Polymers

As discussed in the previous chapter, polymer crystallization is a phase transition process in the first order from a disordered isotropic melt to a semicrystalline state. The amorphous phase which is the disordered isotropic melt has interfaces made of chain entanglements, end groups, bulky side groups and chain defects which during the formation of the crystalline lattice are excluded (Müller et al., 2016). Thermodynamics and Kinetics are important variables when describing polymer crystallization. However, the kinetics study of polymer crystallization is of great importance as compared to thermodynamics. A crystal can have the

lowest activation energy but can grow at a slow rate which would not favor crystallization at a specific temperature. Metastability is one of the major characteristics of polymer crystals because of their lamellar structure, hence depending on the crystallization kinetics these crystals can vary in size and form.

Polymer crystallization studies are of high importance, especially in the field of polymer chemistry, polymer processing and polymer testing. To understand the structure, morphology and properties of polymer for practical applications, one must be able to know the kinetics governing crystallization to model a polymer of choice. Certain factors such as temperature, pressure, flow of the polymer, nucleating agents and stereo-defects affect the outcome of crystallization. These factors will be briefly highlighted below.

A.   Temperature

Kinetically and thermodynamically, temperature has a massive effect on both growth and nucleation during crystallization. Cooling transforms the polymer into its lowest energy state which reduces the diffusion of chains leading to a reduction of diffusion coefficient (Yang et al., 2005). During nucleation, when the polymer is cooled below its T_g, there is a seizure of nucleation because the random coiled molecules in this region have less energy to overcome the diffusion-resistant barrier above which chain alignment and aggregation can occur efficiently (Yang et al., 2005). According to classical nucleation theory (Yang et al., 2005), the influence of temperature on nucleation rate is because of the interfacial energy gradient and equilibrium solubility variation at various temperatures. Experimental data by Yang supports this classical nucleation theory and goes further to prove that supersaturation is influenced by temperature which affects nucleation rate efficient (Yang et al., 2005). A decrease in supersaturation rate is a result of an increment in temperature which leads to a lowering of nucleation rate (increase in energy barrier, W^*) and when supersaturation approaches unity, termination of the nucleation rate occurs

Growth rate is also affected by chain diffusion, hence at higher temperatures the chains re-disperse due to the disorderliness of the chains resulting from thermal energy. The variables involved in the influence of temperature on growth rate are pre-factors of growth rate co-efficient (Yang et al., 2005), Gibbs-Thomson effect of particle curvature (D W Oxtoby, 1992) and the heat of solidification. The activation energy during the growth rate needs to be

overcome for growth to happen. An increase in temperature leads to an increase in the activation energy leading to a slow growth rate.

Recent experiments performed by Yang et al (Yang et al., 2018), Nakurama et. al (Nakamura et al., 2008) show the dependence of growth and nucleation rate on temperature and hence temperature is one of the most important parameters to be considered during polymer crystallization.

B.   Pressure

Pressure is relevant in crystallization studies because most polymer processing techniques at the industrial level such as injection molding, extrusion and compression molding apply pressure during processing as high as 1000 bar (Speranza et al., 2023). Melting and Crystallization are pressure-dependent due to the presence of weak Van Der Waal's forces between the molecular chains. The effect of pressure on crystallization was first investigated by Matsouka (Matsuoka, 1960) on linear polyethylene crystallization under high pressure. Wunderlich and Arakawa discovered that high pressure influences the spherulite size i.e. at isothermal temperature and high pressure, there is an increase in spherulite size with time (Wunderlich and Arakawa, 1964). Osugi et al. experimented on the effect of elevated pressure on the crystallization kinetics of polyethylene under pressure of up to 2000atm and analyzed their results by using the Lauritzen-Hoffman equation (Osugi et al., 1964). It was discovered that an increase in pressure leads to an increase in Tm which in effect reduces the surface free energy and favors crystallization. Other experiments (Chitoshi Nakafuku, 1994; Kanetsuna et al., 1973; Speranza et al., 2023) show that pressure has a huge impact on melting and crystallization. Haudin and Boyer (J.-M. Haudin and S. A. E. Boyer, 2017) investigated the growth rate of PP under different conditions and with regards to pressure, the growth rate increased as pressure increased. Figure 2.11 shows the growth rate of PP at different pressures.
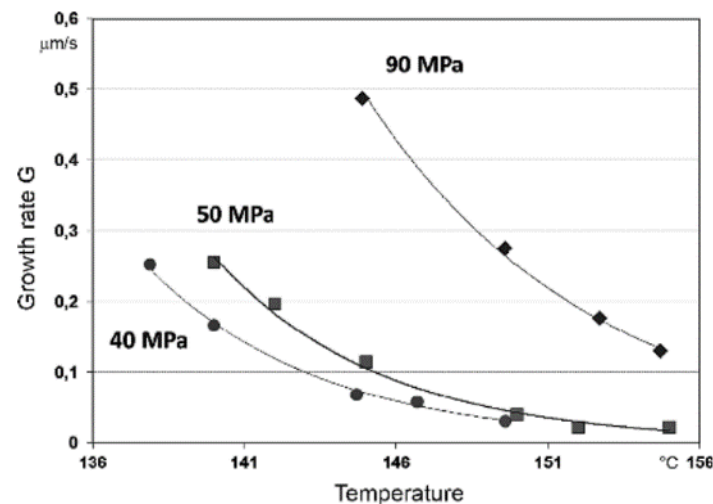
Fig. 2.11: Effect of Pressure on Growth rate at different isothermal temperatures (S. A. E. Boyer, 2017)

C.   Other factors

Apart from temperature and pressure, other factors affecting crystallization are nucleating agents, stereoregularity of the polymer, and rheological properties of polymers. Yanjie An et al. (Yanjie An et al., 2019) investigated the effect of different nucleating agents namely i.e. carboxylate, phosphate, sorbitol and rosin type nucleating agent on the crystallization of isotactic PP. Although different types of nucleating agents affect crystallization in their independent ways, the conclusion drawn was an increase in nucleating agents increases the rate of crystallization (Yanjie An et al., 2019). The spherulite size of PP decreases as nucleating agents increase due to the spike in the number of nucleating sites in the polymer. Several experiments, for example Jing et al. (Jiang, 2007), and Harun et al. (KANDEMİR et al., 2022) prove that nucleating agents influence crystallization kinetics, polymer morphology, and properties. Stereoregularity also affects the crystallization behavior and melting of polymers. Research performed by Martuscelli et al. (E. Martuscelli et al., 1983) on isotactic polypropylene with different degrees of stereoregularity shows that stereoregularity affects melting and crystallization temperature. The findings demonstrate that, for a given Tc, the overall crystallization rate constant reduces as configurational chain defects increase (E. Martuscelli et al., 1983). Di Lorenzo et al also worked on the effect of stereoregularity on PLLA and the results showed that an increase in stereoregularity increases crystallization rate (Di Lorenzo and Androsch, 2018).

2.6.1 Crystallization Kinetics of Polymer Blends

Polymer blends have become an interesting and sought-after topic in the field of polymer science due to the advanced properties that are obtained from polymer blending. This is an economic way of producing polymers with improved properties although there might be problems with compatibility. The compatibility of these blends is improved through the process of compatibilization to modify the interfacial bonds by the addition of compatibilizers such as block copolymers (Paul and Bucknall, 2000). Polymer blends such as co-elastomer of polyvinylchloride and butadiene acrylonitrile, polystyrene (impact polystyrene), and acrylonitrile-styrene copolymers were some of the first commercialized polymer blends in the 1940s (Robeson, 2007). The addition of butadiene acrylonitrile to polyvinylchloride improves the toughness property of PVC and increases its resistance to plasticizers and oils. Polymer blends can be categorized under miscible and immiscible blends which are further divided into amorphous/crystalline blends and crystalline/crystalline blends. During crystallization, these two types of blends exhibit different kinetics. In this work, more attention would be paid to crystalline/crystalline blends since this research work is mostly focused on crystalline/crystalline blend crystallization. However, the amorphous/crystalline blends will be briefly discussed.

A.   Amorphous/Crystalline Blend Crystallization

The crystallization of this system can exhibit either of the two behaviors; the amorphous and crystalline parts mix without any separation observed or they separate into their respective phases (Han et al., 2013). According to the proximity of their glass transition temperature (T_g), these blends can be dynamically symmetrical or dynamically asymmetrical (Han et al., 2013). Dynamically symmetrical blends have similar Tg whereas dynamically asymmetrical blends have a huge difference between the Tg of the amorphous and Tc of the crystalline phases (Han et al., 2013). Several experiments (Han et al., 2013; Takahashi et al., 1992; Woo et al., 2010) show that these kinds of mixtures are majorly miscible and affect the overall Tm, Tg, and crystal morphology of the mixture. NMR results of analyzing PEO and PMMA blends in Martuscelli et al. (Martuscelli et al., 1983) showed that they exhibited a single Tg which reduces the tendency of interphase segregation of the amorphous part from the crystalline part. Again, an increase in the PEO content led to a decrease in the growth rate. This is supported by an experiment by Nishi and Wang (Wang and Nishi, 1977). The modes of

segregation of the amorphous part are separation into interspherulitic zones or interfibrillar zones or interlamellar zones (Hsin-Lung Chen and Shi-Fang Wang, 2000).

 Some examples of amorphous/crystalline mixtures are poly (1,6-hexamethylene adipate)/ poly (vinyl methyl ether), poly(e-caprolactone) / poly (vinyl methyl ether), poly (methyl methacrylate) (PMMA) /poly (ethylene oxide) (PEO).

B. Crystalline/crystalline Polymer Blends

These blends can also be miscible and immiscible blends depending on the components involved. Phase morphology, processing properties, interfacial properties, and molecular characteristics determine the properties of immiscible blends (Humberto Lovisi et al., 2001). The most studied immiscible crystalline/crystalline blends are PE/PP blends, and studies have shown that the properties of these blends are reliant on crystalline conditions, crystallization conditions, and composition (Karger-Kocsis, 1994). Research works show that the presence of the PE component affected the overall crystallization kinetics by reducing the growth rate and creating heterogeneous nucleating sites, leading to an increase in nucleation density (Martuscelli et al., 1980; Martuscelli et al., 1984).

In miscible crystalline/crystalline blends there are three possible modes of crystallization namely separate crystallization, concurrent crystallization and co-crystallization (Pracella, 2013). Concurrent crystallization happens when there is a coincidence in the crystallization temperature range of the individual components of the polymer blends (Pracella, 2013). Co-crystallization occurs in polymer chains of isomorphous polymers leading to the creation of a single-phase (Pracella, 2013). Separate crystallization occurs when the individual components crystallize individually due to difference in their Tc. The phenomenon of co-crystallization is common in isotactic poly (4-methyl pentene)/isotactic poly (4- methyl hexene), poly (isopropyl vinyl ether)/poly (sec-butyl-vinyl ether) and poly (vinyl fluoride)/poly (vinylidene fluoride) blends (Pracella, 2013). The spherulite morphologies of these blends reported by several experimental works are spherulitic crystallization, "interpenetrating," or "interfilling" crystallization dependent of heat treatment (Pracella, 2013). Studies by Arai et al. (Arai et al., 2013) on the crystallization of isotactic-poly (methyl methacrylate) (i-PMMA) and poly (vinylidene fluoride) (PVDF) increasing the i-PMMA content in the blends improved the overall crystallization rate and reduced the induction crystallization time since i-PMMA acts as a

nucleating agent in the polymer. Liau et al (Wen-Bin Liau et al., 2006) also backed these findings with their research on poly(butylene terephthalate) [PBT] and polyacrylate, although it should be noted that adding a polymer with a low Tg to a polymer with a high Tg slows down crystallization whereas adding a polymer with a high Tg to a low Tg polymer accelerates crystallization hence the processing techniques and conditions of the blends is very important in crystallization. Research by Yaping et al on the crystallization of isotactic polybutene-1 with isotactic polypropylene (PP) resulted in the block co-polymer blended with the pure iPP having a higher nucleation and crystallization rate as compared to the pure IPP (Yaping Ma et al., 2021)

2.7   Crystallization Theories

2.7.1   Flory's Copolymer Crystallization Theory

To understand the crystallization and melting in copolymers, Flory (Flory, 1949) derived a theory which would describe the effects of comonomer inclusions on primarily the equilibrium melting points of high crystalline copolymers. His study assumed that firstly, one of the constituents of the comonomers was not crystallizable and hence excluded from the crystalline parts during crystallization. Secondly, the polymer chains' configuration in the liquid phase dictates the structure of the polymer making entropy dependent on the flexibility and chain size (Flory, 1949). In his studies, chain length and comonomer composition play an important role in understanding the thermal and crystallization behavior of copolymers and that the chain length *l*, is a rigid part connected to other chains by flexible bonds (Flory, 1949). Flory, Mandelkern et al. (Flory et al., 1951) experimentally proved Flory's theory by performing dilatometry to investigate the melting temperature of polyamide poly-(N, Pu-sebacoylpiperazine) with different mixtures. The observations made were that an increase in the comonomer concentrations (non-crystallizable part) led to a decrease in the melting points of the mixtures by an unspecified degree and this becomes higher as comonomer concentration increases (Flory et al., 1951). In Flory's work (Flory, 1955), he stated that long crystallites i.e. the crystallizable constituents of a copolymer system, could exist in a metastable condition with the melt at temperatures just below the melting point. The melting point of copolymers has a broad range in comparison to homopolymers that have a single melting temperature (Flory, 1955). This was because of the bonding of the non-crystallizable

regions along the crystallizing chains and as the length of the crystallizable chains increases, it causes a reduction in the non-crystallizable regions and improves the stability of the copolymer leading to an increase in the melting point of the system (Flory, 1955). In describing the melting and crystallization in copolymers, Flory named the copolymer constituents A and B, where A is the crystallizable part and B is the non-crystallizable part. The growth of the A chains is favored laterally only that it can be inhibited by the presence of different sequences in the amorphous region. The A chains which are represented by ζ have varying lengths running from one end of the crystallite to the other. Longitudinal growth is not favored due to the presence of the B constituents along the chains which blocks the growth in that direction (Flory, 1955). Entropically, when there is an increase in entropy due to the phase transition from orderly to highly disordered phase, there is a possibility of A and B constituents mixing which contributes to an additional entropy to the overall system (Handbook of Polymer Crystallization, 2013). This additional entropy is accounted for by a probability term $P\zeta$ (Flory, 1955) which is a representation that the crystallizable unit in the copolymer is one of the selected amorphous units. A comonomer that is a component of the equilibrium sequence that is at least ζ units long (Handbook of Polymer Crystallization, 2013). Therefore, the condition $P^o\zeta > P^e\zeta$ must be met under equilibrium conditions for crystallization to occur where superscripts o and e are the initial and equilibrium copolymer sequence distributions, respectively (Flory, 1955). From this theory, the copolymer melting temperature is determined solely by the crystallizable portion A.

Richardson, Flory et al (Richardson et al., 1963) and Crist and Finerman (Crist and Finerman, 2005) utilized the Flory theory to investigate the effect of different weight fractions of comonomers of polymethylene and ethylene/butene comonomers respectively. Their observations supported the Flory theory in that the presence of comonomers reduces the melting point and sequential folding can be a barrier to nucleation. Flory's model is only limited to the qualitative analysis of the crystallization behavior of copolymers but not quantitatively. The Flory model suggests that the Tm of copolymer AB can depend on the concentration of B and their sequential distribution (non-crystallizable constituent) if $p \neq X_a$ yet not dependent on the chemical nature of the constituents (Handbook of Polymer Crystallization, 2013). Experiments performed by Alamo and Mandelkern (Alamo and Mandelkern L., 1994) and Kale et al. (Kale et al.) proved otherwise, although both

experiments had varying results. Alamo and Mandelkern investigated the melting temperatures of copolymers of ethylene–alkene with varying short-chain branches. They concluded that melting temperatures show a relative dependence on the constituents' concentrations irrespective of their chemical nature only if there is an exclusion of the constituents from the crystalline phase (Alamo and Mandelkern L., 1994). Whereas Kale et al. (Kale et al.) observed that an increase in comonomer concentration in ethylene–butene comonomers led to elevated melting temperature peaks debunking Flory's hypothesis that melting temperatures are independent of comonomer concentrations at equilibrium.

2.8   Bulk Crystallization Kinetics: Avrami's Equation

Phase transformation of materials and the theory governing it was first postulated by Johnson and Mehl, Volmer and Weber and Avrami (Jiří Málek, 1995). Johnson-Mehl-Avrami theories are however the most researched postulate in polymer crystallization with it being utilized mostly in isothermal crystallization. Avrami's review of the kinetics of change became the basis on which nuclei growth, density of nuclei growth, and the volume of nuclei could be quantitatively characterized with time (Avrami, 1939). The Avrami theory can be applied to secondary nuclei (new nuclei or phase grown from an existing one) which occur above equilibrium conditions whereas the rate-limiting factor is temperature with external factors being constant (Avrami, 1939). It is used to scrutinize the crystal growth and crystal geometry of a polymer melt undergoing crystallization i.e. cooling under different isokinetic temperatures and concentrations by using temperature-time curves and transformation time curves (Avrami, 1939).

Temperature-time curves according to Avrami (Avrami, 1939), have 'S' shapes which is because of variation at extremely low cooling temperatures (supercooling). The transformation, or crystallization temperature in our case, has a relation with the crystallization time. Lowering the crystallization temperature shortens the time required for the crystallization of the polymer sample. However, it should be noted that this is dependent on the mobility of the chains in the crystals (Avrami, 1939). The occurrence of secondary nucleation is catalyzed by the presence of heterogeneities such as foreign particles with an adsorbed layer of the new phase or crystal molecules of the new phase (Avrami, 1939). Avrami made assumptions according to other experimental research related to his work.

Firstly, in the work of deCoppet, Hammer, Scheil-Lange-Weise, and others, there is an indication that during nucleation only a specific number of nuclei can grow from the nucleation stage to the growth stage (Avrami, 1939). Secondly, Goler-Sachs and Mehl-Johnson postulated that the surface area of crystals influences the rate of volume growth of the crystals (Avrami, 1939). Avrami combined these two assumptions to generate the relationship between the 'germ nuclei', 'growth nuclei', and transformation volume. He stated that the germ nuclei can be transformed either into growth nuclei through free energy perturbation giving them the ability to overcome the nucleation barrier or be dormant when growing crystals 'swallows' them. The two scenarios are expressed mathematically as follows respectively:

$$n(T)=Ke^{-Q+A(T)/R(T)} \tag{2.23}$$

where n(T) is the probability of a nuclei transforming and Q, a constant, is activation energy (per gram molecule), R is the gas constant, and A(T) is the work per gram molecule required for forming a growth nucleus at temperature T

$$dN=-dN^{'}-dN^{''} \tag{2.24}$$

where

$$dN^{'}=nNdt \tag{2.25}$$

and

$$dN^{''}=NdV \tag{2.26}$$

The volume of the new phase per unit volume of space is represented by dV, which is the increase in time dt. One could argue that (2.25) must be amended even more by deducting in the second term from d V. (dN"), the involvement of the dN' development nuclei that emerged in dt, as these have been granted permission for by the initial period. Nonetheless, it is simple to confirm that this adjustment is of the kind (dtP, making it insignificant by comparison with the additional phases that belong to the arrangement dt. From the equations above, the temperature of supercooling affects the total number of active nuclei formed (Avrami, 1939). Therefore,

$$dN/dt = -dN'/dt = -nN \tag{2.27}$$

$$N = Ne^{-nt} \tag{2.28}$$

for n constant with time (that is, under constant temperature and concentration) follows. At time t, the quantity of growing nuclei would be

$$N' = \int_0^t nNdt = N(1-e^{-nt}) \tag{2.29}$$

and N' = N, the total number that appears. This does not provide the dependency of the upper limit of the number of growth nuclei on the temperature of supercooling.

Expressing the equations in terms of volume and time (τ):

$$ndt = d\tau \qquad N(t) \rightarrow N(\tau) \qquad V(t) \rightarrow V(\tau) \tag{2.30}$$

Substituting into equation

$$dN/d\tau + N(\tau) + NdV/d\tau = 0 \tag{2.31}$$

After integrating the above equation

$$N(\tau) + \int_0^\tau N(z)dz = N(\tau) + N'(\tau) = N((1-V(\tau)) \tag{2.32}$$

Physically speaking, the functional equation (2.52) connecting N and V can be explained as follows: 1-V(τ) is the volume (per unit volume of space) that has not yet been transformed at time r, and N[l- V(τ)] is the number of germ nuclei that would have existed if their density had not changed. These relations with regards to nuclei growth are also described extensively using physical parameters precisely its geometry and the relationship it has with kinetics in his work (Avrami, 1939). Avrami also formulated the relationship between the actual transformed volume and an extended volume in a crystallization system (Avrami, 1940). He also investigated the time dependent transformation of randomly distributed nuclei in the major types of crystalline growth such as plate-like, polyhedral and linear during impingement (Avrami, 1940). His work in 1941 (Avrami, 1941) focused on the densities of the extended volume of crystals as they grew without impingement.

The probability, p_x, that a location inside the crystallizing volume will be traversed by x fronts growing independently from randomly positioned centers is derived from the Poisson relationship and represented by:

$$p_x = \frac{E^x}{x!} \exp(-E) \tag{2.33}$$

where E is the average number of fronts over all the system's such sites. Next, given x = 0, the likelihood that the point stays uncovered is

$$p_o = \exp(-E) \tag{2.34}$$

In a crystallizing system, p_o represents the proportion of uncrystallized material, or 1 - Xt, and Vt is the entire volume of crystalline material (the volume fraction of crystalline material is denoted by Xt in this case). Therefore:

$$1 - X_t = \exp(-V_t) \tag{2.35}$$

Since they deal with the formation of spherulitic crystallization, only two modes of crystallization have physical significance in the study of polymer melt crystallization. These are: (a) predetermined; and (b) sporadic sphere formation.

(a) The volume increase in the period t to t + dt, for crystallization growing from L spherical nuclei arranged randomly and expanding at a constant rate, g, is

$$dV_t = 4\pi r^2 L dr \tag{2.36}$$

$$r = gt \tag{2.37}$$

$$V_l = \int_0^t 4\pi g^2 L g dt \rightarrow \frac{4}{3}\pi g^3 L t^3 \tag{2.38}$$

(b) In terms of increase in the number of spherulites linearly with respect to time, t and rate, l, volume increase at time, t is represented as

$$dV_t = 4\pi g^2 (t-t_1)^2 l t g dt \tag{2.38a}$$

Hence $V_t = \frac{2}{3}\pi g^2 l t^4$ (2.38b)

Avrami's work on Kinetics of Phase Transformation (Avrami, 1939, 1940, 1941) which was on phase transformation of materials such as metals, ceramics and polymers is the basis of the formulation of Johnson-Mehl-Avrami's equation. This equation is used to describe, analyze and understand the crystallization kinetics of polymers and other solid-state transformation under isothermal conditions and is expressed as:

$$\alpha=1-\exp(-kt^n) \tag{2.39}$$

Where α is the fraction of melt crystallized with respect to time, t and k and n are constants. n is called the Avrami's exponential, and it relies on the growth geometry and nucleation type whereas k is the Avrami's constant which depends on the growth and nucleation rates and molecular weight, and secondary nucleation (Long et al., 1995). The equation assumes that nucleation rate is constant and the constant decrease in the volume of the untransformed material is negligible whilst considering nuclei impingement (Long et al., 1995). The graphical representation of the Avrami Equation is represented below.
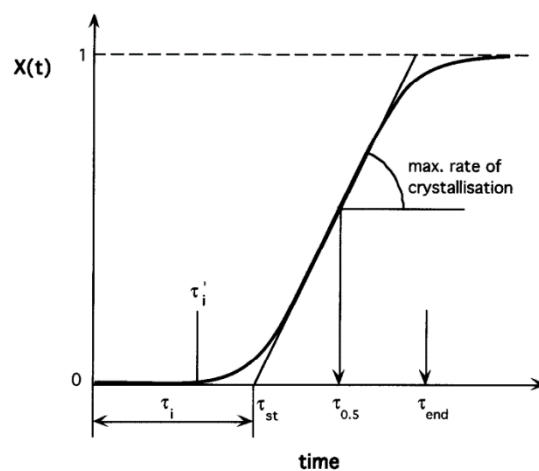
Fig. 2.12: Graphical Representation of the Avrami Equation (Blázquez et al., 2022)

Table 2.1: Avrami exponents for various types of crystal growth geometry's (Hiemenz, 1984)

Avrami Exponent (n)	Crystal Geometry	Nucleation Type	Rate Determination
0.5	Rod	Athermal	Diffusion
1	Rod	Athermal	Nucleation

1.5	Rod	Thermal	Diffusion
2	Rod	Thermal	Diffusion
1	Disc	Athermal	Diffusion
2	Disc	Athermal	Nucleation
2	Disc	Thermal	Diffusion
3	Disc	Thermal	Nucleation
1.5	Sphere	Athermal	Diffusion
2.5	Sphere	Thermal	Diffusion
3	Sphere	Athermal	Nucleation
4	Sphere	Thermal	Nucleation

Specifically, the line that is drawn at the point of inflection perpendicular to the curve defines three distinctive quantities:

The line's gradient equals the maximum crystallization rate. The incubation time, τ_i, is defined as the point where the line and the time axis connect. The crystallization half-time, 0.5 is the time at which X = 0.5.

τ_{st} can also be taken as the incubation time, and time at which crystallization stops is expressed as $\tau_{end}= 2(\tau_{0.5} - \tau_{st}) + \tau_i$

Practically, the Avrami equation is used in the analysis of the evolution of the degree of crystallinity with respect to time and is usually applied in techniques such as DSC, dilatometry and XRD. When used in DSC, the equation is expressed in terms of enthalpy as:

$$\theta = \frac{\Delta H_t}{\Delta H_\infty} \tag{2.40}$$

For volumetric measurement:

$$\theta = \frac{V_t - V_O}{V_\infty - V_O} \tag{2.41}$$

The results from DSC analysis and volumetric analysis are graphically represented below.
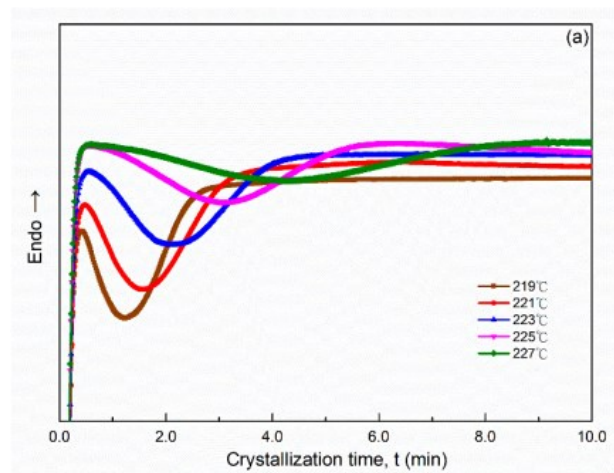
Fig. 2.13: Isothermal exothermic DSC peaks of Polyamides (Tseng and Tsai, 2022)
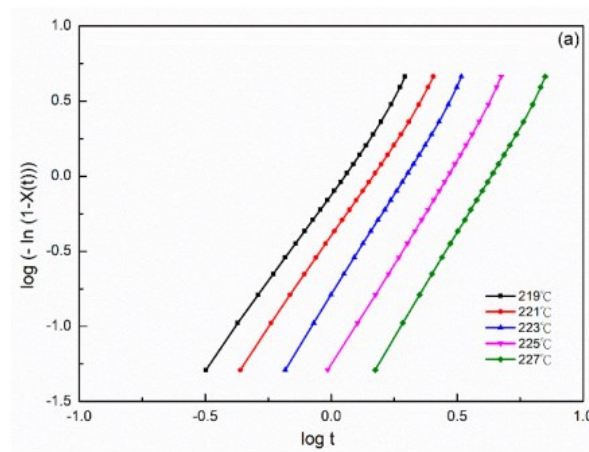
Fig. 2.14: Plots of log {− ln[1 − x(t)]} versus log t at the indicated temperature for isothermal crystallization of Polyamide (Tseng and Tsai, 2022)

Taking the double logarithm of the Avrami equation

$$\log\left(-\mathrm{Ln}(1-\theta)\right) = \log K + n\log t \tag{2.42}$$

yields a straight line as shown in figure 2.13, whereby the slope represents the Avrami constant, n and K can be obtained by using the equation

$$K = \frac{\ln 2}{t_{1/2}^{\,n}} \tag{2.43}$$

Although the Avrami's equation is limited to isothermal conditions, it can be modified to be applied to non-isothermal conditions. These modifications by Nakurama et al. (Nakamura et al., 1972; Nakamura et al., 1973), Harnisch and Mushick (Harnisch and Muschik, 1983) and

Ozawa (Ozawa, 1971) are an extension of the Avrami equation which helps in the study of crystallization kinetics under different cooling rates and these theories are practical for industrial applications since plastic fabrications are mostly under non-isothermal conditions.

## 2.9	Types of Crystallization

### 2.9.1	Crystallization during polymerization

This phenomenon usually occurs in flexible linear polymers whereby crystallization and polymerization occur either simultaneously, successively, or separately in the system depending on the processing parameters. The most investigated pathways are successive and simultaneous occurrences of polymerization and crystallization. Simultaneous polymerization and crystallization are synonymous with chain polymerization, here part or full of a mobile monomer is positioned on the desired point of a lattice in a growing crystal leading to simultaneous rearrangement of the covalent bonds together with the creation of secondary bonds (Wunderlich, 1968a, 1968b). Thermodynamically, the heat of transition of this reaction and its entropy is the summation of both the heat of polymerization and the heat of crystallization and their entropies, respectively (Wunderlich, 1968a). On the other hand, when crystallization happens after polymerization is completed then the process is termed a successive polymerization crystallization process. Since the two processes are mutually exclusive yet dependent on each other, a detailed kinetic description of each reaction is necessary for a comprehensive study on how these two processes affect each other. The difference between the simultaneous and the successive processes can be deciphered when the reactions are carried out close to their ceiling temperature. Separate polymerization and crystallization occur when the covalent bonds during polymerization are completely formed in the molten or dissolved state before crystallization takes place (Wunderlich, 1968a). Five different nucleation paths can be created during the three different types of polymerizations during crystallization (Wunderlich, 1968b):

- Path 1: a simultaneous polymerization and crystallization close to the ceiling temperature, followed by intermolecular nucleation.

- Path 2: an intermolecular nucleation that occurs much below the ceiling temperature, followed by simultaneous polymerization and crystallization.

- Path 3: intermolecular nucleation, which is followed by crystallization and polymerization in turn.

- Path 4: an intramolecular nucleation that is followed by crystallization and polymerization occurring simultaneously.

- Path 5: an intramolecular nucleation that is followed by crystallization and polymerization in turn.

One of the challenges associated with this kind of crystallization is in polymers with only regularity (arrangement). This kind of crystallization can cause imperfections in crystal arrangements, for example in cellulose, polycaprolactam, and polyhydroxybutyrate which folds in anti-parallel arrangement (Wunderlich, 1968b). Kubo and Wunderlich worked on crystallization during polymerization of p-xylylene from the gas phase between 200°C and -196°C (Kubo and Wunderlich, 1972). They observed that in this system either simultaneous or successive crystallization during polymerization can occur and the mechanisms occur either at high or low temperatures extrema (Kubo and Wunderlich, 1972).

2.9.2 Crystallization Induced by orientation

Shear stresses, deformation, and elongation flow fields are some of the external factors that affect polymer crystallization during the processing of polymers for industrial use. Techniques such as extrusion, calendaring, blow molding, etc. are all processes that require some form of tensional or contractional force. These forces induce a form of molecular and chain orientation in the polymer, depending on the direction of the force. Crystallization is thermodynamically possible in a network of polymer chains because applying external deformation forces creates a low interchain configurational entropy leading to TΔS<ΔH. Kornfield also argued that shearing polymers during crystallization introduces nucleation precursors into the polymer chains which increases the rate of crystallization in the polymer (Kornfield et al., 2002). This can be observed in elastomeric polymers such as butyl rubbers and natural rubbers because they possess a network structure and can easily be stretched. This stretching orients the polymers in a direction during manufacturing (Flory, 1947). Liu et al. investigated the effect of shear and elongation on the nucleation of iPP and its microstructure. It was discovered that an increase in the shear rate of the PP increases flow which increases the overall crystallization (Liu et al., 2013). Shearing in the polymer melt

even at the minimum shearing leads to the formation of highly oriented polymer chains. Polymorphism is also affected by orientation of the crystals i.e. α crystals or β crystals would be formed dependent on the amount of shearing which affects the direction of flow and the orientation. The α crystals of iPP are common and produced under quiescent conditions whilst the β crystals are complicated to produce under such conditions. Hence there have been considerable investigations by scientists on the application of deformational forces to produce such crystals.

2.9.3   Crystallization Under Quiescent Conditions

Most papers on polymer crystallization, especially of long-chain flexible polymers, are done under quiescent conditions because it is a stable condition where we can understand polymer growth without a lot of external influence. Crystallization under this condition can be investigated either isothermally or non-isothermally with isothermal crystallization kinetics being more studied than non-isothermal crystallization, although most industrial polymer processing is done under non-isothermal. The crystals grown from this type of crystallization are categorized into Solution Growth Single Crystals and Melt Growth Single Crystals.

As the name suggests, solution growth single crystals crystallize in dilute solutions whereby the crystal is considered as a single chain due to the isolation of the molecular chains in the solution. This system is an isolated system which is very difficult to design however Bu et al. (Bu et al., 1991) came about this concept by spraying heavily diluted polymer solutions (PEO of concentration 2.5wt%) drop by drop on hot water, to comprehend the morphology and diffraction patterns of single crystals confirming a folded chain formation.

Melt-grown polymer crystals are formed from melting and are the most investigated category during polymer crystallization since it is easy to experimentally model this system. Chains in melt-grown crystals are adjacent to each other and the folding of these chains can be described by using the Fringed Cell model, lamellar models, and the interlamellar Adjacent Models. These models have already been described in the sub-chapters above. In the next chapter, the experimental procedure describing spherulite growth and crystallization using Polarized Light Optical Microscope with heating stage and Differential Scanning Calorimetry would be discussed.

3   EXPERIMENTAL

3.1   Materials

Commercially available extrusion grades PP-H, PP-R, PP-B were used for the crystallization kinetic analysis and spherulite growth analyses. The co-monomer constituent infused in PP-B and PP-R is ethylene. The properties of the PP-H, PP-R and PP-B are summarized in table 3.1.

Table 3.1: Material Properties of PP-H, PP-B and PP-R

PP-Type	Density (kg/m³)	Melt Flow Rate (g/10min)
PP-H	0.905	0.3g/10min (230/2.16)
PP-B	0.900	0.3g/10min (230/2.16)
PP-R	0.900	2.2g/10min (230/2.16)

To produce blends of PP-H, PP-B and PP-R, the PP samples were mixed in a compounder and molded into tensile specimens (Type A) via injection molding. The compounder was used to ensure homogenization of the pure PP samples and the mixture for uniformity of the blends. The ratio of the blends of PP types are tabulated in table 3.2.

Table 3.2: PP constituents and its blends ratio

Material Name	Constituents / Blend Composition		
	PP-H	**PP-B**	**PP-R**
PP-H	100	-	-
PP-B	-	100	-
PP-R	-	-	100
PP-HB	50	50	-
PP-HR	50	-	50
PP-BR	-	50	50

3.2   Thermal Analysis

Thermal analysis using PerkinElmer DSC 8000 was used to perform classical DSC runs on all six samples. This thermal run was conducted to measure the melting temperatures and crystallization temperatures of PP-H, PP-B, PP-R, PP-HB, PP-HR and PP-BR. The melting and crystallization temperature values were further applied in the isothermal crystallization studies of the PPs via DSC.

3.2.1   Sample Preparation

The tensile samples of the PP types were cut using a cutting blade. Hermetic Aluminum pans and lids are used for thermal analysis of PP and its blends due to their good thermal conductivity and their ability to prevent mass loss and contamination. The aluminum pans and lids were weighed on a Precision Digital Balance, the measured weight was then tared to zero. The cut PP sample was then measured in the pan to obtain the weight of the PP for thermal analysis. The weight of all six PP samples used for the thermal analysis was 7mg (+-0.5mg). This process was carried out for all six samples.

The sample was then placed in the well of the PerkinElmer crimping dye and pressed with a lever to cover the pan securely. It should be noted that the sample was handled with tweezers, not with bare hands to avoid contamination. Subsequently the specimens were then loaded in the DSC for normal DSC analysis on PP samples.

This process was repeated for the isothermal crystallization kinetics studies via DSC. The repititions for each PP type were five samples each (representing isothermal temperatures of 110°C, 115°C, 120°C, 125°C, 130°C) totaling thirty samples for the isothermal kinetics studies via DSC.

3.2.2   Applied Methodology

3.2.2.1   Normal DSC Analysis of PP and its Blends

The samples were then loaded into the furnace of the PerkinElmer DSC 8000 machine using a special vacuum holder attached to the DSC machine and an empty pan was also loaded into the other furnace in the machine as a reference. The purging gas used for this process was nitrogen gas at a volumetric flow rate of 50ml/min. Nitrogen gas was used because it is non-reactive with PP. Before the analysis started, the machine was calibrated to a cooling rate of

30 °C/min with indium and zinc as reference materials. The thermal profile of the DSC was set as follows:

- Holding the sample temperature at 25°C for 3 minutes,

- Heating of the sample from 25°C to 210°C at a rate of 30 °C/min and hold it for five minutes to eliminate thermomechanical history in the PP samples. Cooling the sample at a rate of 30°C/min to a temperature of -30°C.

- Heating the sample back to room temperature (25°C).

The thermal profile is represented below.
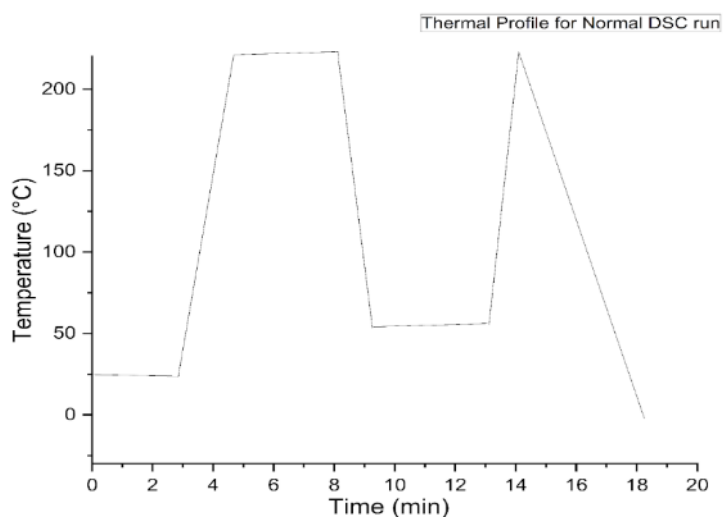
Fig. 3.1: Thermal profile for normal DSC runs of PP

3.2.2.2   Isothermal Crystallization Kinetics Via DSC

The samples were loaded into the furnace of the Perkin Elmer Machine DSC machine using a special vacuum holder attached to the DSC machine. An empty pan was also loaded into the other furnace in the machine as a reference. The purging gas used for this process was Nitrogen gas at a volumetric flow rate of 50ml/min, nitrogen gas was used because it is non-reactive to PP. The thermal profile of the DSC was set as follows:

Holding the sample temperature at 25°C for 3 minutes, Heating of the sample from 25°C to 210°C at a rate of 30 °C/min and hold it for five minutes to eliminate thermomechanical history in the PP samples. Cooling the sample at a rate of 30°C/min to different isothermal

temperatures i.e. 110°C,115°C,120°C, 125°C, 130°C. These temperatures range were chosen because they were the range in which crystallization took place for PP and its blends in DSC measurements. These temperatures were held at 10 minutes for 110°C and 115°C, 15 min for 120 °C and 125 °C and 20 minutes for 130°C to ensure complete crystallization of the samples. Below is a graphical representation of the thermal protocol for the DSC measurement of PP and its blends:
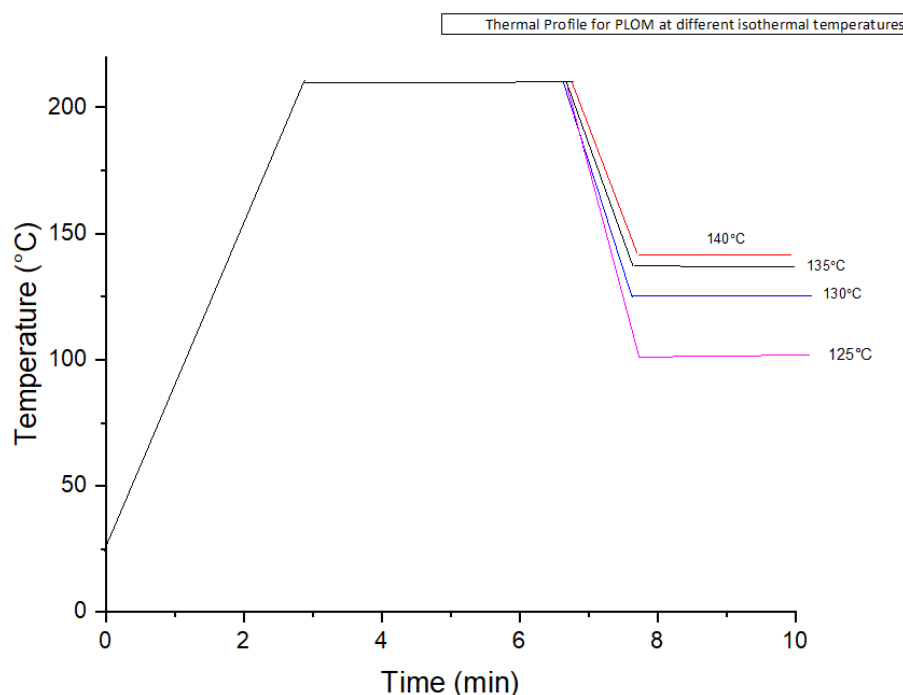
Fig 3.2: Thermal profile of DSC runs for isothermal crystallization kinetics of PP

The isothermal crystallization temperatures and their corresponding melting temperatures are used to find the equilibrium melting temperatures ($T°m$) of PP-H, PP-B, PP-R, PP-HB, PP-HR and PP-BR by using the Hoffman-Week's Linear Extrapolation. Equilibrium temperatures are used for the LH equation whereby nucleation constant (K_g) and pre-exponential growth rate (G_o) and represented below:

$$G=G*\exp(\frac{-U*}{R(T-T_\infty)})*\exp(\frac{K_G}{T\Delta Tf}) \tag{3.1}$$

Where U^* is the energy that macromolecules in the melt use for transportation and is given by 6300J/mol is taken from literature, T_∞ , given by T_g-30K for Polypropylene, is the temperature below which polymer chain movement stops, ΔT is the undercooling temperature represented by $T°m-T_C$, Tc being the crystallization temperature and $T°m$ being

the equilibrium melting temperature. K_G is the nucleation constant, ´f´ is the correction factor

represented by $\frac{2Tc}{Tc-Tm}$, R is the universal gas constant given by 8.314J/mol/K whilst G and Go

are the Growth rate and pre-exponential growth rate factor respectively.

To analyze the exothermic isothermal graphs from the DSC analysis, the area below the curve

is first fully integrated from the time when crystallization started to the time when

crystallization ended using Pyris Software. The equation used to represent this integration is

given as:

$$X_t=\int_0^t (\frac{dH}{dt})/\int_0^\infty (\frac{dH}{dt})dt \qquad (3.2)$$

The resulting graph from the integration of the area under the enthalpy-time graph of the

isothermal curves results in the Avrami graph. This graph is used to describe the evolution of

crystallization with respect to time. The Avrami exponential fit which is obtained from the full

integration of the enthalpy-time graph is represented as:

$$X_t=\exp(-Kt^n) \qquad (3.3)$$

To simplify the above equation from an exponential graph to a linear graph, the natural log is
taken on both sides and the equation transforms into:

$$\log(-\ln(1-Xt))=n\log t+\log k_n \qquad (3.4)$$

The Avrami number, which is K and the Avrami, n can be used to theoretically calculate for the

half time to crystallization as follows:

$$t_{1/2}=(\frac{\ln 2}{K})^{1/n} \qquad (3.5)$$

Replacing $t_{1/2}$ in the LH equation (3.1), the equation is rewritten as:

$$t_{1/2}=t_{1/2}{}^* \exp(\frac{-U^*}{R(T-T_\infty)})*\exp(\frac{K_G}{T\Delta Tf}) \qquad (3.6)$$

To obtain the parameters K_G and $t_{1/2}{}^*$, a plot of $Int_{1/2}+ \frac{U^*}{R(Tc-To)}$ against $1/Tc*(\Delta T) *f$ is drawn,

and the result is a straight line with the slope being Kg and intercept being $t_{1/2} *$, accordingly

The Avrami exponent and Avrami number can also be used in the calculation of the Activation

energies of the PP samples by the equation below:

$$Lnk^n=\frac{\Delta E}{RTc} \qquad (3.7)$$

Equation (3.7) is plotted on a graph to obtain a linear curve. The values of the slopes of the

curve represents $\Delta E/R$, to obtain ΔE which is the activation energy, the value of the slope is

multiplied by R which is the universal gas constant 8.314J/Kmol.

3.3   Insitu Polarized Light Microscopy with Heating Stage

3.3.1   Sample Preparation

Already mechanically tested tensile samples (type A) of PP-H, PP-B, PP-R, PP-HR and PP-BR were used. The unstrained shoulders of these samples were sliced into thin slices with a thickness of 70µm to 100µm using a Leica RM 2255 microtome with disposable blade types inserted in the knife holder. The part of the samples cut was the undeformed sections usually at the clamping area. This is shown in Figure 3.3.

The slicing was carefully done automatically to ensure uniform thickness for all samples. The thickness of each sample was then measured using micrometer screw gauge. They were then placed on a clean rectangular transparent glass slide (cleaned with ethanol) and covered with circular glass slide for the heating and crystallization observation under the microscope.

Fig. 3.3: PP-H clamped in the Leica RM 2255 microtome ready for slicing

3.3.1.1   Applied Methodology

The thermal protocol utilized for the sample preparation and crystal growth of PP and its blends was done under standard atmospheric temperature and pressure. The prepared sample was placed in a Linkam 2028 heating stage and heated above its melting temperature to 210ºC at a rate of 50ºC/min. The heat was held there for about 3 minutes to erase any thermomechanical history of the structure which may influence the crystallization and crystal growth of the PP. Then cooling of the sample took place at a rate of 30ºC/min to the desired

crystallization temperature of 140°C ,135 °C, 130°C and 125°C then held at adequate time to observe crystal growth and crystallization. As soon as the heating stage hits the intended isothermal temperature, a stopwatch is started to observe simultaneously the time intervals as the crystals start to grow. The heating and cooling were observed under a polarized 3D Keyence VHX 7000 optical Microscope using polarization filters, differential Interference Contrast (DIC) and analyzers. The magnification used for the observation of crystals growth is 400 times. This protocol was done three times for each isothermal crystallization temperature for PP-H, PP-B and PP-HB totaling twelve times for each sample and thirty-six times for the overall experiment. PP-R, PP-HR and PP-BR were also evaluated. However, it was not possible to document the crystal growth at the chosen temperatures using this method.

Fig. 3.4: Linkam 2028 Heating Stage for heating the PP samples

Afterwards, VHX 7000 software which is used for evaluation of images obtained from the microscope was used to measure the crystals' diameters at specific times. For temperatures 140°C and 135 °C, the number of crystals measured averaged 10 crystals per temperature and repetition. Since the crystals appeared in small quantities, the tracing of the increase in the diameter of crystals was easy to accomplish.For temperatures of 130°C and 125°C, the crystals appeared in a great number, hence the averaged diameter of 20 crystals at specific time intervals were traced visually and measured as their isothermal times increased. This was done for all three samples. The average of the crystal diameters was then taken for each isothermal temperature and samples.

To measure the rate at which these crystals grow, the average of the crystal diameters was plotted against time, linear curves are obtained, and the resulting slopes represent growth rate of the crystals. This is represented as:

dG=dØdt   (3.8)

Where dG is the change in growth and Ø is diameter and t represent time.

To understand and compare the growth rate of PP-H, PP-B and PP-HB, the calculated growth rates of each sample were plotted against their isothermal temperatures.

4   RESULTS AND DISCUSSION

For brevity's sake, graphs and images represented in this section are that of PP-HB except when comparisons are being made on the same graph for all six samples. Graphs and images of the remaining five samples (PP-H, PP-B, PP-R, PP-HR and PP-BR) can be found in the Appendix of this thesis.

4.1   Thermal Analysis

4.1.1   Normal DSC Runs

The normal DSC analysis was performed on the PP samples to determine their crystallization temperatures and melting temperatures. This analysis serves as a preliminary study to understand and know the melting temperatures of the six different PP types and their crystallization temperatures at the heating and cooling rate later on used for the other tests. This is to identify the thermal history of the samples and which temperature ranges would be used during isothermal crystallization analysis in the next stage. In this study, the endothermic peaks which are the melting peaks are up (maxima) whereas the exothermic peaks which are the crystallization peaks are down (minima). The graphs below show the endothermic and exothermic peaks of PP-HB. The endothermic and exothermic peaks were analyzed by extrapolating the peaks using originPro software and the results of the melting temperature and crystallization temperature of PP-H, PP-B, PP-R, PP-HB, PP-HR and PP-BR are tabulated in table 4.1.

Table 4.1 Melting and crystallization Temperatures of PP-H, PP-B, PP-R, PP-HB, PP-HR and PP-BR

PP-type	Melting Temperature (°C)	Crystallization Temperature (°C)
PP-H	164.47	110.18
PP-B	167.8	118.50
PP-R	141.32	104.46
PP-HB	166.11	116.02
PP-HR	163.17	115.73

PP-BR	160.33	116.8

From the table above, the melting temperatures of the samples except for PP-R are within the range of 166.11°C and 160.33°C. The difference in melting temperatures is because of their difference in chain architecture and the presence of comonomers. PP-R has the lowest melting temperature because of its random stereoregularity (E. Martuscelli et al., 1983)**.** The blending of PP-R with PP-H led to a decrease in the melting temperature by 1.29°C whereas the mixing of PP-B with PP-H led to an increase in the melting temperature by 1.67°C and a decrease in the melting temperature of PP-B by 1.69°C. The lowering of the melting temperatures is an indication of the imperfection of the crystals formed after mixing of PP-H and PP-R (Cao et al., 2014). An increase in the melting temperature of the resulting PP-HB can possibly be crystals arrangement of PP-H induced by PP-B (Flory, 1955). Hence, homogeneous mixing of the different PP-types leads to either an increase or decrease in their melting temperatures depending on the types of PPs being blended. The crystallization temperatures of the samples also change when blended. The product of blending PP-H with PP-R had a higher crystallization temperature than the individual constituents. Blending of PP-R with PP-B led to a reduction in crystallization temperature in PP-B with respect to PP-BR and increased in crystallization temperature in PP-R with respect to PP-BR.
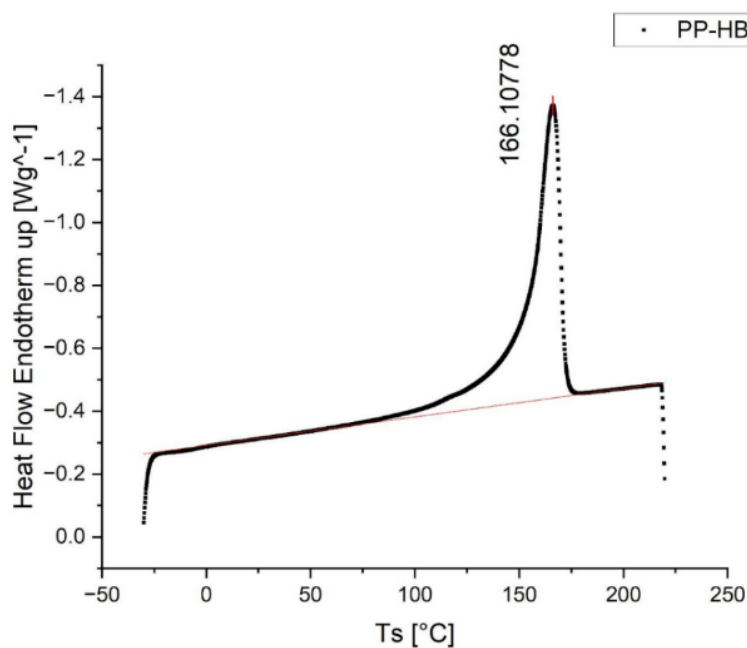
Fig 4.1: Endothermic Melting Peak of PP-HB
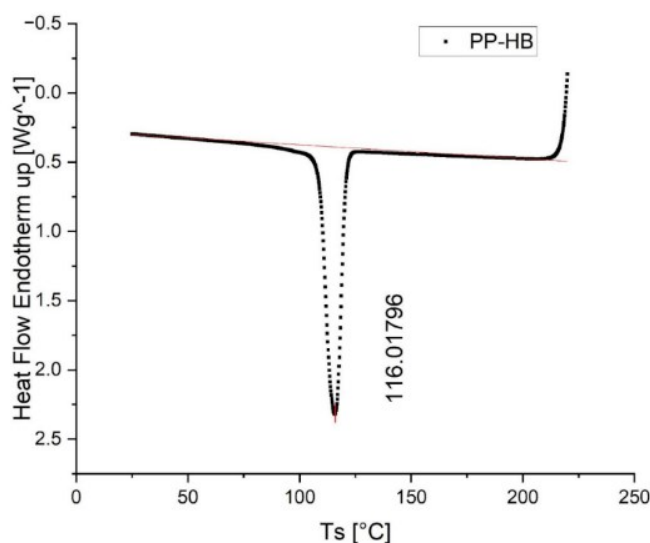
Fig 4.2: Exothermic crystallization curve of PP-HB

4.1.2   DSC runs for Isothermal crystallization Kinetics

Isothermal crystallization kinetics is used to observe the crystal growth of the PP types at constant temperature with varying times. In this study, the peaks usually observed are the exothermic peaks which in this case are represented at a minimum. The exothermic curves are a representation of heat dissipation and the enthalpy of reactions of all six samples are negative representing exothermic reactions and are shown in table 4.2. The chain behavior of polymer molecules with nearby neighboring chains is what causes this exothermic reaction. When the variables influencing the relative positions are favorable, chain mobility and chain arrangement occur. This chain arrangement forms a nucleus by first forming a parallel array and is supported by secondary valence forces that maintain stable molecular packing as the nucleus forms. For the exothermic isothermal curves of the blended samples (PP-HB, PP-HR and PP-BR), they all exhibited single peaks. This shows homogeneity and miscibility of the components of the blends and the absence of phase separation.

The exothermic peaks at different isothermal temperatures (135°C,125°C,120°C,115°C,110°C) experienced a shift towards the right as temperature increases from 110°C to 135°C. This shifting is an indication that as isothermal crystallization temperature increases, the time needed for crystallization to start (induction time) also increases which is in accordance with literature ((Avrami, 1939). The width of the exothermic peaks also broadens as crystallization

temperature increases, this means that at higher temperatures more energy needs to be dissipated for crystallization to occur. This wide width also indicates slow nucleation rate and crystallization kinetics. As the crystallization temperature approaches the melting point, the probability for the occurrence of crystallization becomes slimmer. The isothermal exothermic peaks of PP-HB are represented in figure 4.2.
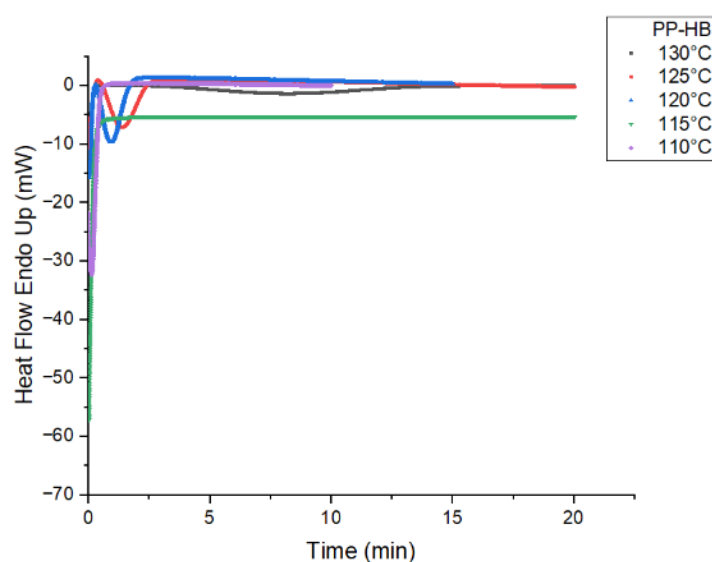
Fig. 4.3: Isothermal crystallization peaks of PP-HB at different isothermal temperature

4.1.3   Relative Crystallinity

As mentioned in the methodology, the relative crystallinity is obtained by integrating the area under isothermal exothermic curves. This integration resulted in a sigmoid-shaped curves which agrees with literatures (Avrami, 1939) .These curves quantitatively describe the evolution of PP crystallinity with respect to time. From these curves, the induction time, time required for crystallization to reach 50% (time to half crystallization) and time needed to reach 100% crystallization can be obtained. From the curve, isothermal temperatures affect formation of crystalline parts over time. As the isothermal crystallization temperature increases, formation of crystalline parts slows down because the degree of supercooling decreases and the PP system exhibits high entropy. This affects the overall time needed for the completion of crystallization, induction time and time needed for half crystallization to occur. The nucleation barrier is also increased because of high entropy and lower degree of supercooling. Due to this, a high amount of energy is needed for nucleation and crystallization to start at higher temperatures explaining the broadening of the peaks with increased in

isothermal temperatures. Conclusively, temperature plays a very important role during isothermal crystallization, an increase in temperature translates to an increase in induction time, an increase in time for half crystallization to occur, an increase in the enthalpy of crystallization and increase in the overall crystallization time (Yang et al., 2018).

Comparing the six PP samples from the Avrami's graph, PP-HR, PP-R and PP-BR have the fastest rate of evolution of crystallinity even at higher temperatures (Yang et al., 2018). PP-R has the lowest melting temperature and nucleating agents, hence it crystallizes fastest amongst the three non-blended PP although at higher temperatures (120°C and 125°C), PP-R lags PP-BR and PP-HR. PP-HR and PP-BR are also nucleated because of the nucleation agents present in the PP-R. These nucleating agents increases the number of nucleating sites in the PP samples accelerating nucleation rates in PP-R, PP-HR and PP-BR (Martuscelli et al., 1980; Martuscelli et al., 1984).
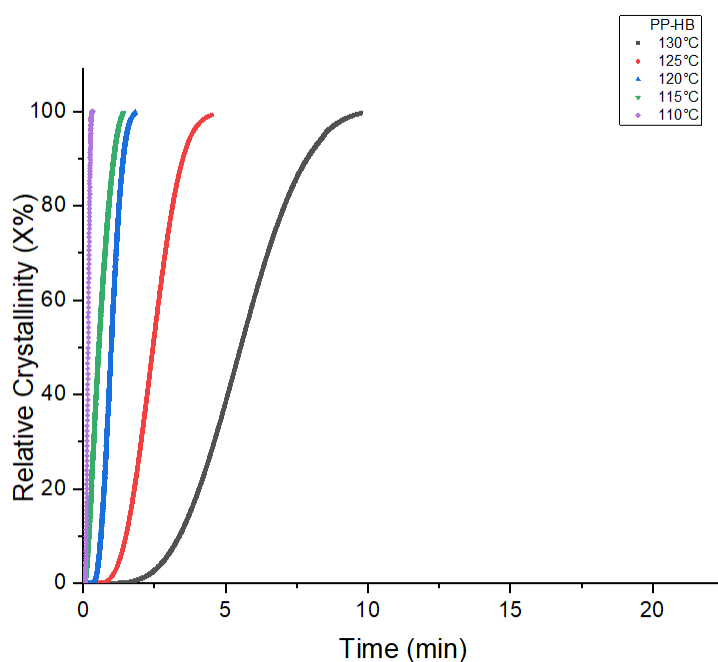
Fig. 4.4: A graph of relative crystallinity with respect to time

4.1.3.1 Avrami Analysis

The obtained sigmoid-shaped graphs are transformed into linear curves for simplification and make analysis easier. The transformed curve is represented in figure 4.5.
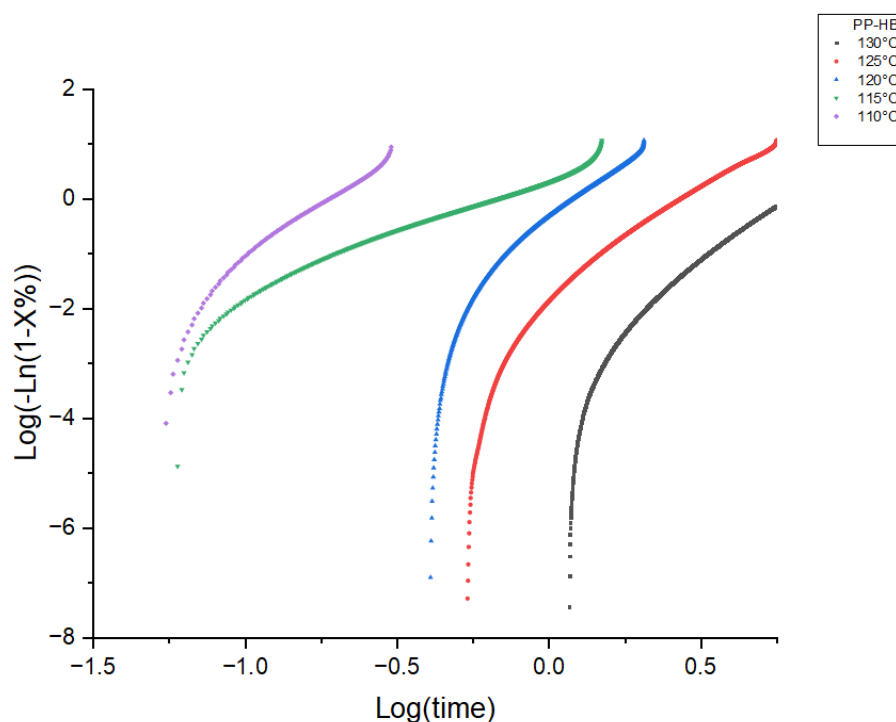
Fig: 4.5: Linear transformation of the Avrami Curve of PP-HB

The transformed Avrami curve is not completely linear. It becomes non-linear at the end of the curve. The graphs are divided into two parts namely primary nucleation and secondary nucleation. The linear part of the graph which is the first part is the primary nucleation whereas the non-linear part is the secondary nucleation. It can be said that the polymer melt undergoes both primary nucleation and secondary nucleation from the graphs above. The slopes of the curve representing the Avrami exponents for all six samples are between 2 and 4. Avrami numbers for polymer crystallization are between 2 and 4 hence the obtained data agrees with literature results (Lu et al., 2002; M. Gordon and I.H. Hillier, 1965). These numbers are represented in table 4.3**.** The Avrami exponents suggest that the geometry of the PP samples is either 2D disc-like or 3D spherulitic crystals.

Table 4.2: Values for Avrami exponent, Nucleation rate constant (K), time for half crystallization ($t_{1/2}$) and induction time (t_0)

PP type	T_c (°C)	Avrami exp. (n)	Log K	K (min)$^{-1}$	t_0 (min)	$t_{1/2, exp.}$ (min)	$t_{1/2, calc.}$ (min)	R^2
PP-B	110	1.859	2.003	100.723	0.002	0.070	0.069	0.992
	115	3.489	1.713	51.624	0.075	0.285	0.291	0.993
	120	3.919	0.289	1.927	0.220	0.753	0.770	0.992
	125	3.884	-1.231	0.059	0.414	1.825	1.888	0.991
	130	4.317	-2.912	1.224×10^{-3}	1.390	4.317	4.421	0.991
PP-HB	110	3.923	2.856	717.794	0.003	0.170	0.170	0.988
	115	2.079	0.414	2.594	0.003	0.555	0.530	0.990
	120	4.083	-0.353	0.443	0.013	0.983	1.116	0.996
	125	3.780	-1.6501	0.023	0.258	2.453	2.462	0.996
	130	4.253	-3.303	4.997×10^{-3}	1.062	5.568	5.485	0.993
PP-H	110	3.735	1.337	21.727	0.043	0.385	0.398	0.990
	115	3.485	0.947	8.851	0.065	0.468	0.472	0.992
	120	3.535	-2.012	9.727×10^{-3}	0.35	3.345	3.343	0.999
	125	2.662	-2.536	2.911×10^{-3}	0.856	7.908	7.814	0.999
	130	3.462	-3.340	4.569×10^{-4}	1.063	9.368	8.926	0.999
PP-R	110	2.344	3.442	2767.70	0.002	0.023	0.010	0.999
	115	4.770	1.277	18.94	0.075	0.500	0.507	0.995

	120	2.465	-0.301	0.500	0.220	0.983	1.004	0.992
	125	3.695	-1.663	0.022	0.414	2.452	2.468	0.991
	130	3.798	3.742	5523.70	1.390	8.297	8.326	0.994
PP-BR	110	3.052	2.892	780.171	0.003	0.098	0.1	0.995
	115	1.667	1.782	60.477	0.002	0.082	0.068	0.992
	120	1.894	1.791	61.759	0.002	0.082	0.093	0.996
	125	3.567	1.693	49.317	0.003	0.298	0.303	0.991
	130	3.900	0.118	1.314	0.258	0.822	0.848	0.999
PP-HR	110	2.293	3.382	2107.677	0.002	0.028	0.030	0.999
	115	1.437	1.824	53.035	0.003	0.04	0.049	0.983
	120	3.213	2.392	246.422	0.003	0.160	0.125	0.998
	125	3.054	1.556	35.977	0.003	0.273	0.274	0.999
	130	3.648	0.016	1.038	0.283	0.875	0.895	0.993

From table 4.2, the PP samples exhibit disc-like shapes at lower crystallization temperatures (110°C and 115°C) and spherulitic structures at higher crystallization temperatures (Hiemenz, 1984).

The intercepts of the curves represent nucleation rate constant (K) which decreases as temperature increases. This means that as isothermal crystallization temperature increases the rate of nucleation decreases which results in a smaller number of nucleation sites.

4.1.3.2   Lauritzen-Hoffman Analysis

The most utilized model for the studies of crystallization kinetics in quiescent melt polymers is the Lauritzen-Hoffman Model (Lauritzen, JR and Passaglia, 1967). As discussed in the experimental section, the Hoffman-Week's linear extrapolation is used for obtaining the equilibrium melting temperature, it is graphically represented for PP-HB in figure 4.6.
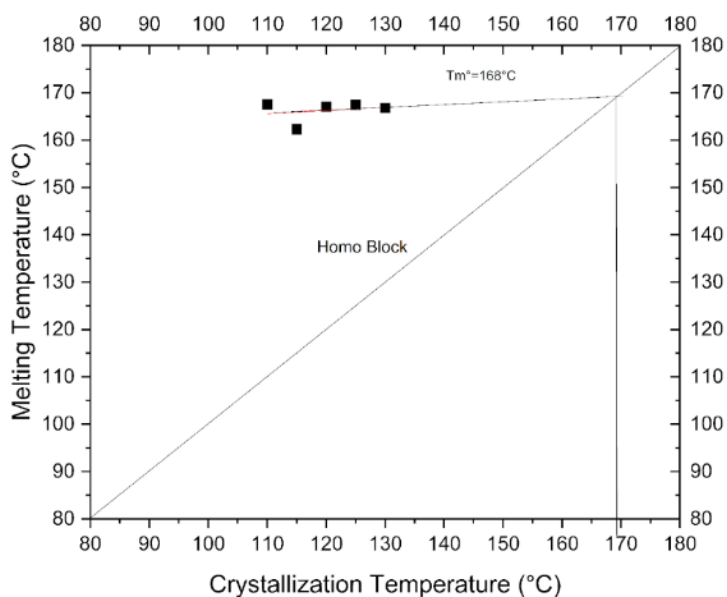
Fig. 4.6: Hoffman Week's Extrapolation for finding Tm° of PP-HB

The LH analysis using the time for half crystallization ($t_{1/2}$) obtained from isothermal crystallization DSC analysis and Growth rate constant (G) from spherulites growth analysis using PLOM and heating stage is graphically shown below.
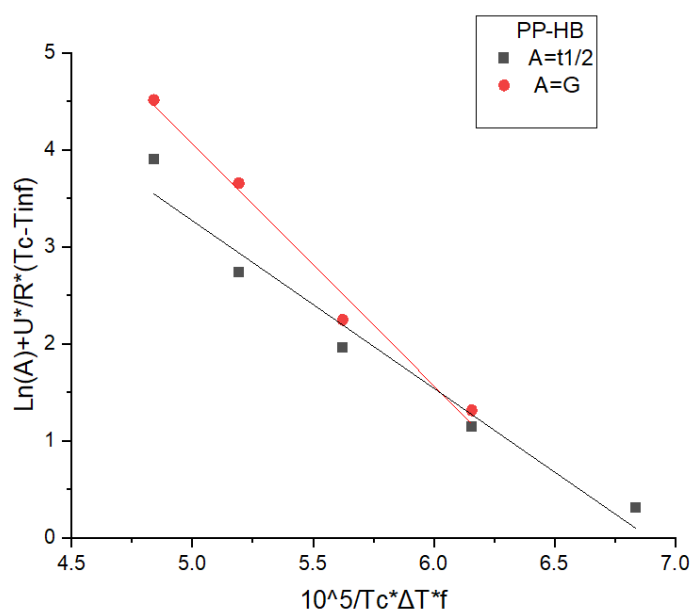
Fig. 4.7: Lauritzen Hoffman representation for finding Go and Kg

The comparison of the two different curves (DSC and PLOM analysis) could not be made for PP-HR, PP-BR and PP-R because they underwent spontaneous nucleation hence their crystals could not grow to a measurable size. This would be discussed in section 4.2. From the LH graphs, the graphs for PLOM and DSC have similar inclinations and slopes although they are not the same. The slight difference in their slope is due to the different methods used in arriving at the same results. Additionally, the isothermal crystallization temperatures used in the two separate experiments differed (PLOM was 120°C,125°C, 130°C and 135 °C whereas DSC 110 °C, 115 °C, 120 °C,125 °C and 130 °C). This difference in temperature was because during the PLOM experiment, extremely low temperatures could not be achieved because of the cooling rate used which was the same cooling rate for the DSC experiment. Hence, the slopes were not the same but similar so it can be argued that $G^{DSC} \approx G^{PLOM}$ although there were slight differences in the values. These values are represented in table 4.4

Table 4.3: Kg and Go values for PP types from PLOM and DSC analysis

Values	Homo	Homo Block	Block
Kg from DSC *10^5 (K^2)	2.18	1.20	1.50
Kg from PLOM *10^5 (K^2)	2.75	1.72	2.76
Go from DSC (μm/s)	15.54	11.73	12.45
Go from PLOM (μm/s)	14.68	11.91	16.40

The values of Kg in all PP-types are in the range of literature values (Clark and Hoffman, 1984; Hao et al., 2019). PP-HB has the lowest Kg values for both DSC and PLOM measurements, an indication of increasing crystal growth upon addition of PP-B (Hao et al. 2019). The surface growth energy of the crystal (σ_e) can be calculated if the regime in which secondary nucleation and crystallization occurs is accurately known. In this experiment, the regime is predicted to be from Regime II→Regime III due to the degree of supercooling (34K and 54K) of the crystallization and also the Kg values obtained in comparison to literature (Clark and Hoffman 1984). The nucleation constant of PP-H in both PLOM and DSC is the highest amongst the three PP types and are 2.18 and 2.75 respectively whereas PP-HB had the lowest nucleation constant. The reduction of Kg in PP-HB indicates a decrease in the energy required to form the critical nucleus of the spherulites hence fast nucleation rate is favored in PP-HB

compared to PP-H and PP-B (Kocic et al., 2012). The DSC method and PLOM method are all used for LH analysis. However, to get precise and accurate results, it is highly recommended to use the DSC. The DSC provides quantitative results specifically enthalpy of fusion, enthalpy of crystallization, melting temperature and crystallization temperature on the crystallization kinetics of PP whereas PLOM only provides qualitative results focusing on just the spherulite growth rate and through visual analysis of the growth of the spherulites. Again, in terms of accuracy and precision, DSC produces more accurate and precise results as compared to PLOM because during analyzing with the PLOM human errors can occur when measuring the spherulite growth and the time.

4.1.4   Activation energy

The activation energy is the energy needed to overcome nucleation barrier for crystallization to commence. From the bar graph below, random PP has the highest activation energy of 359.0kJ/mol which is not in accordance with literature and its overall molecular structure. PP-R should have had the lowest activation energy because it is highly nucleated and has a low melting temperature hence the energy needed to overcome nucleation would be low. The high value in PP-R may be as a result of human error or operational error on the part of the DSC. PP-HR and PP-BR have the lowest activation energy of 191.3kJ/mol and 142.5kJ/mol respectively due to the possible presence of high amount of nucleating agents or the nucleating effect of the random polymer in the PP-H and PP-B which reduces the activation barrier of the PP-types. PP-B had the highest activation energy (255.320kJ/mol) followed by PP-H (217.324kJ/mol) whose activation energy is closer to that of PP-HB (215.553kJ/mol). The activation energy of PP-B is highest because of its molecular structure (Li et al., 2002). The presence of ethylene comonomers bonding with propylene monomer in PP-B in addition to its alternating molecular structure provides stronger intermolecular bonds in the PP-B leading to a more stable structure in comparison to PP-R and PP-H. This means more energy is required for crystallization reaction to occur. Activation energy and crystallization reaction are mutually dependent on each other, this is because for crystallization reaction to occur, the activation energy barrier must be overcome. However, a polymer can have a low activation energy barrier and slow crystallization and vice versa although the in the case of PP-HR and PP-BR they both had low activation energies and fast crystallization rates due to the presence of nucleating agents in PP-R. PP-H had a slow crystallization rate yet a low

activation energy whereas PP-B had a faster crystallization rate yet a high activation energy. The activation energies of different PP types vary with different literatures, because this value is affected by several factors such as processing conditions, grade of PP and crystallization conditions, hence there are no exact values or ranges to describe the exact activation energy of the PP and its blends.
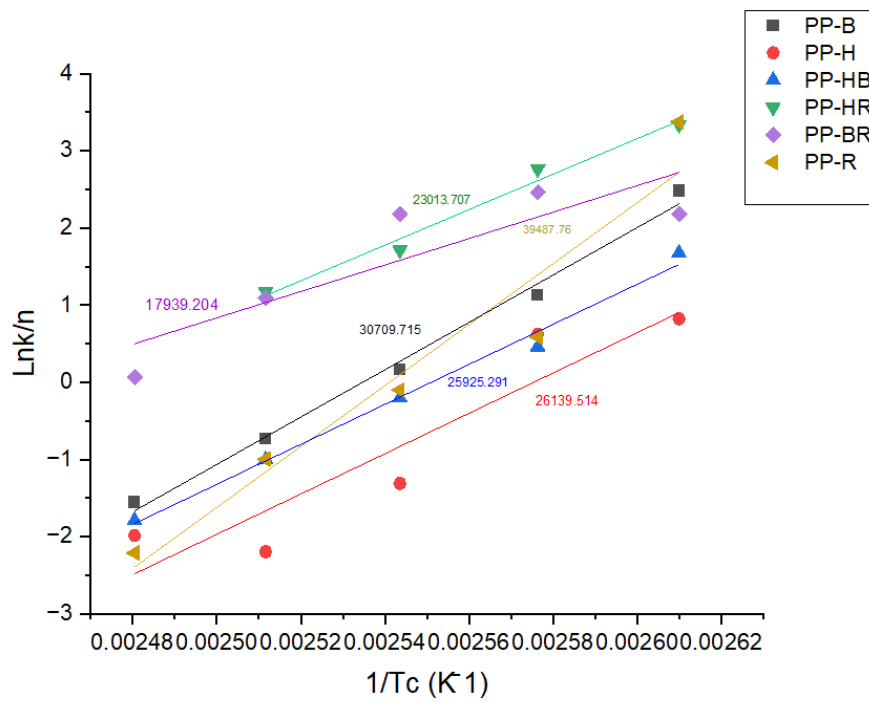
Fig. 4.8: Plot of Lnk/n versus 1/Tc to determine activation energy of PP types
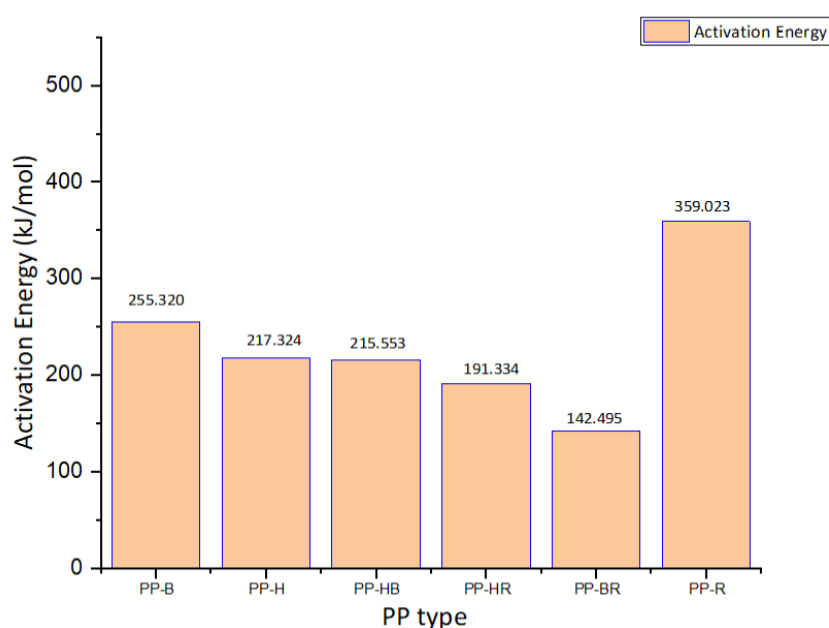
Fig. 4.9: Activation energies of PP and its blends

4.2   Spherulite structure

In molten state (210°C), there was no observable segregated phases of propylene-ethylene in the block and homo block melts in the liquid-liquid phase, this shows that the optical microscope cannot capture the domain dimension of the liquid-liquid phase since the dimension is very nanoscopic and too small for the resolution of the optical microscope to capture. At specific isothermal temperatures and their induction times, the spherulites begin to appear from the melt and we can see a distinct separation between the liquid phase and the solid phase. However as time elapses there is a disappearance of the liquid domain in favour of the solid domain indicating spherulite growth and also crystallization approaching termination. This behaviour is in agreement with Avrami review work on phase transformation during crystallization of melt (Avrami, 1939).

The crystals seen in the PP melts and their blends possess a spherical geometry hence the crystals can be referred to as spherulites. In terms of the type of spherulite growth of all three samples under the isothermal temperatures of 120 °C, 125 °C, 130 °C and 135°C, there were all category one growth since the growth started from the centre (nucleus) and spred radially from the nucleation site (Gránásy et al., 2005). It could also be observed that during crystal growth, the intensity of the polarized light interacting with the polymer melt increases as the

spherulites grow, this is because the polymer chains in the spherulites aligns in a regular pattern which refracts the polarized light along the directions of the aligned chains as it passes through it whereas the random orientation of chains in the melt at high temperature diffuses polarized light reducing the intensity of the light. The spherulites in all three samples exhibited birefringence due to their dual colors exhibition of blue and yellow perpendicularly inclined to each other, this hints that PP homo, PP Block and PP Homo Block have anisotropic properties (Handbook of Polymer Crystallization, 2013). In terms of the type of birefringence, the spherulites block PP exhibits negative birefringence whereas most of the spherulites of homo PP exhibit positive birefringence although the birefringence of about 10% of its spherulites are unknown due to the irregular color patterns. The spherulites of PP-HB had a uniform spherulite distribution of both positive and negative spherulites, this indicates that the melt is a blend of both PP-H and PP-B.

In the blends of the Homo and Block PP there was no inter spherulitic region whereby the spherulites of the Homo and Block PP separated which is indicated by tight impingement of the spherulites, hence the phase was a singular miscible phase indicating that there was coalescence between the blends. The PP-HB sample exhibits co-crystallization due to the absence of separate phases and miscibility of the PP-H and PP-B (Pracella, 2013). Hence, it appears that PP-H and PP-B can be blended to achieve a single-phase polymer system in equal ratios (50:50) during PP recycling.

PP-H spherulite has a star branched morphology whereas PP-HB and PP-B has a regular maltese cross patterns at high temperatures (135ºC and 140ºC) and irregular maltese pattern at lower temperatures. This maltese morphology is due to folding of polymer chains in a regular pattern to form lamellae during crystallization in the spherulite whereas the star branched chain morphology is because of chain branching which is caused by screw dislocations during crystal growth. The isothermal crystallization temperatures also affect the texture, size and shape of the spherulites in all the PP samples. At higher temperatures (140 ºC and 135ºC), the spherulites have fine texture, bigger size and an almost symmetrical spherical shape. This is because spherulite growth at this temperature is non-spontaneous and takes enough time for the PP spherulites to orient into their original shapes. At lower temperatures, spherulites possess smaller sizes, irregular spherical shape and coarser texture. This is as result of nucleation and growth being instantaneous and sporadic in this region

hence the spherulites do not take enough time to grow. Via visual observations, we infer that the nucleation density of the PP samples decreases with increasing crystallization temperature i.e. the number of nuclei formed in the volume of the melt. This is because at lower temperatures, the melt has lower entropically level and low supercooling hence less energy is required to overcome nucleation barrier encouraging the formation of more nuclei during crystallization whereas at higher temperatures, the nucleation density is low due to melt having high entropy and high supercooling making it difficult to form nuclei. The spherulites growth of PP-HB are represented in the figures below.
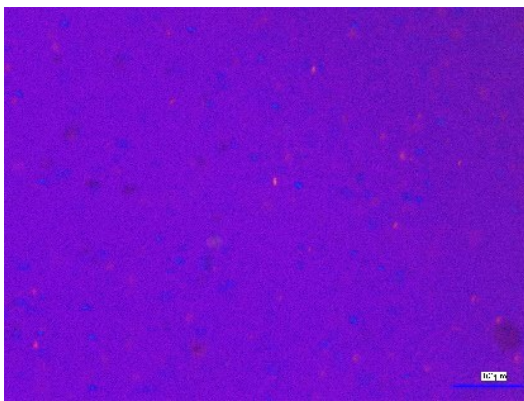
t= 2s

t= 5s
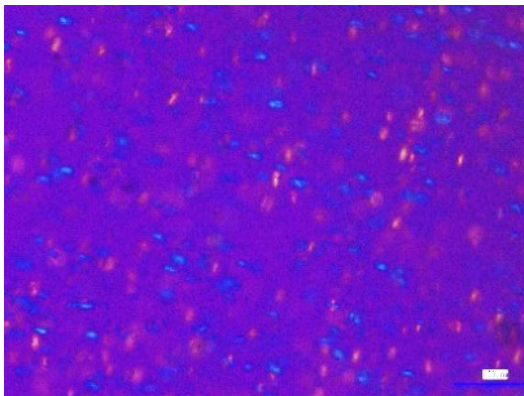
t= 15s
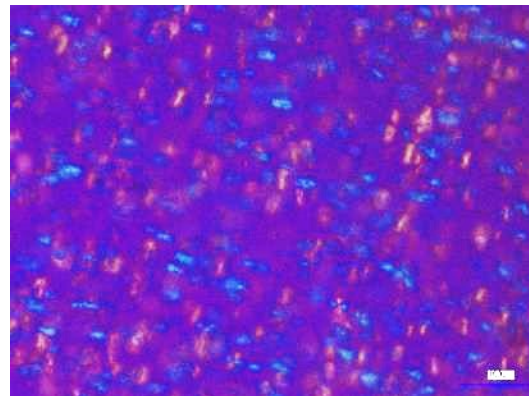
t= 24s
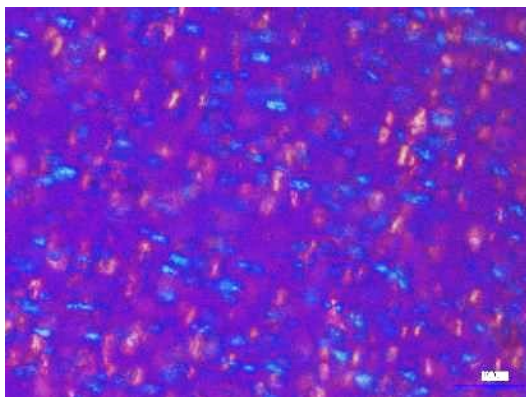
t=60s

Fig. 4.4.100: Growth of Spherulites of Homo Block PP observed under the Polarized Optical Microscope at specific intervals at 125°C
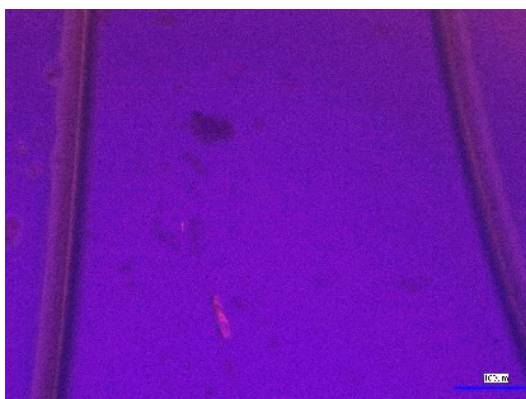
t=4s

t=20s
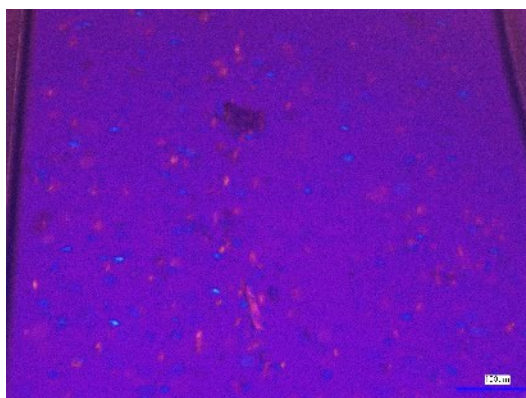
t=30s
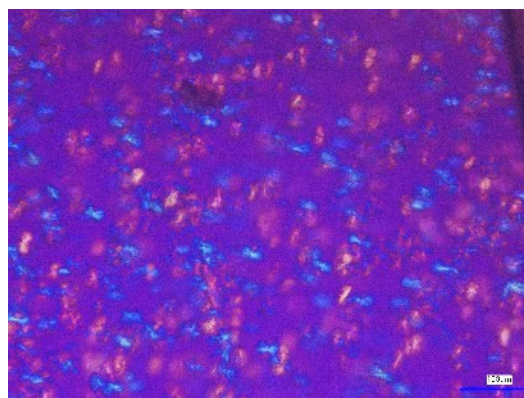
t=60s
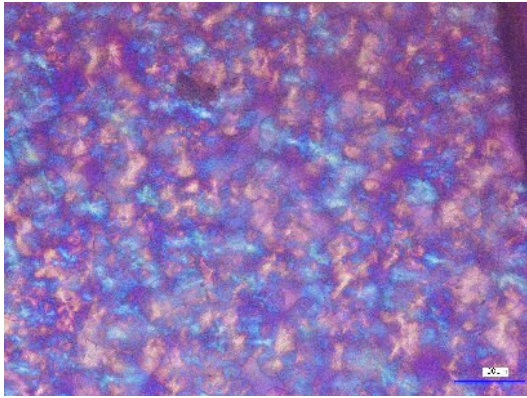
t=120s

Fig.4.11: Growth of Spherulites of Homo Block PP observed under the Polarized Optical Microscope at specific intervals at 130 °C
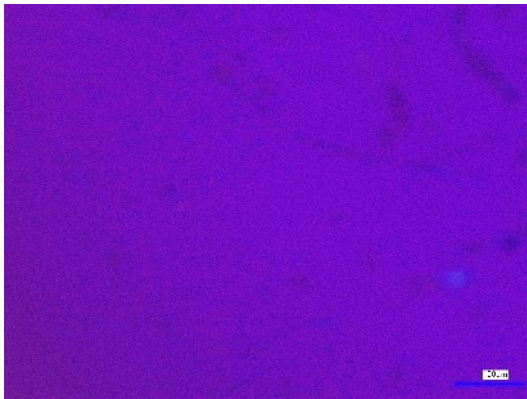
t=20s
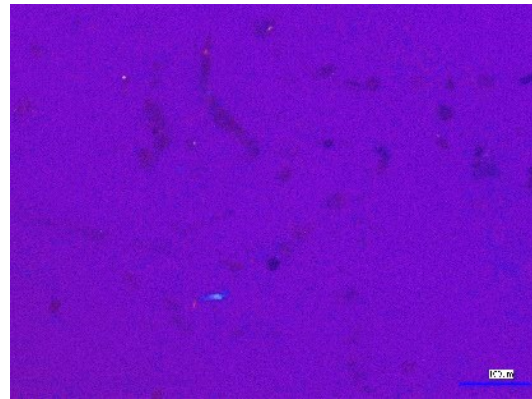
t=30s
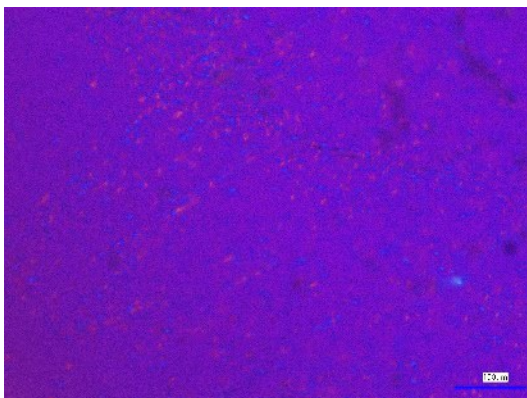
t=60s
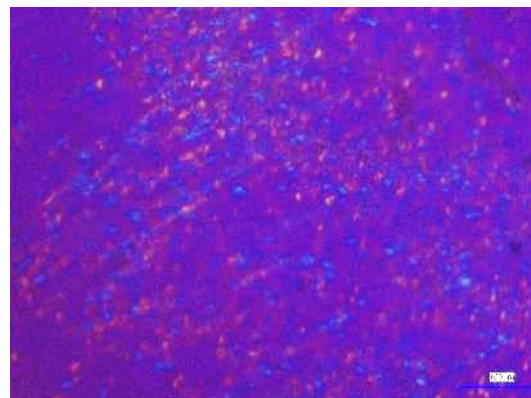
t=120s
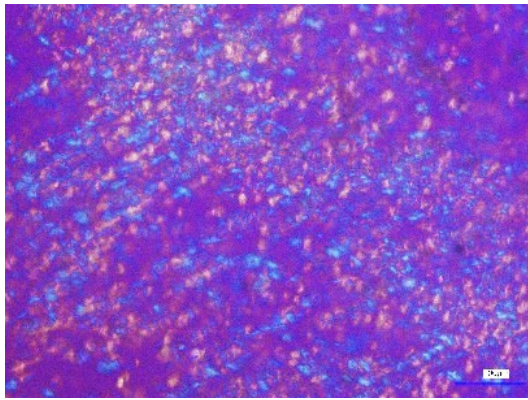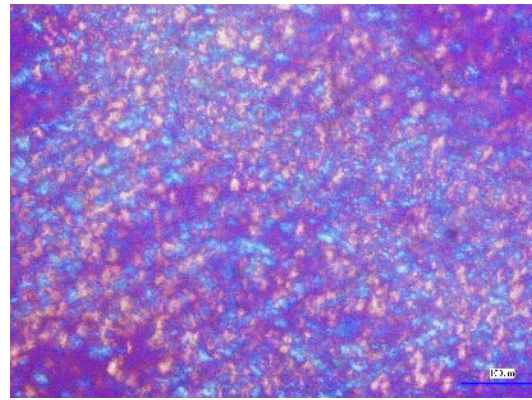
t=180s   t=240s

Fig. 4.12: Growth of Spherulites of Homo Block PP observed under the Polarized Optical Microscope at specific intervals at 135 °C
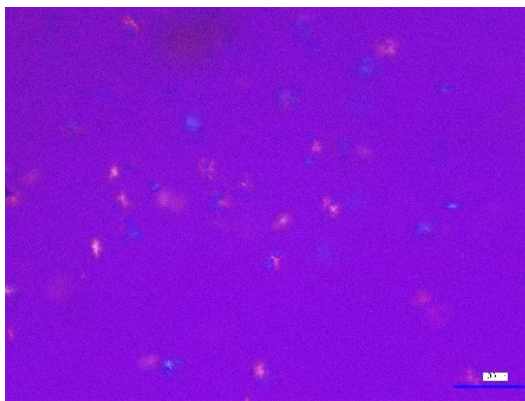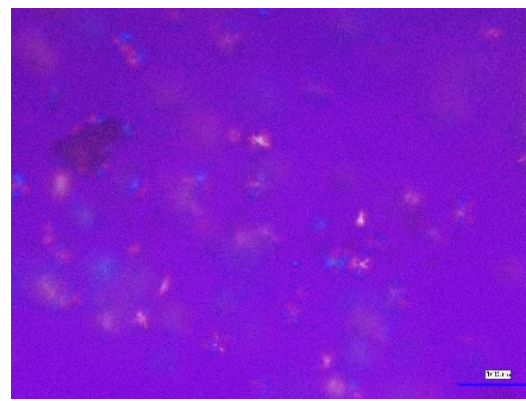
t=600s   t=900s
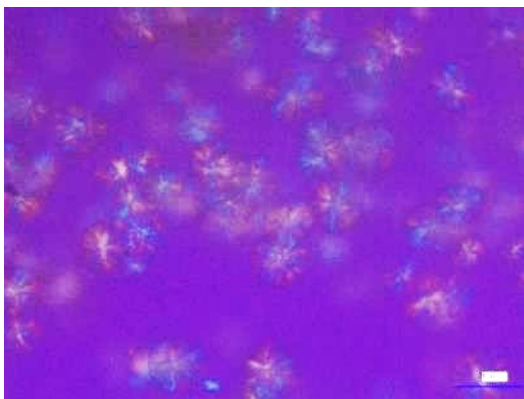
t=1200s   t=1800s
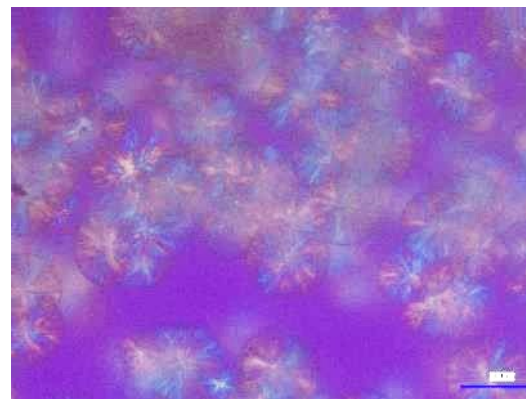
t= 2400s   t=3000s
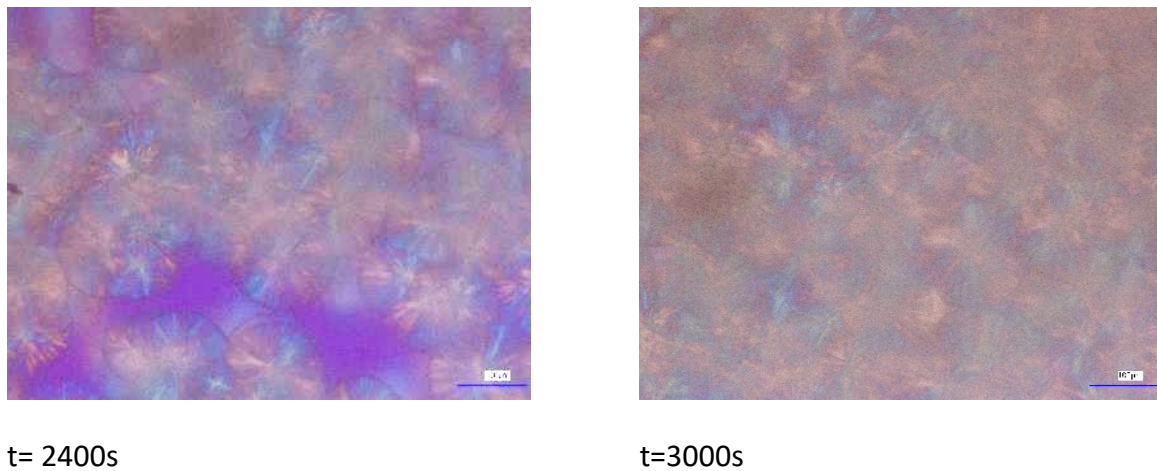
Fig. 4.13: Growth of Spherulites of Homo Block PP observed under the Polarized Optical Microscope at specific intervals at 140 °C

4.3   Spherulite Growth Rate

The average diameters of measured spherulites of PP-H, PP-B and PP-HB were plotted against time and represented in the graphs below. The graphs representing the growth for PP-H, PP-HB and PP-B were all linear graphs which means that the spherulites exhibited a constant growth rate under all isothermal temperatures. The radial growth rate for all three samples decreases with an increased in crystallization temperature due to enthalpic and entropic contributions. According to Gibbs Free energy (Raka and Bogoeva-Gaceva, 2008), an increase in crystallization temperature leads to an increased in entropy and the energy needed to crystallize the polymer melt increases leading to less negative Gibbs Free energy hence crystallization in the system becomes difficult to reach. Comparing all three samples, Homo PP has the slowest crystallization rate within the isothermal temperature range of 125°C to 130°C and Homo Block and Block had similar growth rate. This may be because of the presence of the ethylene comonomers in the Homo Block and Block PP acting as nucleating agents or sites in the PP to help in crystallization (Yanjie An et al., 2019). Another possibility is that the presence of the ethylene comonomer in PP-B and PP-HB reduced the viscosity of the melts helping crystallization to occur faster (Yaping Ma et al., 2021)**.** Finally, there may be a possibility of the effect of processing conditions of the samples, since the samples were already preformed before cut, we can argue that processing parameters such as screw shearing of the injection molding machine, holding time and pressure and most importantly the presence of nucleating agents could affect the crystallization growth of the PP and its

blends. However, at higher temperatures, the growth rate of PP-HB blends was the slowest. The table and graphs below represent the growth rate of the samples.

PP-HR and PP-BR were highly nucleated hence small sized spherulites were instantaneously formed and crystal growth was hardly observed. This is because of the high nucleation density in the PP-HR and PP-BR which created several nucleation sites and smaller nuclei sizes. Hence, the nucleus of the crystals could not overcome their critical radii leading to spontaneous nucleation in the melt (Sihan Wang et al., 2005). Therefore, the spherulite size of PP-HR and PP-BR cannot be controlled during crystallization regardless of the isothermal crystallization temperature. This means that, if spherulite size control is the goal, highly nucleated PP-R should not be blended with PP-H and PP-B.
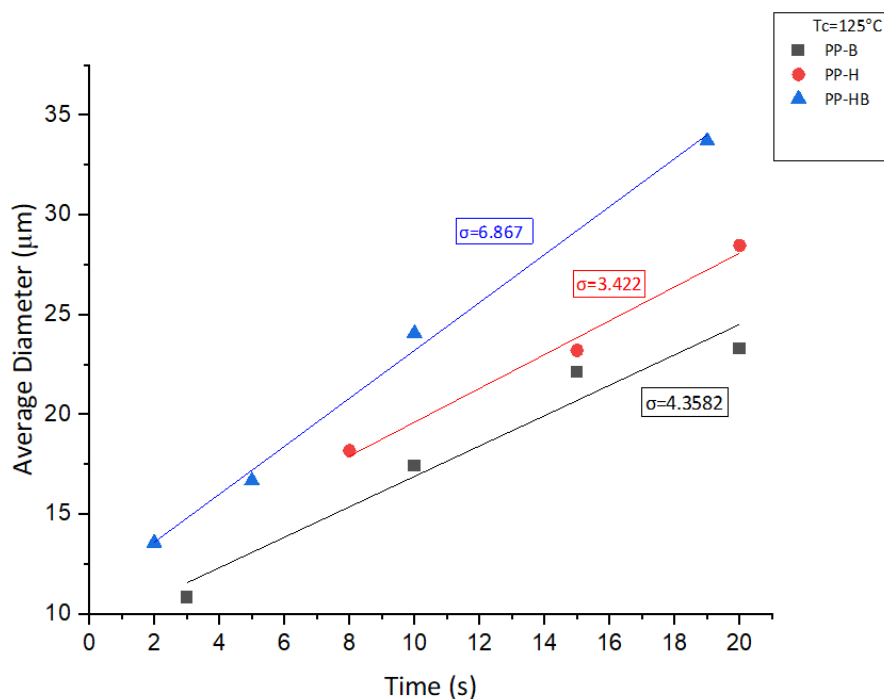
Fig. 4.14: Average diameter versus Time at isothermal temperature 125 °C
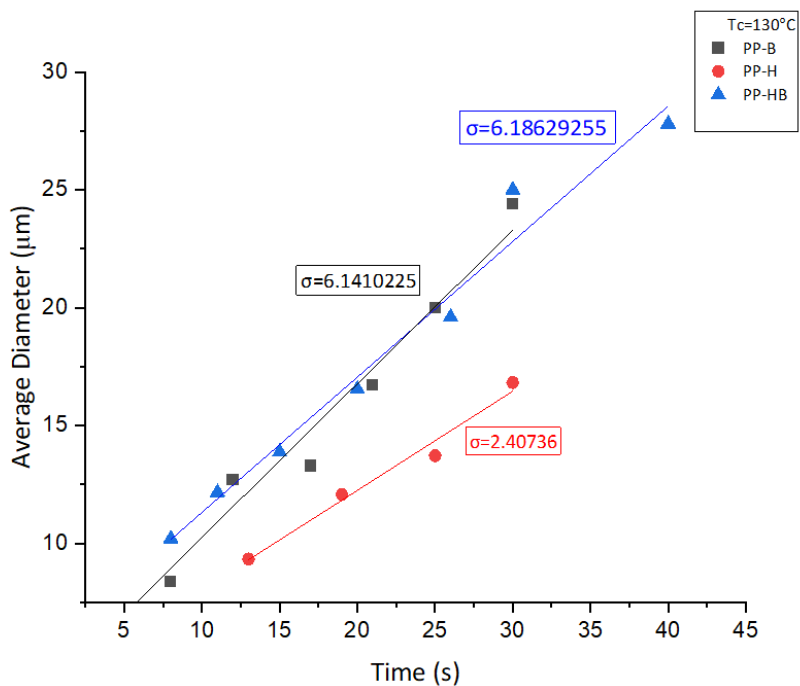
Fig. 4.15: Average **d**iameter versus Time at isothermal temperature 130 °C
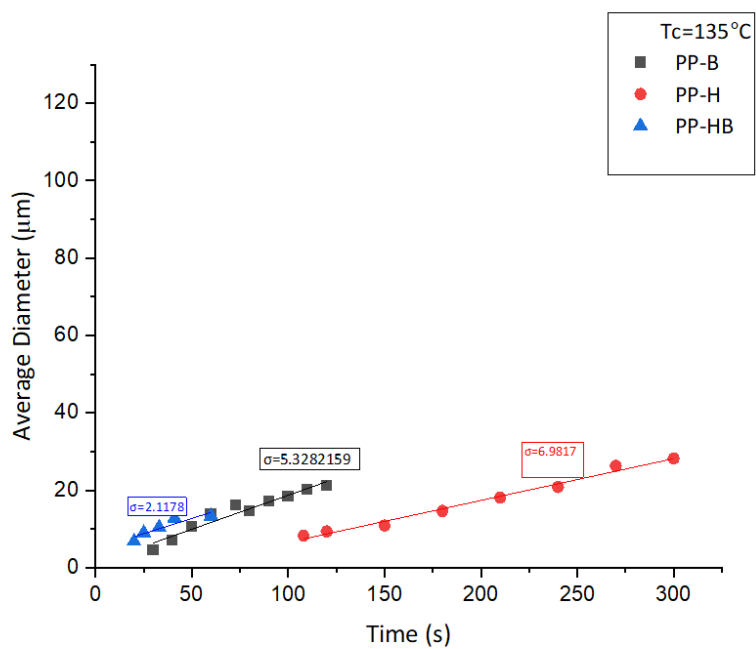
Fig 4.16: Diameter versus Time at isothermal temperature 135 °C
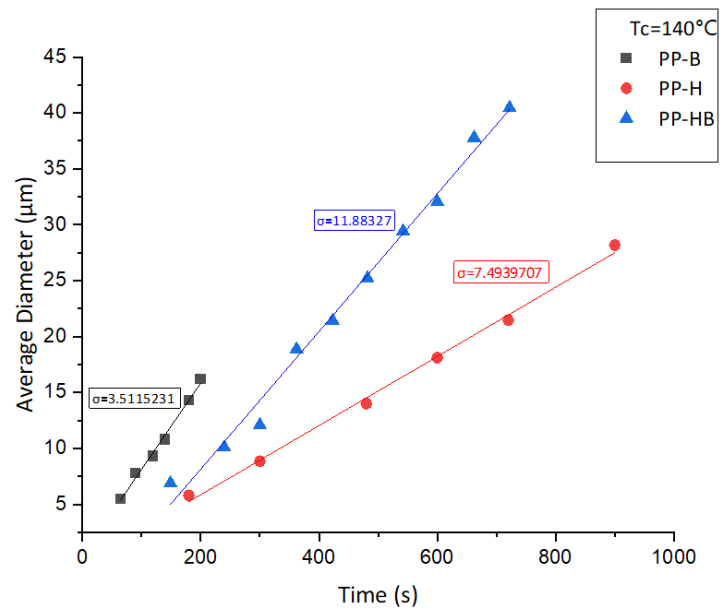
Fig. 4.17: Diameter versus Time at isothermal temperature 140 $^{\circ}$C

Table 4.5: Growth rates for Homo, Block and Homo Block at different isothermal crystallization temperature

Temperature ($^{\circ}$C)	Growth Rate (μm/s)	Growth Rate (μm/s)	Growth Rate (μm/s)
125	1.25204	0.84771	1.20085
130	0.52191	0.42095	0.57467
135	0.17489	0.10809	0.1574
140	0.10209	0.06165	0.03094
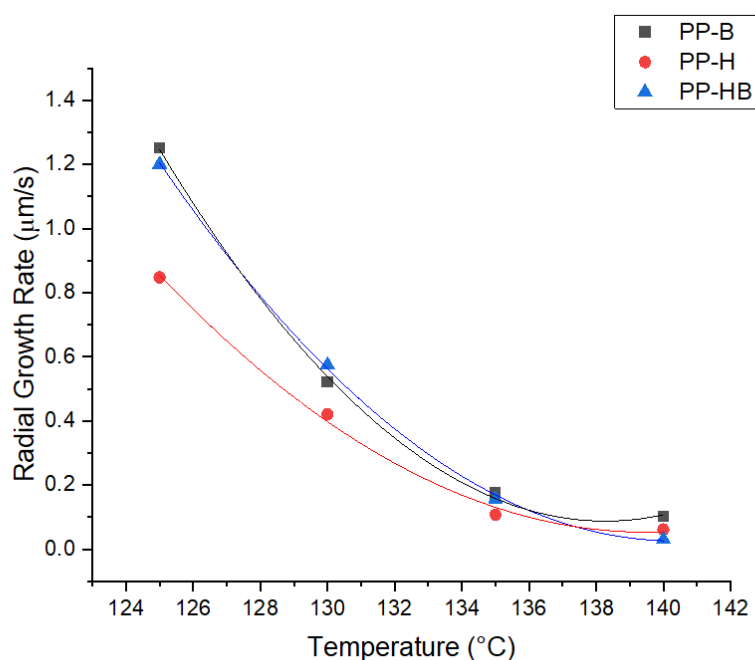
Fig. 4.18: Radial Growth Rate with respect to temperature

The graph above is a plot of growth rate with respect to isothermal crystallization temperature. The radial growth rate versus temperature curve if measured to extremely low isothermal crystallization temperatures of about 10°C requiring very high cooling rates would have a down bell curve. The graph above is a representation of the downward slope part of the curve which is similar to literature (Huang et al., 1994) . This is because the cooling rate of the Leica RM 2255 heating stage had a cooling rate limit of 50°C/ s and the refrigerated water coolant used could not rapidly cool to an isothermal temperature below 125°C without spherulite forming through the cooling process. To achieve an extremely low isothermal crystallization temperature, the cooling rate must be very fast above 50°C/s.

Crystallization temperature plays a vital role in growth rate of spherulite. From the graph, as crystallization temperature increases the growth rate of PP decreases because crystals formation is very difficult at high supercooling **.** And at high temperatures, nucleating sites are fewer hence spherulites take a lot of time and energy to grow and impinge each other. At a lower temperature of 125°C, due to low supercooling resulting in decreased in enthalpy of crystallization, several nucleating sites are formed within few seconds with smaller sizes and this is translated to high radial crystal growth rate.

Overall, the crystallization rate of PP-H was the slowest amongst the three samples which is in accordance with results obtained from LH theory and Avrami analysis. PP-B and PP-HB had intercepting radial growth rate at 135°C, the closeness in the growth of curves of PP-B and PP-HB indicates that both samples exhibit similar growth rate. When PP-B is blended with PP-H to form PP-HB its growth rate is improved.

5   SUMMARY, CONCLUSIONS AND OUTLOOK

In summary, the spherulite growth, spherulite growth rate and the overall crystallization kinetics of PP and its blends were studied using Polarized Optical Microscope coupled with heating stage and Differential Scanning Calorimetry under isothermal conditions. The results from these characterization techniques were analyzed using Avrami Model of crystallization, Lauritzen Hoffman Secondary Crystallization Model and Arrhenius equation to investigate Relative crystallinity with respect to time, to observe and predict the geometry of the crystals formed under specific isothermal conditions and their growth rates and finally to calculate the activation energy needed for crystallization to start in the different PPs inclusive of nucleation, growth and overall crystallization parameters.

The spherulite growth and crystallization kinetics of PP-B, PP-R, PP-H, PP-HB, PP-BR and PP-HR were investigated. The DSC exothermic peaks of the blends recorded only single peaks, an indication of the miscibility of the blends. The observation of the melt of the different types of PP and it blends under Polarized Optical Microscope during crystallization showed that they are geometrically spherical and disc like dependent on the maxima or minima of their crystallization temperatures which was confirmed through Avrami analysis. The size and texture of the spherulites grown from the melting of PP and its blends were also dependent on the crystallization temperatures with the size increasing with elevated crystallization temperatures. The blend of the PP-B and PP-H i.e. PP-HB had no distinct separate spherulite phases when observed under the Polarized Microscope indicating interpenetrating co-crystallization of the blends however the blends of PP-HR and PP-BR underwent spontaneous crystallization immediately, they reached their crystallization temperatures (140 °C, 135 °C,130 °C,125 °C) an indication of the presence of nucleating agents. Due to this spontaneous crystallization, only nucleation occurred in the melt and no observable growth of the nuclei was observed due to the high nucleation density of the melt of the PPs on the onset of crystallization. The spherulite growth rate of PP-H was shown to be the slowest whereas PP-B and PP-HB exhibited similar growth rates both in DSC analysis and PLOM analysis. The Avrami equation and its curves were used to predict the increase of crystallinity with respect to time at different isothermal temperatures and from the results higher isothermal temperatures gives slower evolution of crystallinity whereas lower isothermal temperatures

lead to faster evolution of crystallinity. Amongst the six samples, PP-H had the highest time to half crystallization followed by PP-B this indicates that PP-H crystallizes the slowest, PP-R, PP-BR and PP-HR had the lowest time to half crystallization indicating that they have relatively fast crystallization rate. The Avrami exponents of all six samples predict that they had spheres and disc like geometries depending on the crystallization temperature which was backed by the observation under the PLOM. The Lauritzen Hoffman equation was used for both DSC and PLOM calculations to understand the crystallization kinetics of PP and its blends and the Arrhenius equation was used for the calculation of the activation energy. The blending of PPs improved the crystallization growth rate, reduced activation energy needed to overcome nucleation barrier. In terms of crystal morphology, PP-HB showed no separation between its constituents indicating miscibility and co-crystallization of PP-H and PP-HB. In the case of PP-HR and PP-BR, the spherulite size could not be studied because of instantaneous nucleation leading to formation of several small nuclei sizes. Comparing the two characterization methods i.e. PLOM with heating stage and DSC, PLOM should be an option when studying in-situ crystals growth during polymer crystallization and morphology of polymer crystals as they grow whereas DSC should be an option when study the kinetics of crystallization.

In conclusion:

1) Crystals growth rate is dependent on the molecular architecture of the chains and the isothermal temperatures of PP and their blends.

2) To optimize PP and its blends spherulite size and morphology during recycling and processing into final products, temperature control is a very important parameter.

3) The spherulite size, induction time and time needed for half crystallization increases as isothermal crystallization temperature decreases nucleation rate and nucleation density can be controlled by crystallization temperatures during processing.

4) The blends of PP were miscible hence they can be mixed in specific percentages for PP recycling.

5) The Lauritzen Hoffman equation helped to determine the crystallization kinetics in both PLOM and DSC and the parameters obtained i.e. Go and Kg can be used to investigate the surface energy and chain folding energy of the PP samples if specific parameters such as chain folding energy, surface energy, width and length of the are known.

6) The Avrami exponent can be used to predict the geometry of the spherulite of PPs and their blends and are mostly between 2 and 4.

Further studies can be done on the blends by varying the blend ratios of block and random PP in the homo polymer to investigate how different ratios affect the spherulite growth rate and crystallization kinetics of blends, this would help recycling scientists and engineers to optimize blends ratios during processing. Again, the mechanical properties of the PP and its blends can be studied on a microscale to develop a relationship between blends proportion, crystallization kinetics and the mechanical properties of the blend to know which type of PP and blends to use for specific applications. Non-isothermal crystallization studies can also be performed on the PP and its blends to study their crystallization kinetics and spherulites growth rate under different cooling rates using Nakurama theory and Ozawa model

6   LITERATURE

Alamo, R. G. and Mandelkern L., "The crystallization behavior of random copolymers of ethylene", Thermochimica Acta, **238**, 155 – 201 (1994), DOI:10.1016/S0040-6031(94)85210-3

Arai, F., Shinohara, K., Nagasawa, N., Takeshita, H., Takenaka, K., Miya, M. and Shiomi, T., "Crystallization behavior and higher-order structure in miscible crystalline/crystalline polymer blends", Polymer Journal, **45**, 921 – 928 (2013), DOI:10.1038/pj.2013.5

Ariff, Z., Ariffin, A., Jikan, S. and Abdul Rahim, N., "Rheological Behaviour of Polypropylene Through Extrusion and Capillary Rheometry", p. 29 – 48 (2012)

Avrami, M., "Kinetics of Phase Change. I General Theory", The Journal of Chemical Physics, **7**, 1103 – 1112 (1939), DOI:10.1063/1.1750380

Avrami, M., "Kinetics of Phase Change. II Transformation-Time Relations for Random Distribution of Nuclei", The Journal of Chemical Physics, **8**, 212 – 224 (1940), DOI:10.1063/1.1750631

Avrami, M., "Granulation, Phase Change, and Microstructure Kinetics of Phase Change. III", The Journal of Chemical Physics, **9**, 177 – 184 (1941), DOI:10.1063/1.1750872

B. Malpass, D. and Band, E. I., Introduction to Industrial Polypropylene. Properties, Catalysts, Processes, Scrivener Publishing LLC; John Wiley & Sons, Inc, Hoboken, New Jersey, Salem, Massachusetts (2012)

Bao Wang, 03/20/2020, "Heterogeneous Nucleation in Semicrystalline Polymers". Dissertation, University of Genova, Genova

Bassett, D. C., Frank, F. C. and Keller, A., "Lamellae and their Organization in Melt Crystallized Polymers", Philosophical Transactions: Physical Sciences and Engineering, **348**, 29 – 43 (1994)

Benarab, A., Blázquez-Blázquez, E., Krache, R., Benavente, R., Cerrada, M. L. and Pérez, E., "Composites of a Polypropylene Random Copolymer and Date Stone Flour: Crystalline Details and Mechanical Response", Polymers, **13** (2021), DOI:10.3390/polym13172957

Binhong Lin, Devin Lawler, Gregory P. McGovern, Christopher A. Bradley and Christopher E. Hobbs, "Terminal functionalization of atactic polypropylene: a new soluble polymer support", Tetrahedron Letters, **54**, 970 – 974 (2013), DOI:10.1016/j.tetlet.2012.12.046

Blázquez, J. S., Romero, F. J., Conde, C. F. and Conde, A., "A Review of Different Models Derived from Classical Kolmogorov, Johnson and Mehl, and Avrami (KJMA) Theory to Recover Physical Meaning in Solid-State Transformations", physica status solidi (b), **259** (2022), DOI:10.1002/pssb.202100524

Bryan B. Sauer and Benjamin S. Hsiao, "Effect of the heterogeneous distribution of lamellar stacks on amorphous relaxations in semicrystalline polymers", Polymer, **36**, 2553 – 2558 (1995), DOI:10.1016/0032-3861(95)91200-Q

Bu, H., Pang, Y., Song, D., Yu, T., Voll, T. M., Czornyj, G. and Wunderlich, B., "Single-molecule single crystals", J. Polym. Sci. B Polym. Phys., **29**, 139 – 152 (1991), DOI:10.1002/polb.1991.090290201

Bunn, C. W. and Alcock, T. C., "The texture of polythene", Trans. Faraday Soc., **41**, 317 (1945), DOI:10.1039/tf9454100317

Burnett, B. B. and McDevit, W. F., "Kinetics of Spherulite Growth in High Polymers", JOURNAL OF APPLIED PHYSICS, **28**, 1101 – 1105 (1957), DOI:10.1063/1.1722586

Busico, V., "Microstructure of Polypropylene", Progress in Polymer Science, **23**, 443 – 533 (2001)

C. Virone, J.H. ter Horst, H.J.M. Kramer and P.J. Jansens, "Growth rate dispersion of ammonium sulphate attrition fragments", Journal of Crystal Growth, **275**, e1397-e1401 (2005), DOI:10.1016/j.jcrysgro.2004.11.167

Cao, X.-W., Lin, H., Luo, J., He, G.-J., Zhang, Y.-J. and Xu, B.-P., "Comparison Study on CO2-Promoted Crystallization and Melting Behavior of Polypropylene: Homopolymer and Copolymers", Journal of Macromolecular Science, Part B, **53**, 1726 – 1738 (2014), DOI:10.1080/00222348.2014.966892

Chen, F., Qiu, B., Shangguan, Y., Song, Y. and Zheng, Q., "Correlation between impact properties and phase structure in impact polypropylene copolymer", Materials & Design, **69** (2015), DOI:10.1016/j.matdes.2014.12.052

Chitoshi Nakafuku, "High Pressure Crystallization of Poly(L-lactic acid) in a Binary Mixture with Poly(ethylene oxide)", Polymer Journal, **26**, 680 – 687 (1994)

Clark, E. J. and Hoffman, J. D., "Regime III crystallization in polypropylene", Macromolecules, **17**, 878 – 885 (1984), DOI:10.1021/ma00134a058

Cox, S. J., Kathmann, S. M., Slater, B. and Michaelides, A., "Molecular simulations of heterogeneous ice nucleation. II. Peeling back the layers", The Journal of Chemical Physics, **142**, 184705 (2015), DOI:10.1063/1.4919715

Crist, B. and Finerman, T. M., "Copolymer crystallization: Approaching equilibrium", Polymer, **46**, 8745 – 8751 (2005), DOI:10.1016/j.polymer.2005.03.124

D W Oxtoby, "Homogeneous nucleation: theory and experiment", Journal of Physics: Condensed Matter, **4**, 7627 (1992), DOI:10.1088/0953-8984/4/38/001

David M. Sadler, "Roughness of growth faces of polymer crystals: Evidence from morphology and implications for growth mechanisms and types of folding", Polymer, **24**, 1401 – 1409 (1983), DOI:10.1016/0032-3861(83)90220-3

Di Lorenzo, M. L. and Androsch, R., "Crystallization kinetics of blends of two poly(lactic acid) grades with diverse stereoregularity and molar mass", AIP Conference Proceedings, **1981**, 20008 (2018), DOI:10.1063/1.5045870

DiMarzio, E. A., "Some Contributions to the Kinetics of Growth of Multicomponent Chains with Application to the Problems of Ciliation and Fractionation in Polymer Crystallization", The Journal of Chemical Physics, **47**, 3451 – 3469 (1967), DOI:10.1063/1.1712411

Douwe-Wiebe, M., "Structure-property relationships in isotactic polypropylene : the influence of chain architecture and nucleation on crystallization, morphology and mechanical properties", Physical Review Letters - PHYS REV LETT (2003)

E. Martuscelli, M. Pracella and L. Crispino, "Crystallization behaviour of fractions of isotactic polypropylene with different degrees of stereoregularity", Polymer, **24**, 693 – 699 (1983), DOI:10.1016/0032-3861(83)90005-8

European Plastic Joint Stock Company, "7 different types of polypropylene and their applications", Blog, https://europlas.com.vn/en-US/blog-1/7-different-types-of-polypropylene-and-their-applications (2024), accessed June 26, 2024

Feng Luo, Chenlong Xu, Ke Wang, Hua Deng, Feng Chen and Qiang Fu, "Exploring temperature dependence of the toughening behavior of β-nucleated impact polypropylene copolymer", Polymer, **53**, 1783 – 1790 (2012), DOI:10.1016/j.polymer.2012.02.024

Fischer, S., Jiang, Z. and Men, Y., "Analysis of the Lamellar Structure of Semicrystalline Polymers by Direct Model Fitting of SAXS Patterns", The Journal of Physical Chemistry, **115**, 13803 – 13808 (2011)

Flory, P. J., "Thermodynamics of Crystallization in High Polymers. I. Crystallization Induced by Stretching", J. Chem. Phys., **15**, 397 – 408 (1947), DOI:10.1063/1.1746537

Flory, P. J., "Thermodynamics of Crystallization in High Polymers. IV. A Theory of Crystalline States and Fusion in Polymers, Copolymers, and Their Mixtures with Diluents", The Journal of Chemical Physics, **17**, 223 – 240 (1949), DOI:10.1063/1.1747230

Flory, P. J., "Theory of crystallization in copolymers", Trans. Faraday Soc., **51**, 848 (1955), DOI:10.1039/TF9555100848

Frank, F. C. and Tosi, M., "On the theory of polymer crystallization", Proceedings of the Royal Society of London. Series A. Mathematical and Physical Sciences, **263**, 323 – 339 (1961), DOI:10.1098/rspa.1961.0163

Gahleitner, M., Tranninger, C. and Doshev, P., "Heterophasic copolymers of polypropylene: Development, design principles, and future challenges", Journal of Applied Polymer Science, **130**, 3028 – 3037 (2013), DOI:10.1002/app.39626

Galeski, A., "Strength and toughness of crystalline polymer systems", Progress in Polymer Science, **28**, 1643 – 1699 (2003)

Gibbs, J. and Bumstead, H., Thermodynamics, Longmans; Green and Company (1906)

Goran Ungar and Andrew Keller, "Time-resolved synchrotron X-ray study of chain-folded crystallization of long paraffins", Polymer, **27**, 1835 – 1844 (1986), DOI:10.1016/0032-3861(86)90169-2

Gránásy, L., Pusztai, T., Tegze, G., Warren, J. A. and Douglas, J. F., "Growth and form of spherulites", Physical review. E, Statistical, nonlinear, and soft matter physics, **72**, 11605 (2005), DOI:10.1103/PhysRevE.72.011605

Guerin, G., Rupar, P. A. and Winnik, M. A., "In-Depth Analysis of the Effect of Fragmentation on the Crystallization-Driven Self-Assembly Growth Kinetics of 1D Micelles Studied by Seed Trapping", Polymers, **13** (2021), DOI:10.3390/polym13183122

Guo, Q. (Ed.), Polymer Morphology, John Wiley & Sons, Inc, Hoboken, New Jersey (2016)

Guth, E. and Mark, H., "Zur innermolekularen, Statistik, insbesondere bei Kettenmolekiilen I", Monatshefte fr Chemie, **65**, 93 – 121 (1934), DOI:10.1007/BF01522052

Hamley, I. W., "Diffuse Scattering from Lamellar Structures", Soft Matter, **18**, pp. 711-721 (2022)

Han, C., Shi, W. and Jin, J., "Morphology and Crystallization of Crystalline/Amorphous Polymer Blends", p. 1 – 19 (2013)

Handbook of Polymer Crystallization, John Wiley & Sons, Ltd (2013)

Harnisch, K. and Muschik, H., "Determination of the Avrami exponent of partially crystallized polymers by DSC- (DTA-) analyses", Colloid & Polymer Sci, **261**, 908 – 913 (1983), DOI:10.1007/BF01451668

Hao, Z., Li, L., Yang, B., Sheng, X., Liao, X., He, L. and Liu, P., "Influences of Hyperbranched Polyester Modification on the Crystallization Kinetics of Isotactic Polypropylene/Graphene Oxide Composites", Polymers, **11** (2019), DOI:10.3390/polym11030433

Helfand, E. and Lauritzen, J. I., "Theory of Copolymer Crystallization", Macromolecules, **6**, 631 – 638 (1973), DOI:10.1021/ma60034a031

Herrmann, K., Gerngross, O. and Abitz, W., "Zur röntgenographischen Strukturerforschung des Gelatinemicells", Zeitschrift für Physikalische Chemie, **10B**, 371 – 394 (1930), DOI:10.1515/zpch-1930-1028

Hiemenz, P. C., "Polymer Chemistry: The Basic Concepts Marcel Dekker,", 219 (1984)

Huang, T., Rey, A. D. and Kamal, "Linear radial growth velocity of isolated spherulites in polymer free solidification", 0032-3861, **35**, 5434 – 5440 (1994)

Hoffman, J. D., Davis, G. T. and Lauritzen, J. I., "The Rate of Crystallization of Linear Polymers with Chain Folding", in Treatise on Solid State Chemistry: Volume 3 Crystalline and Noncrystalline Solids, Hannay, N. B. (Ed.), Springer US, Boston, MA, p. 497 – 614 (1976)

Hoffman, J. D., Frolen, L. J., Ross, G. S. and Lauritzen, J. I., JR, "On the Growth Rate of Spherulites and Axialites from the Melt in Polyethylene Fractions: Regime I and Regime II Crystallization", Journal of research of the National Bureau of Standards. Section A, Physics and chemistry, **79A**, 671 – 699 (1975), DOI:10.6028/jres.079A.026

Hoffman, J. D. and Miller, R. L., "Kinetic of crystallization from the melt and chain folding in polyethylene fractions revisited: theory and experiment", Polymer, **38**, 3151 – 3212 (1997), DOI:10.1016/S0032-3861(97)00071-2

Hongjun, C., Xiaolie, L., Xiangxu, C., Dezhu, M., Jianmin, W. and Hongsheng, T., "Structure and properties of impact copolymer polypropylene. II. Phase structure and crystalline morphology", Journal of Applied Polymer Science, **71**, 103 – 113 (1999), DOI:10.1002/(SICI)1097-4628(19990103)71:1<103::AID-APP13>3.0.CO;2-5

Hsin-Lung Chen and Shi-Fang Wang, "Crystallization induced microstructure of polymer blends consisting of two crystalline constituents", Polymer, **41**, 5157 – 5164 (2000), DOI:10.1016/S0032-3861(99)00745-4

Humbert, S., Lame, O., Séguéla, R. and Vigier, G., "A re-examination of the elastic modulus >dependence on crystallinity in semi-crystalline polymers", Polymer, **52**, 4899 – 4909 (2011)

Humberto Lovisi, Maria Inês B Tavares, Naira M da Silva, Sônia M.C de Menezes, Luiz Claudio de Santa Maria and Fernanda M.B Coutinho, "Influence of comonomer content and short branch length on the physical properties of metallocene propylene copolymers", Polymer, **42**, 9791 – 9799 (2001), DOI:10.1016/S0032-3861(01)00528-6

J. Jancar and J. Tochacek, "Effect of thermal history on the mechanical properties of three polypropylene impact-copolymers", Polymer Degradation and Stability, **96**, 1546 – 1556 (2011), DOI:10.1016/j.polymdegradstab.2011.05.013

J.-M. Haudin and S. A. E. Boyer, "Crystallization of Polymers in Processing Conditions: An Overview", International Polymer Processing, **32**, 545 – 554 (2017), DOI:10.3139/217.3415

Javier Arranz-Andrés, Juan L. Guevara, Teresa Velilla, Raúl Quijada, Rosario Benavente, Ernesto Pérez and María L. Cerrada, "Syndiotactic polypropylene and its copolymers with alpha-olefins. Effect of composition and length of comonomer", Polymer, **46**, 12287 – 12297 (2005), DOI:10.1016/j.polymer.2005.10.078

Jiang, X., "Effect of nucleating agents on crystallization kinetics of PET", Express Polymer Letters - EXPRESS POLYM LETT, **1**, 245 – 251 (2007), DOI:10.3144/expresspolymlett.2007.37

Jiří Málek, "The applicability of Johnson-Mehl-Avrami model in the thermal analysis of the crystallization kinetics of glasses☆", Thermochimica Acta, **267**, 61 – 73 (1995)

John D. Hoffman, "Regime III crystallization in melt-crystallized polymers: The variable cluster model of chain folding", Polymer, **24**, 3 – 26 (1983), DOI:10.1016/0032-3861(83)90074-5

Kale, L., Plumley, T., Patel, R. and Redwine, O. D., "Structure-property relationships of ethylene/1-octene and ethylene/1-butene copolymers made using INSITE technology", in Plastic Film Sheet, p. 27 – 40

KANDEMİR, M., Karagöz, İ. and Sepetcioglu, H., "Experimental Investigation of Effects of the Nucleating Agent on Mechanical and Crystallization Behavior of Injection-Molded Isotactic Polypropylene", **10**, 109 – 120 (2022), DOI:10.31202/ecjse.1165527

Kanetsuna, H., Mitsuhashi, S., Iguchi, M., Hatakeyama, T., Kyotani, M. and Maeda, Y., "Effect of pressure on the crystallization of polyethylene", Journal of Polymer Science: Polymer Symposia, **42**, 783 – 793 (1973), DOI:10.1002/polc.5070420228

Karger-Kocsis, J., "Polypropylene: Structure, blends and composites - composites", Engineering Plastics, **3** (1994), DOI:10.1177/147823919400200509

Karger-Kocsis, J., "Amorphous or atactic polypropylene", in Polypropylene: An A-Z reference, Karger-Kocsis, J. (Ed.), Springer Netherlands, Dordrecht, p. 7 – 12 (1999)

Karger-Kocsis, J. and Bárány, T., Polypropylene Handbook Morphology, Blends and Composites: Morphology, Blends and Composites (2019)

Keller, A., "The Morphology of Crystalline Polymers", Molecular Physics and Chemistry, **34**, 1 – 28 (1959)

Keller, A. and Goldbeck-Wood, G., "Polymer crystallization: Fundamentals of structure and crystal growth of flexible chains", 241 – 306 (1996)

Kocic, N., Kretschmer, K., Bastian, M. and Heidemeyer, P., "The influence of talc as a nucleation agent on the nonisothermal crystallization and morphology of isotactic polypropylene: The application of the Lauritzen–Hoffmann, Avrami, and Ozawa theories", J of Applied Polymer Sci, **126** (2012), DOI:10.1002/app.36880

Kornfield, J. A., Kumaraswamy, G. and Issaian, A. M., "Recent Advances in Understanding Flow Effects on Polymer Crystallization", Ind. Eng. Chem. Res., **41**, 6383 – 6392 (2002), DOI:10.1021/ie020237z

Kossel, W., "Zur Theorie des Kristallwachstums", Nachrichten von der Gesellschaft der Wissenschaften zu Göttingen, Mathematisch-Physikalische Klasse, **1927**, 135 – 143 (1927)

Kubo, S. and Wunderlich, B., "Crystallization during polymerization of poly-p-xylylene", Journal of Polymer Science: Polymer Physics Edition, **10**, 1949 – 1966 (1972), DOI:10.1002/pol.1972.180101007

Kumaki, J., Kawauchi, T. and Yashima, E., "Two-Dimensional Folded Chain Crystals of a Synthetic Polymer in a Langmuir-Blodgett Film", The Journal of American Chemical Society, **127**, 5788 – 5789 (2005)

Kundagrami, A. and Muthukumar, M., "Continuum theory of polymer crystallization", The Journal of Chemical Physics, **126**, 144901 (2007), DOI:10.1063/1.2713380

Kurt, G. and Kasgoz, A., "Effects of molecular weight and molecular weight distribution on creep properties of polypropylene homopolymer", Journal of Applied Polymer Science, **138**, 50722 (2021), DOI:10.1002/app.50722

Lauritzen, J. I., JR and Hoffman, J. D., "Theory of Formation of Polymer Crystals with Folded Chains in Dilute Solution", Journal of research of the National Bureau of Standards. Section A, Physics and chemistry, **64A**, 73 – 102 (1960), DOI:10.6028/jres.064A.007

Lauritzen, J. I., JR and Passaglia, E., "Kinetics of Crystallization in Multicomponent Systems: II. Chain-Folded Polymer Crystals", Journal of research of the National Bureau of Standards. Section A, Physics and chemistry, **71A**, 261 – 275 (1967), DOI:10.6028/jres.071A.033

Li, C. Y., "The rise of semicrystalline polymers and why are they still interesting", Polymer, **211**, 2 – 9 (2020)

Li, J., Zhou, C., Wang, G., Tao, Y., Liu, Q. and Li, Y., "Isothermal and nonisothermal crystallization kinetics of elastomeric polypropylene", Polymer Testing, **21**, 583 – 589 (2002), DOI:10.1016/S0142-9418(01)00128-3

Liu, Q., Sun, X., Li, H. and Yan, S., "Orientation-induced crystallization of isotactic polypropylene", 0032-3861, **54**, 4404 – 4421 (2013), DOI:10.1016/j.polymer.2013.04.066

Long, Y., Shanks, R. A. and Stachurski, Z. H., "Kinetics Of Polymer Crystallisation", Progress in Polymer Science, **20**, 651 – 701 (1995)

Lu, H., Qiao, J. and Yang, Y., "Effect of isotactiLicity distribution on crystallization kinetics of polypropylene", Polymer International, **51**, 1304 – 1309 (2002), DOI:10.1002/pi.856

Lugito, G. and Woo, E. M., "Lamellar assembly corresponding to transitions of positively to negatively birefringent spherulites in poly(ethylene adipate) with phenoxy", Colloid and Polymer Science, **291**, 817 – 826 (2013), DOI:10.1007/s00396-012-2793-9

Lupi, L., Hudait, A. and Molinero, V., "Heterogeneous Nucleation of Ice on Carbon Surfaces", Journal of the American Chemical Society, **136**, 3156 – 3164 (2014), DOI:10.1021/ja411507a

Magill, J., "Review Spherulites: A personal perspective", Journal of Materials Science, **36**, 3143 – 3164 (2001), DOI:10.1023/A:1017974016928

Mandal, Š. and Sapcanin, A., "POLYMERIC MATERIALS IN GLUING TECHNIQUES", Journal of Sustainable Technologies and Materials, **3**, 36 – 48 (2023), DOI:10.57131/jstm.2023.4.6

Martuscelli, E., Demma, G., Rossi, E. and Segre, A. L., "Evidence of compatibility in the melt for poly (ethylene oxide)/poly(methyl methacrylate)blends by 15C n.m.r. investigations", Polymer Communications, **24**, 266 – 267 (1983)

Martuscelli, E., Pracella, M., Avella, M., Greco, R. and Ragosta, G., "Properties of polyethylene-polypropylene blends: Crystallization behavior", Die Makromolekulare Chemie, **181**, 957 – 967 (1980), DOI:10.1002/macp.1980.021810417

Martuscelli, E., Pracella, M., Della Volpe, G. and Greco, P., "Morphology, crystallization, and thermal behaviour of isotactic polypropylene/low density polyethylene blends", Die Makromolekulare Chemie, **185**, 1041 – 1061 (1984), DOI:10.1002/macp.1984.021850516

Matsuoka, S., "Pressure-induced crystallization in polyethylene", Journal of Polymer Science, **42**, 511 – 524 (1960), DOI:10.1002/pol.1960.1204214018

Matyjakszewski, K. and Möller, M. (Eds.), Polymer Science: A Comprehensive Reference. Volume 2, Elsevier B.V, Stony Brook, NY, USA (2012)

Meng-Heng Wu, Cheng-Chien Wang and Chuh-Yung Chen, "Chemical modification of atactic polypropylene and its applications as a crystallinity additive and compatibility agent", Polymer, **194**, 122386 (2020), DOI:10.1016/j.polymer.2020.122386

Mercier, J. P., "Nucleation in polymer crystallization: A physical or a chemical mechanism?", Polymer Engineering & Science, **30**, 270 – 278 (1990), DOI:10.1002/pen.760300504

M. Gordon and I.H. Hillier, "The bulk crystallization kinetics of polypropylene and polybutene", 0032-3861, **6**, 213 – 219 (1965), DOI:10.1016/0032-3861(65)90043-1

Müller, A., Michell, R. M. and Lorenzo, A., "Isothermal Crystallization Kinetics of Polymers", p. 181 – 203 (2016)

Murmu, U. K., Adhikari, J., Naskar, A., Dey, D., Roy, A., Ghosh, A. and Ghosh, M., "Mechanical Properties of Crystalline and Semicrystalline Polymer Systems", Encyclopedia of Materials: Plastics and Polymers (2021)

Muthukumar, M., "Nucleation in Polymer Crystallization. 1", in Advances in Chemical Physics, John Wiley & Sons, Ltd, p. 1 – 63 (2003)

Nakamura, K., Katayama, K. and Amano, T., "Some aspects of nonisothermal crystallization of polymers. II. Consideration of the isokinetic condition", J of Applied Polymer Sci, **17**, 1031 – 1041 (1973), DOI:10.1002/app.1973.070170404

Nakamura, K., Shimizu, S., Umemoto, S., Thierry, A., Lotz, B. and Okui, N., "Temperature Dependence of Crystal Growth Rate for and β Forms of Isotactic Polypropylene", Polymer Journal, **40**, 915 – 922 (2008), DOI:10.1295/polymj.PJ2007231

Nakamura, K., Watanabe, T., Katayama, K. and Amano, T., "Some aspects of nonisothermal crystallization of polymers. I. Relationship between crystallization temperature, crystallinity, and cooling conditions", J of Applied Polymer Sci, **16**, 1077 – 1091 (1972), DOI:10.1002/app.1972.070160503

Opperlander, G. C., "Structure and Properties of Crystalline Polymers", Science, **159**, 1311 – 1319 (1968)

Osugi, J., Hara, K., Hirai, N. and Hikasa, J., "Crystallization of polyethylene under high pressure", **34** (1964)

Ozawa, T., "Kinetics of non-isothermal crystallization", Polymer, **12**, 150 – 158 (1971), DOI:10.1016/0032-3861(71)90041-3

Paul, D. R. and Bucknall, C. B., Polymer Blends: Formulation and Performance, Formulation, Wiley (2000)

Peterlin, A., "Crystalline Character in Polymers", A Journal of Polymer Science, **9**, 61 – 89 (1965)

Phillips, P. J. and Tseng, H. T., "Influence of pressure on crystallization in poly(ethylene terephthalate)", Macromolecules, **22**, 1649 – 1655 (1989), DOI:10.1021/ma00194a026

Point, J. J., "A New Theoretical Approach of the Secondary Nucleation at High Supercooling", Macromolecules, **12**, 770 – 775 (1979a), DOI:10.1021/ma60070a047

Point, J. J., Colet, M. C. and Dosiere, M., "Experimental criterion for the crystallization regime in polymer crystals grown from dilute solution: Possible limitation due to fractionation", Journal of Polymer Science Part B: Polymer Physics, **24**, 357 – 388 (1986), DOI:10.1002/polb.1986.090240212

Point, J.-J., "Reconsideration of kinetic theories of polymer crystal growth with chain folding", Faraday Discuss. Chem. Soc., **68**, 167 – 176 (1979b), DOI:10.1039/DC9796800167

Poly Add Co. Ltd, "Resin: Polypropylene (Different Types)", www.polymeradd.co.th

Polypropylene handbook, Springer Berlin Heidelberg, New York NY (2019)

Pracella, M., "Crystallization of Polymer Blends. 10", in Handbook of Polymer Crystallization, John Wiley & Sons, Ltd, p. 287 – 326 (2013)

R Kubo, "The fluctuation-dissipation theorem", Reports on Progress in Physics, **29**, 255 (1966), DOI:10.1088/0034-4885/29/1/306

Rabiej, S. and Rabiej, M., "Determination of the parameters of lamellar structure of semicrystalline polymers using a computer program SAXSDAT", POLIMERY, **56**, 662 – 670 (2011)

Raka, L. and Bogoeva-Gaceva, G., Crystallization of Polypropylene: Application (2008)

Reiter, G. and Sommer, J.-U., "Crystallization of Adsorbed Polymer Monolayers", Phys. Rev. Lett., **80**, 3771 – 3774 (1998), DOI:10.1103/PhysRevLett.80.3771

Richardson, M., Flory, P. J. and Jackson, J., "Crystallization and melting of copolymers of polymethylene", Polymer, **4**, 221 – 236 (1963), DOI:10.1016/0032-3861(63)90028-4

Robeson, L. M., Polymer Blends: A Comprehensive Review, Hanser (2007)

Rosa, C. de, "Structure and physical properties of syndiotactic polypropylene: A highly crystalline thermoplastic elastomer", Progress in Polymer Science - PROG POLYM SCI, **31**, 145 – 237 (2006), DOI:10.1016/j.progpolymsci.2005.11.002

Rowlinson, J. S. and Widom, B., Molecular Theory of Capillarity, Clarendon Press (1982)

Sedighiamiri, A., van Erp, T. B., Peters, G. W. M., Govaert, L. E. and van Dommelen, J. A. W., "Micromechanical modeling of the elastic properties of semicrystalline polymers: A three-phase approach", Journal of Polymer Science Part B: Polymer Physics, **48**, 2173 – 2184 (2010), DOI:10.1002/polb.22099

Shijie Song, Jiachun Feng and Peiyi Wu, "Relaxation of shear-enhanced crystallization in impact-resistant polypropylene copolymer: Insight from morphological evolution upon thermal treatment", Polymer, **51**, 5267 – 5275 (2010), DOI:10.1016/j.polymer.2010.09.008

Shijie Song, Peiyi Wu, Jiachun Feng, Mingxin Ye and Yuliang Yang, "Influence of pre-shearing on the crystallization of an impact-resistant polypropylene copolymer", Polymer, **50**, 286 – 295 (2009), DOI:10.1016/j.polymer.2008.10.054

Shrivastava, A., "Introduction to Plastic Engineering", 1 – 16 (2018)

Sihan Wang, Rui Li, Dezhu Shi, Yuxin Gao and Lei Song, "https://www.degruyter.com/document/doi/10.1515/epoly-2019-0005/xml", e-Polymers, 32 – 39 (0005)

Šimoník, J. and Drexler, J., "Application of atactic polypropylene in technology of chemical foaming of PVC pastes", Journal of Vinyl Technology, **1**, 119 – 121 (1979), DOI:10.1002/vnl.730010214

Speranza, V., Salomone, R. and Pantani, R., "Effects of Pressure and Cooling Rates on Crystallization Behavior and Morphology of Isotactic Polypropylene", Crystals, **13** (2023), DOI:10.3390/cryst13060922

Starkweather Jr., H. W. and Brooks, R. E., "Effect of spherulites on the mechanical properties of nylon 66", Journal of Applied Polymer Science, **1**, 236 – 239 (1959), DOI:10.1002/app.1959.070010214

Takahashi, M., Matsuda, H., Yoshida, H. and He, Y., "Crystallization of crystalline/amorphous polymer blends", AIP Conference Proceedings, **256**, 236 – 237 (1992), DOI:10.1063/1.42355

Tanvir, H. and Abdus, S., "Research and application of polypropylene: a review", Discover Nano, **19** (2024)

Tien, N.-D., Nishikawa, Y., Hashimoto, M., Tosaka, M., Sasaki, S. and Sakurai, S., "Three-dimensional analyses of spherulite morphology in poly(oxyethylene) and its blends with amorphous poly(d,l-lactic acid) using X-ray computerized tomography", Polymer Journal, **47**, 37 – 44 (2015), DOI:10.1038/pj.2014.83

Tseng, C.-H. and Tsai, P.-S., "The Isothermal and Nonisothermal Crystallization Kinetics and Morphology of Solvent-Precipitated Nylon 66", Polymers, **14**, 442 (2022), DOI:10.3390/polym14030442

Turnbull, D. and Fisher, J. C., "Rate of Nucleation in Condensed Systems", The Journal of Chemical Physics, **17**, 71 – 73 (1949), DOI:10.1063/1.1747055

Viana, J. and Cunha, E. M., "Extensibility of the Inter-Lamellar Amorphous Layer and the Mechanical Behaviour of Polyethylene", Materials Science Forum, 1186 – 1190 (2006)

Wang, T. T. and Nishi, T., "Spherulitic Crystallization in Compatible Blends of Poly(vinylidene fluoride) and Poly(methyl methacrylate)", Macromolecules, **10**, 421 – 425 (1977), DOI:10.1021/ma60056a034

Wen-Bin Liau, Shih-Huang Tung, Wei-Chi Lai and Ling-Yueh Yang, "Studies on blends of binary crystalline polymers: Miscibility and crystallization behavior in PBT/PAr(I27-T73)", Polymer, **47**, 8380 – 8388 (2006), DOI:10.1016/j.polymer.2006.09.046

Werner Kuhn, "Über die Gestalt fadenförmiger Moleküle in Lösungen", Kolloid-Zeitschrift, **68**, 2 – 15 (1934)

"What is homopolymer polypropylene used for? - Knowledge", https://www.ifanpiping.com/info/what-is-homopolymer-polypropylene-used-for-84757384.html (2024), accessed August 9, 2024

Wittmann, J. C. and Lotz, B., "Polymer decoration: The orientation of polymer folds as revealed by the crystallization of polymer vapors", Journal of Polymer Science: Polymer Physics Edition, **23**, 205 – 226 (1985), DOI:10.1002/pol.1985.180230119

Woo, E. M., Chou, Y.-H., Chiang, W.-J., Chen, I.-T., Huang, I.-H. and Kuo, N.-T., "Amorphous phase behavior and crystalline morphology in blends of poly(vinyl methyl ether) with isomeric polyesters: poly(hexamethylene adipate) and poly(ε-caprolactone)", Polymer Journal, **42**, 391 – 400 (2010), DOI:10.1038/pj.2010.18

Wu, B., Zheng, X., Ren, Y., Yu, H., Wang, Y. and Jiang, H., "The Crystallization Morphology and Conformational Changes of Polypropylene Random Copolymer Induced by a Novel β-Nucleating Agent", Polymers, **16** (2024), DOI:10.3390/polym16060827

Wunderlich, B., "Crystallization during polymerization", 568 – 619 (1968a)

Wunderlich, B., "Crystallization during Polymerization", Angewandte Chemie International Edition in English, **7**, 912 – 919 (1968b), DOI:10.1002/anie.196809121

Wunderlich, B. and Arakawa, T., "Polyethylene crystallized from the melt under elevated pressure", Journal of Polymer Science Part A: General Papers, **2**, 3697 – 3706 (1964), DOI:10.1002/pol.1964.100020828

Xu, J., Reiter, G. and Alamo, R. G., "Concepts of Nucleation in Polymer Crystallization", Crystals, **11** (2021), DOI:10.3390/cryst11030304

XU, J.-R., 1987, "Investigation Of Trans-1,4 Polyisoprene Crystals From Solution: Morphologies And Quantitative Characterization". Dissertion, The City University of New York, New York

Yandi Fan, Chunyu Zhang, Yanhu Xue, Xuequan Zhang, Xiangling Ji and Shuqin Bo, "Microstructure of two polypropylene homopolymers with improved impact properties", Polymer, **52**, 557 – 563 (2011), DOI:10.1016/j.polymer.2010.12.009

Yang, C.-T., Lee, L.-T. and Wu, T.-Y., "Isothermal and Nonisothermal Crystallization Kinetics of Poly(ε-caprolactone) Blended with a Novel Ionic Liquid, 1-Ethyl-3-propylimidazolium Bis(trifluoromethanesulfonyl)imide", Polymers, **10** (2018), DOI:10.3390/polym10050543

Yang, J., McCoy, B. J. and Madras, G., "Temperature effects for isothermal polymer crystallization kinetics", The Journal of Chemical Physics, **122**, 244905 (2005), DOI:10.1063/1.1924502

Yanjie An, Sihan Wang, Rui Li, Dezhu Shi, Yuxin Gao and Lei Song, "Effect of different nucleating agent on crystallization kinetics and morphology of polypropylene", e-Polymers, **19**, 32 – 39 (2019), DOI:10.1515/epoly-2019-0005

Yaping Ma, Aihua He and Chenguang Liu, "Crystallization kinetics, crystalline structures and properties of PB/PP blends regulated by poly(butene-block-propylene) copolymers", Polymer, **228**, 123901 (2021), DOI:10.1016/j.polymer.2021.123901

Zhang, M. C., Guo, B.-H. and Xu, J., "A Review on Polymer Crystallization Theories", Crystals, **7** (2017), DOI:10.3390/cryst7010004

Zhang, S., Wang, Z., Guo, B. and Xu, J., "Secondary nucleation in polymer crystallization: A kinetic view", POLYMER CRYSTALLIZATION, **4**, e10173 (2021), DOI:10.1002/pcr2.10173

Ziaiea, F., Borhanic, M., Mirjalilib, G. and Bolourizadeh, M. A., "Effect of crystallinity on electrical properties of electron beam irradiated LDPE and HDPE", Radiation Physics and Chemistry, **76**, 1684 – 1687 (2007)
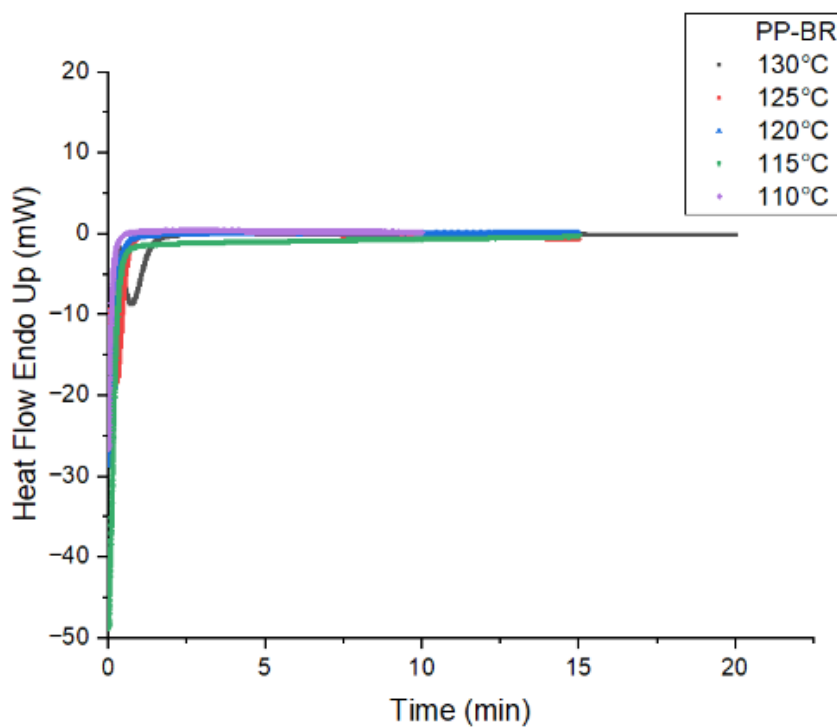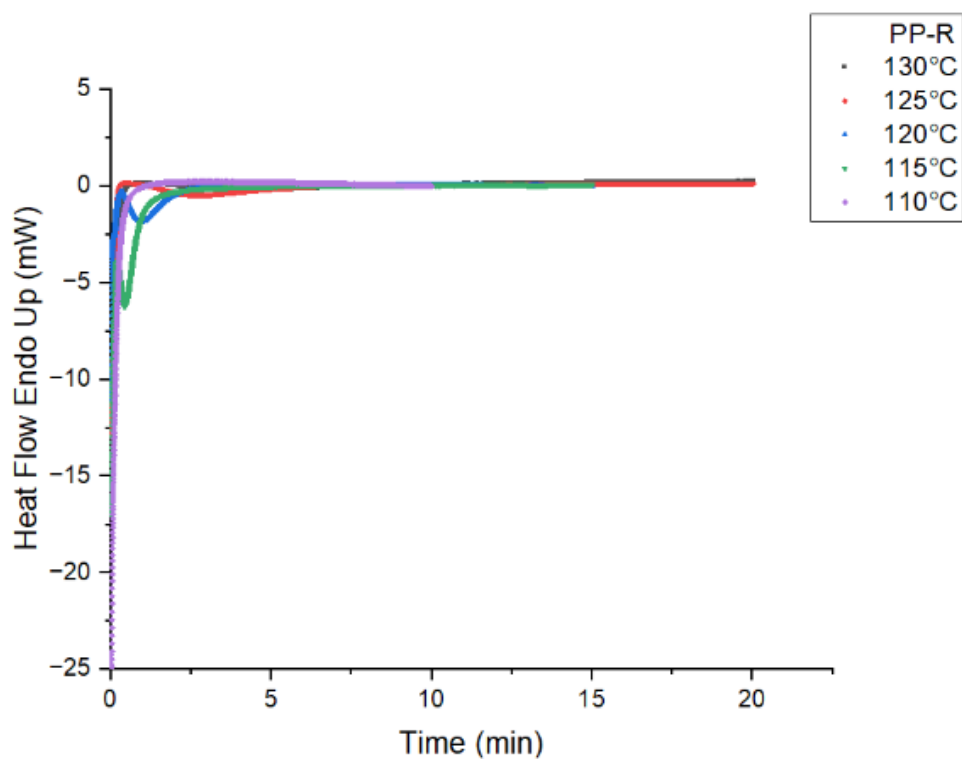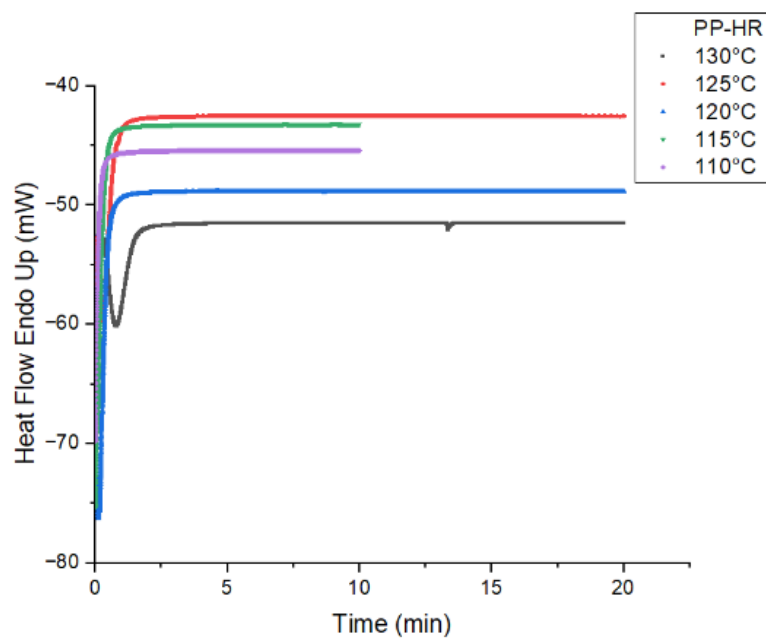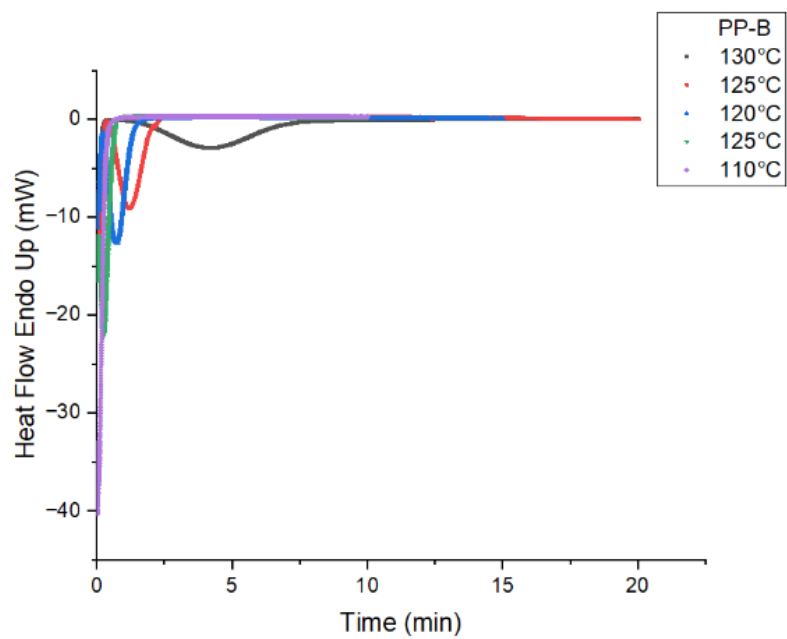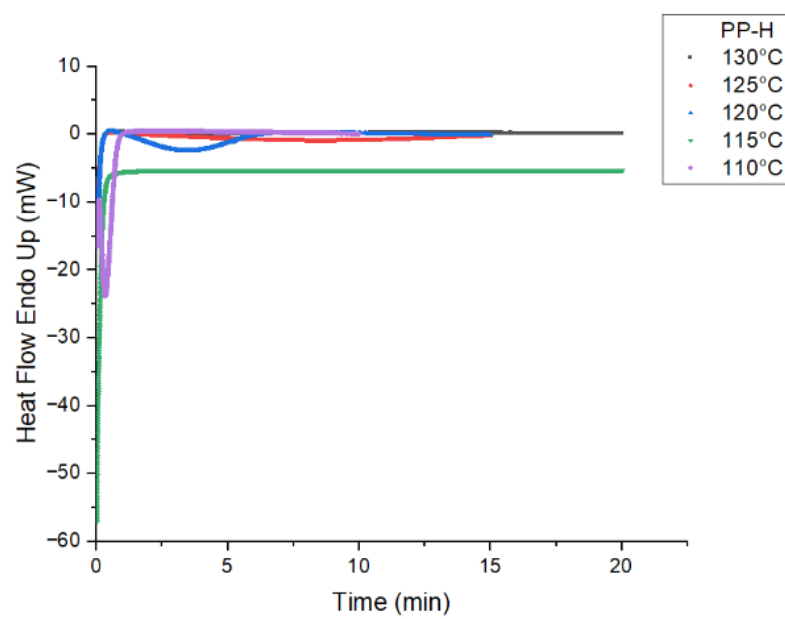
Fig. 5.1: Exothermic isothermal crystallization curves of PP and its blends
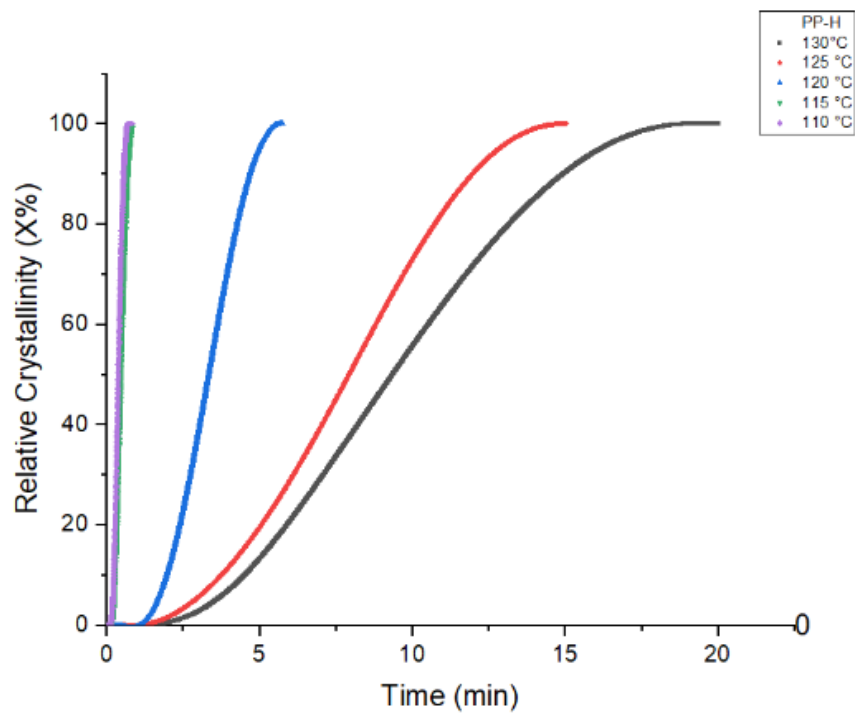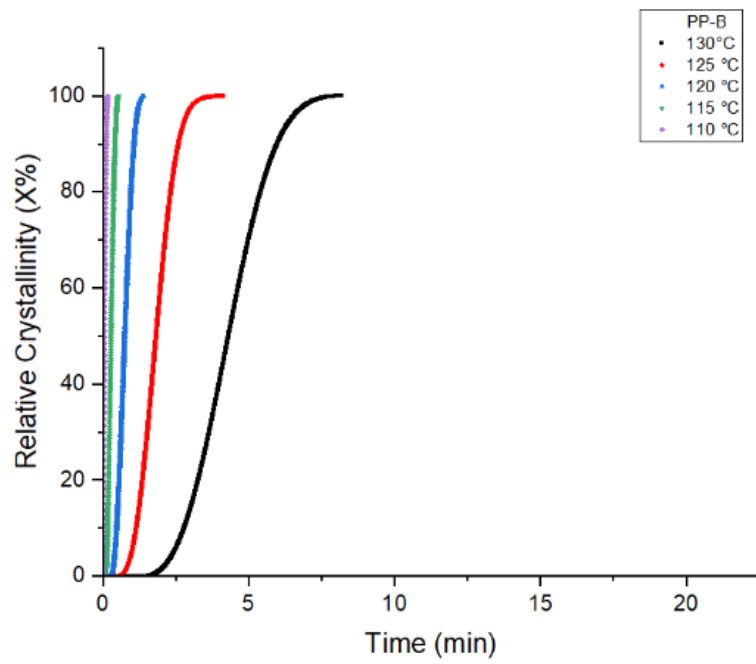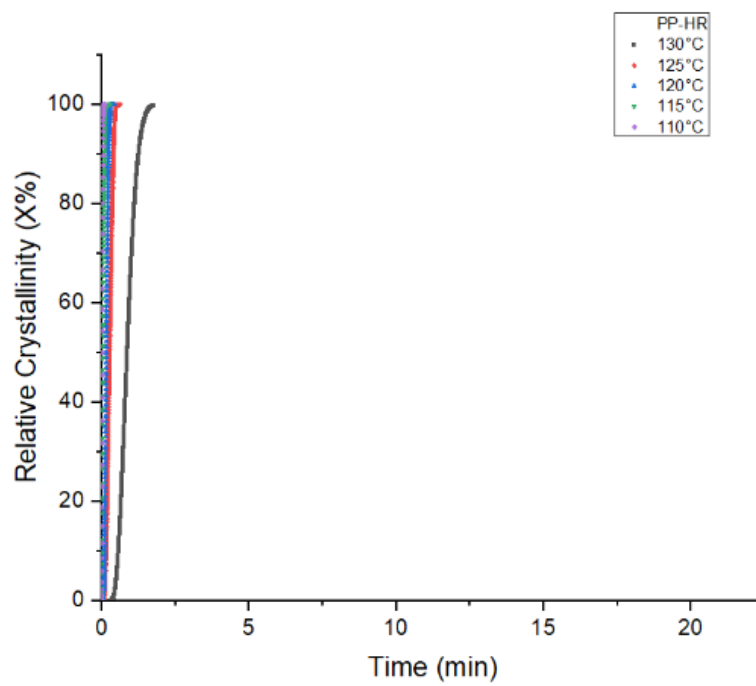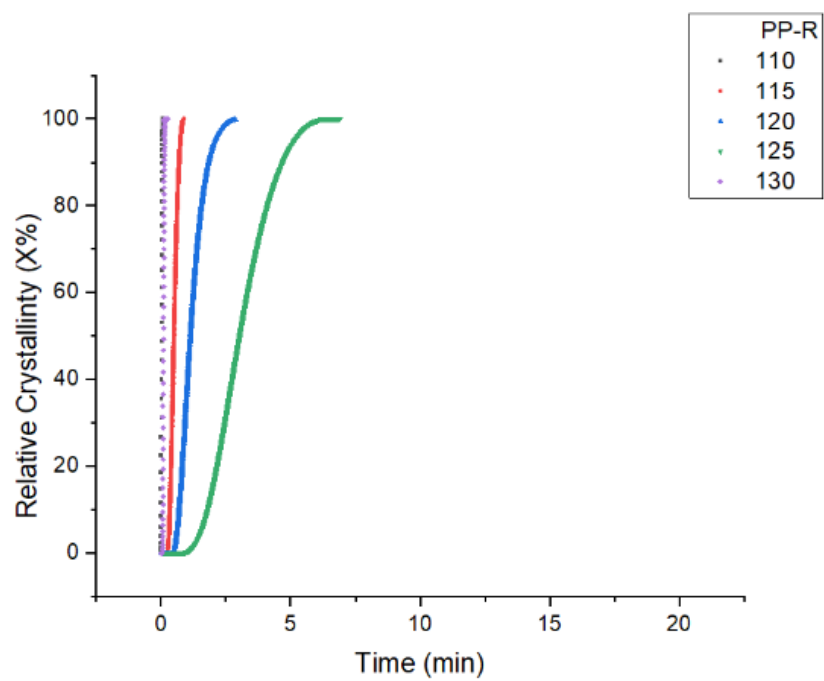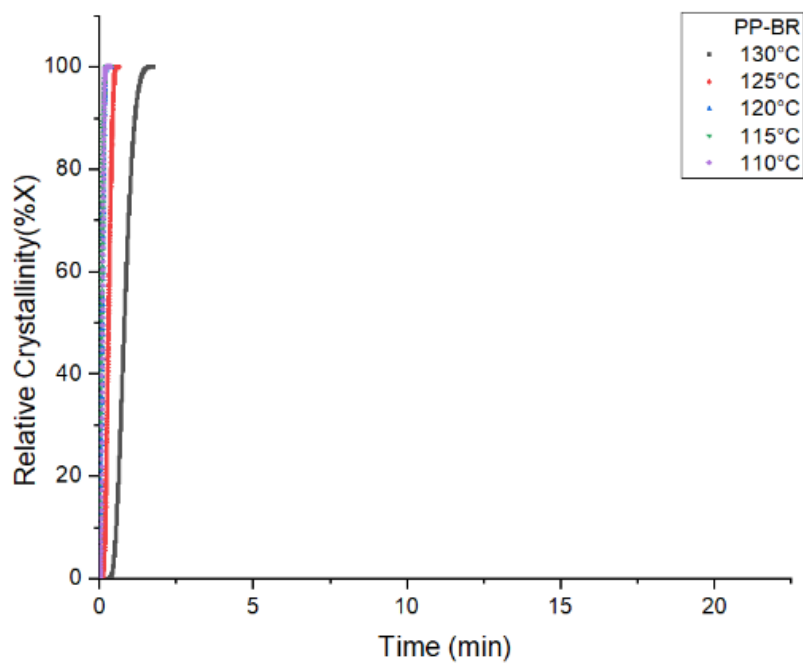
Fig. 5.2 : Avrami representation of evolution of relative crystallinity with respect to time
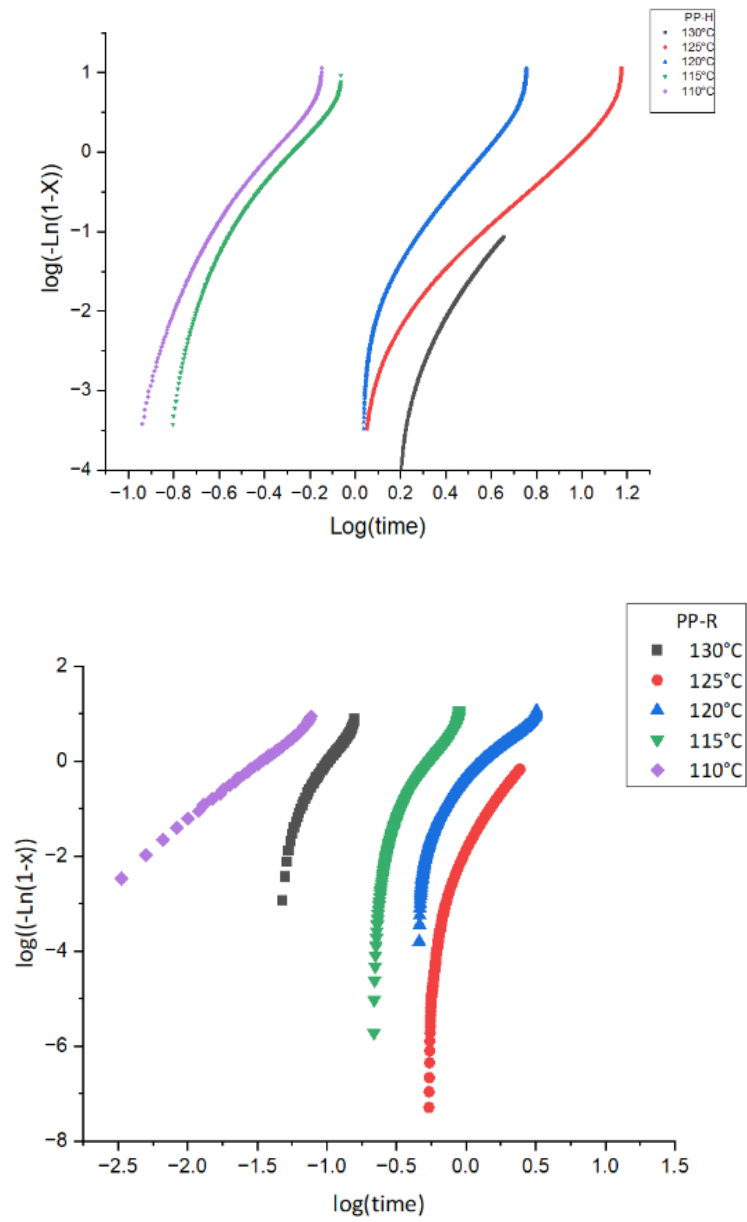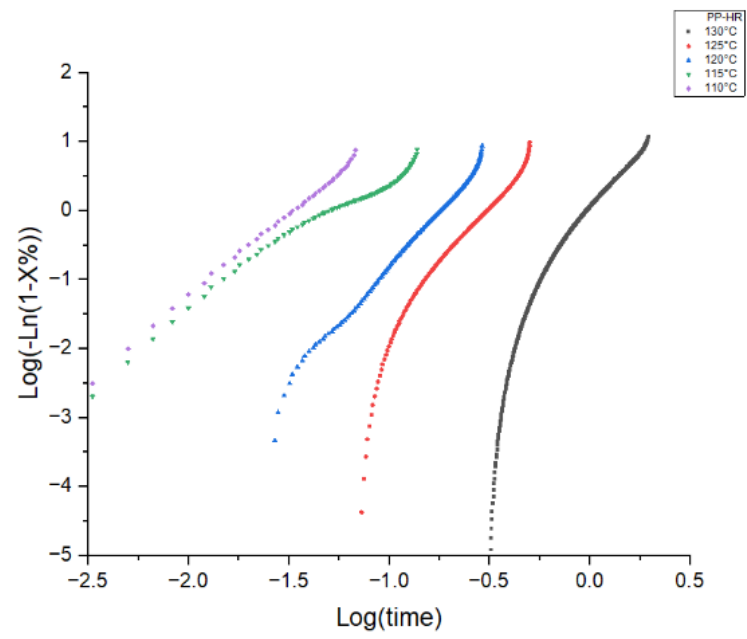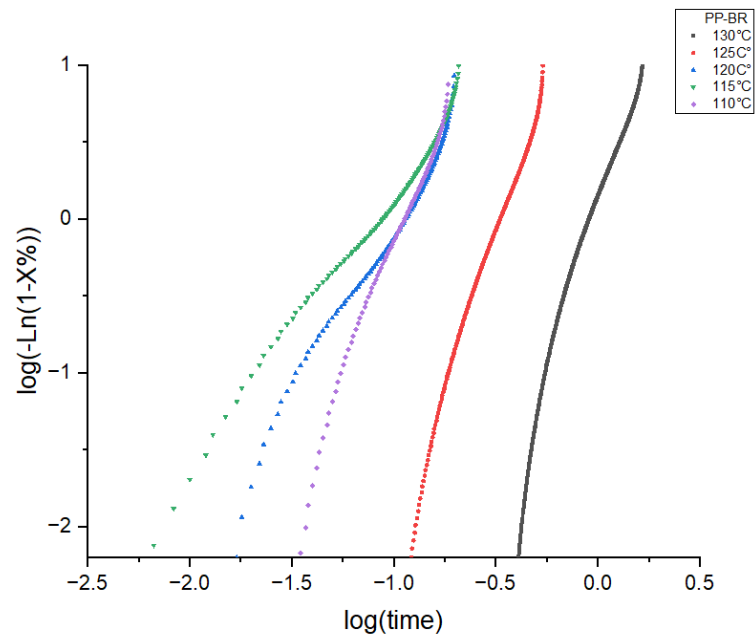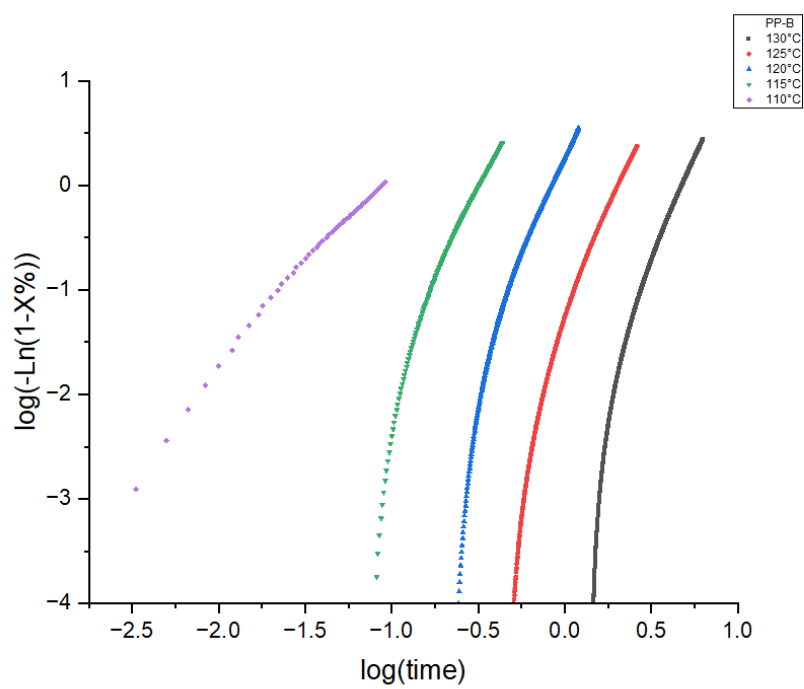
Fig. 5.3: Linear extrapolation of the Avrami crystallinity curve
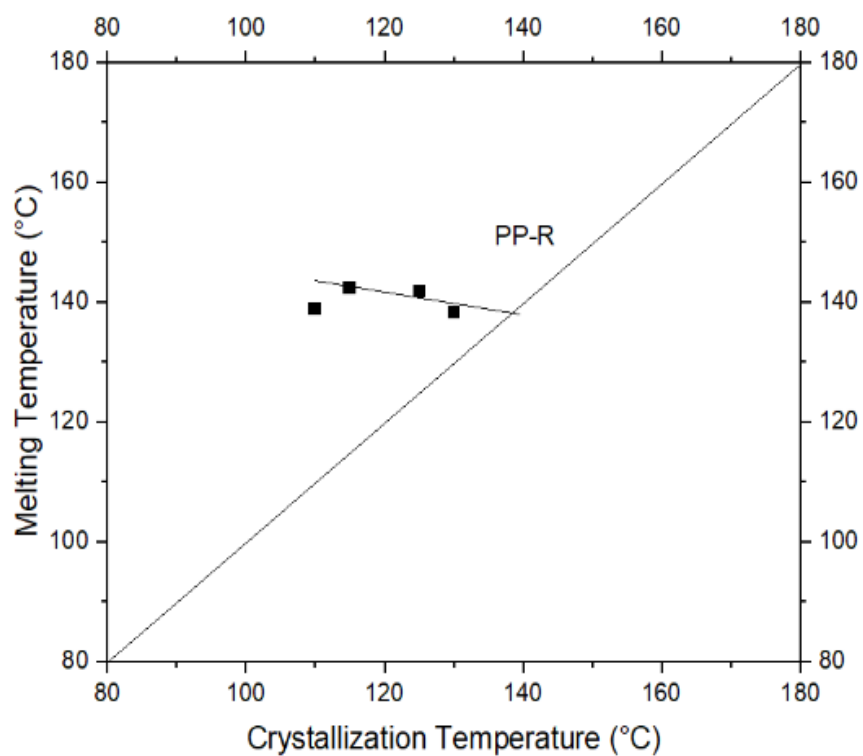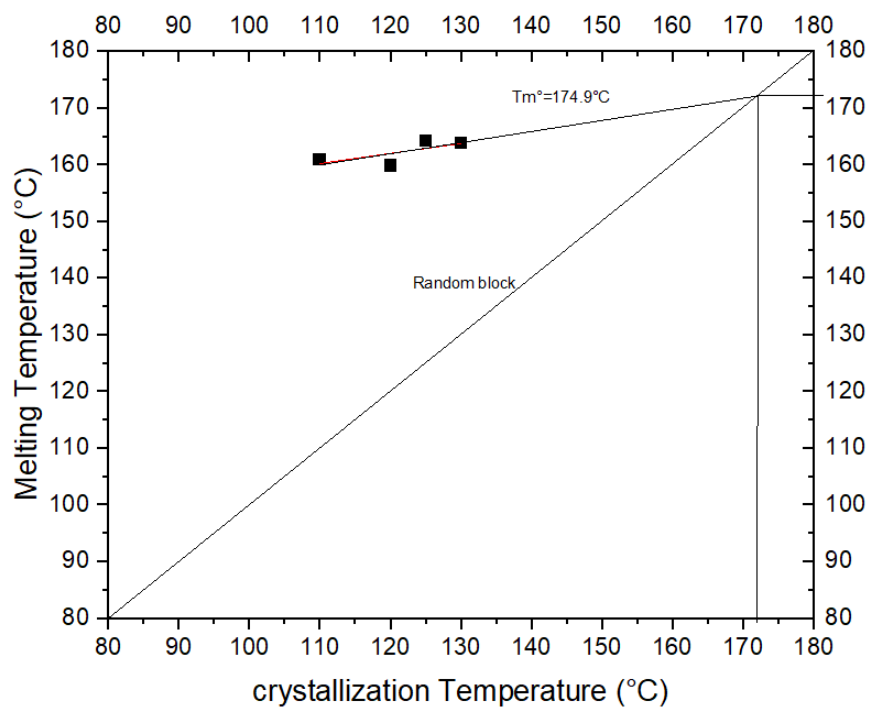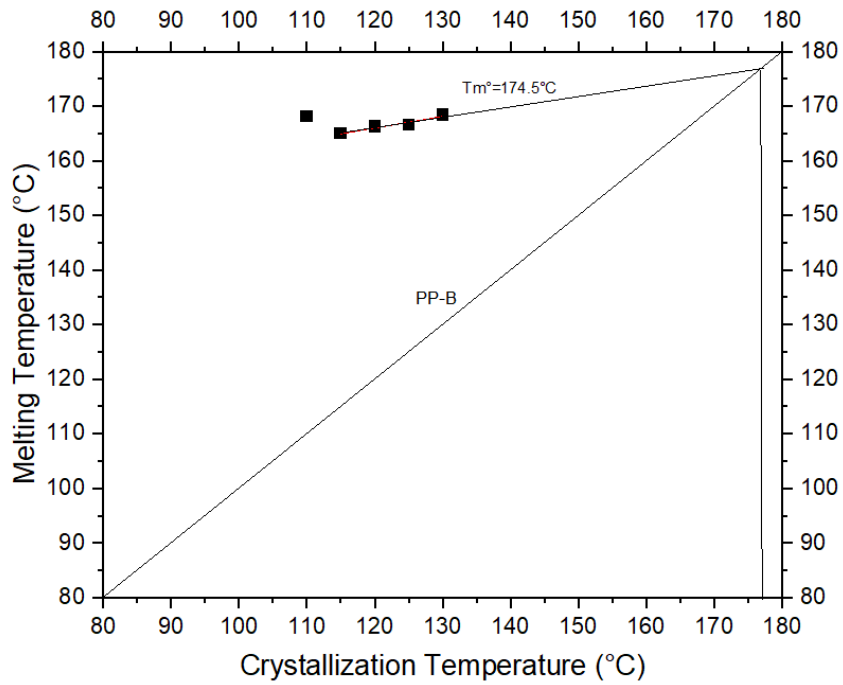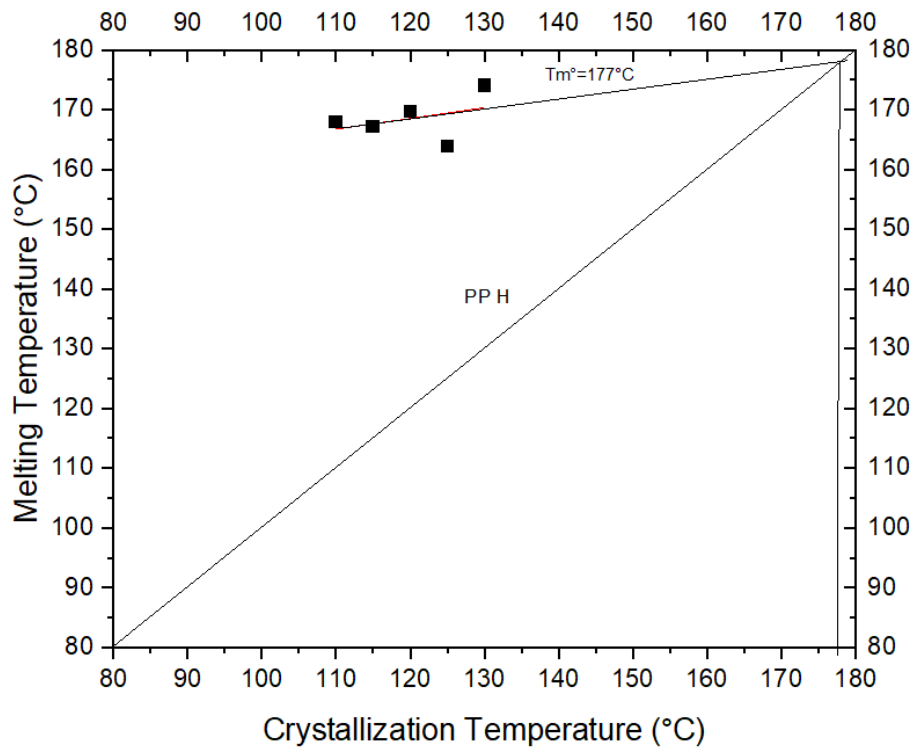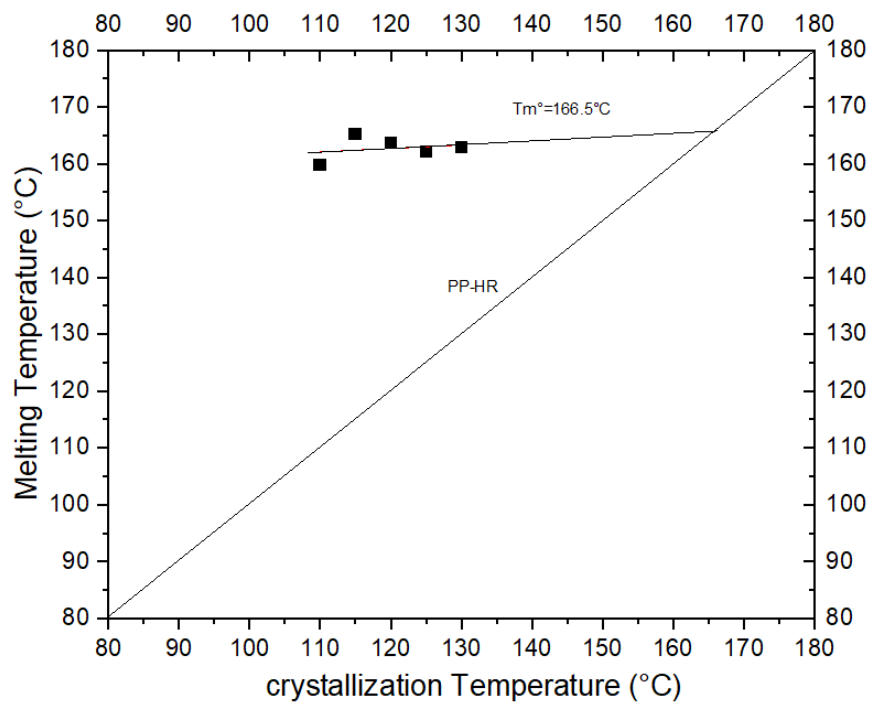
Fig. 5.4 Hoffman Week's Linear Extrapolation to find Tmᵒ
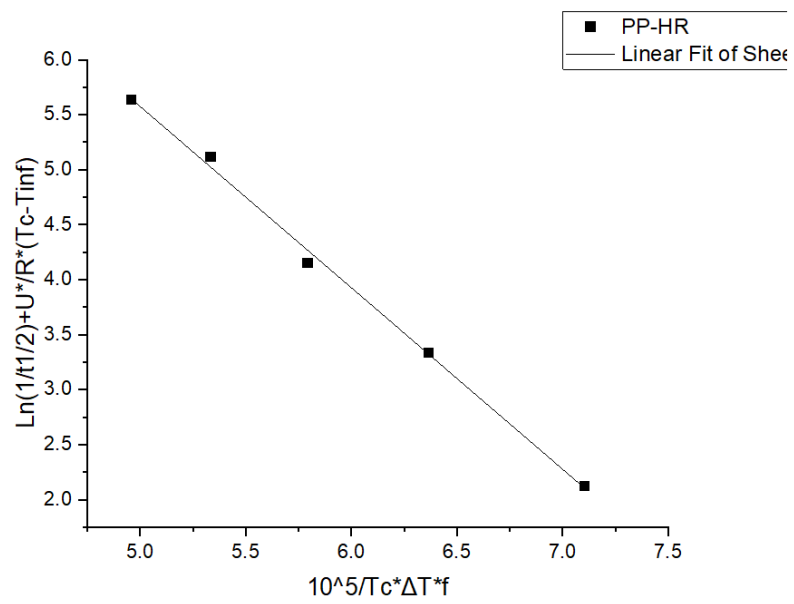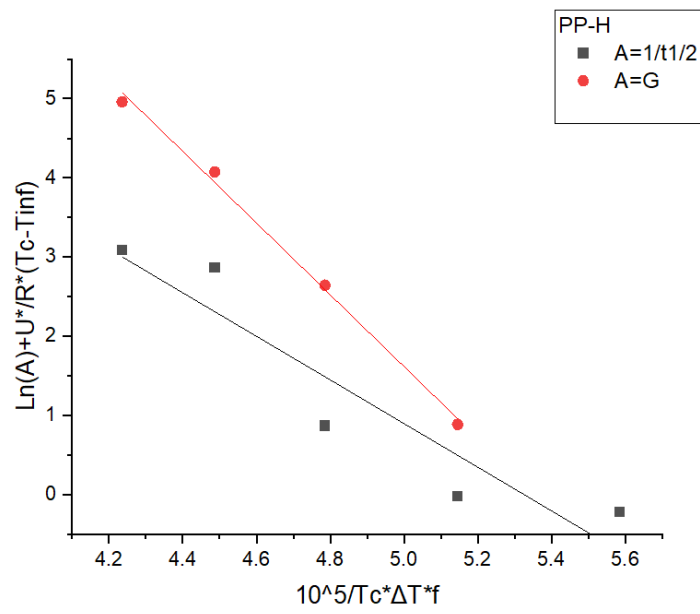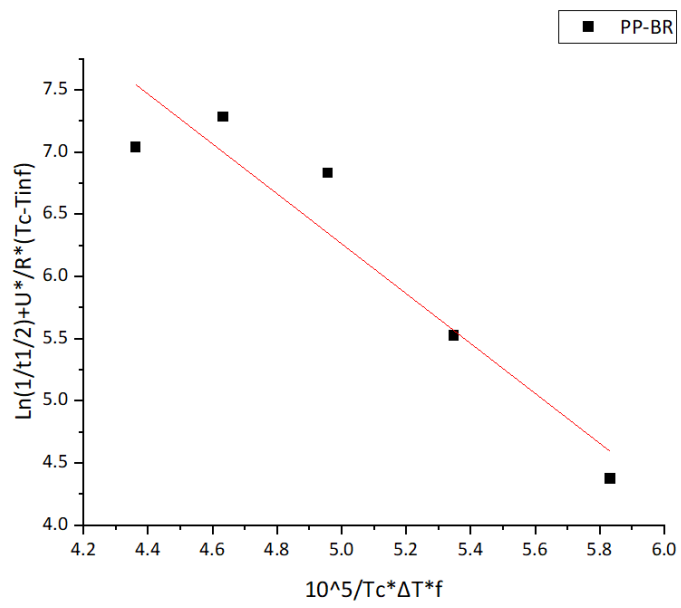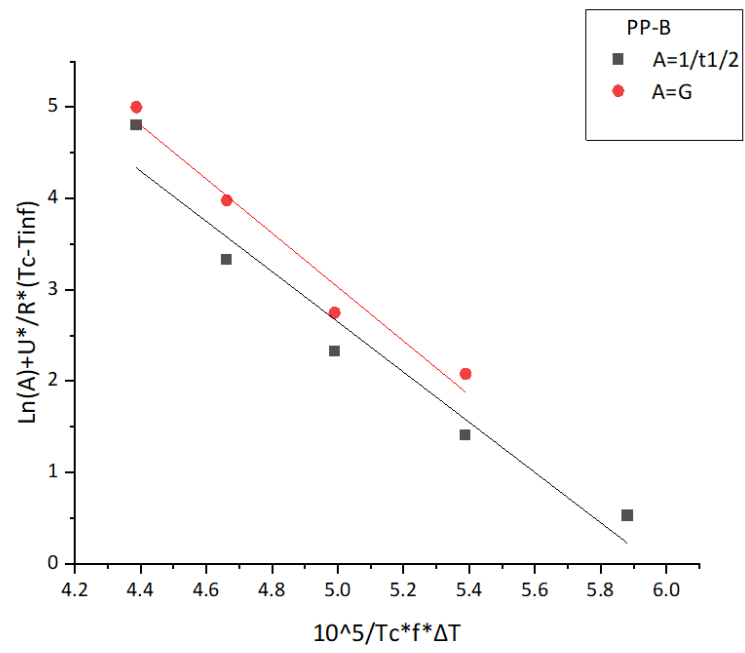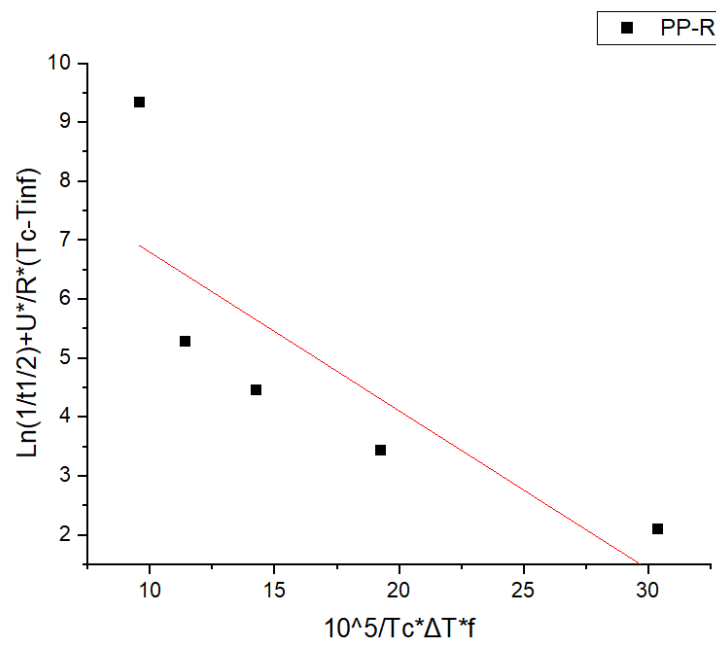
Fig. 5.5: Lauritzen Hoffman representation to find Go and Kg

t= 2s
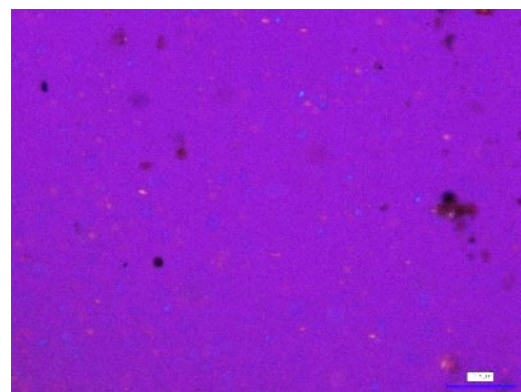
t= 5s
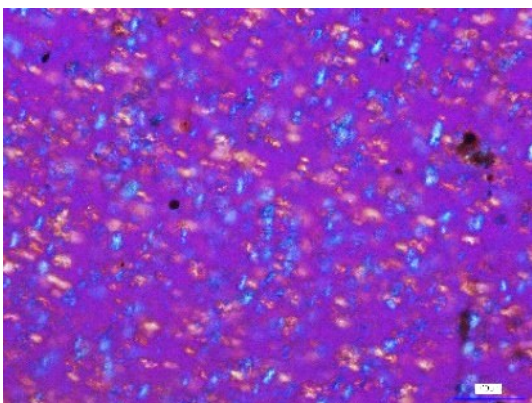
t=20s
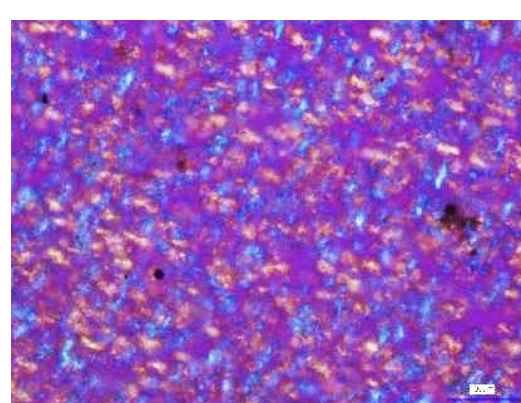
t=30s
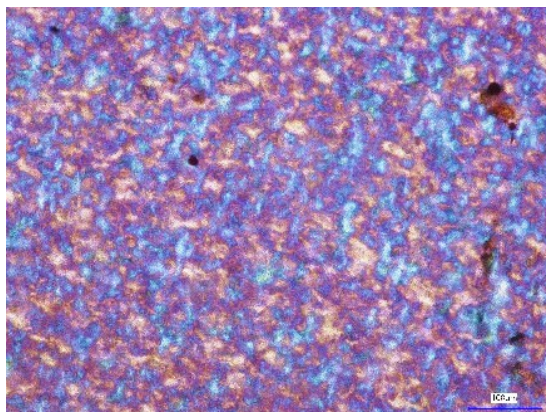
t=60s

Fig. 5.6: Growth of Spherulites of Block PP observed under the Polarized Optical Microscope at specific intervals at 125°C
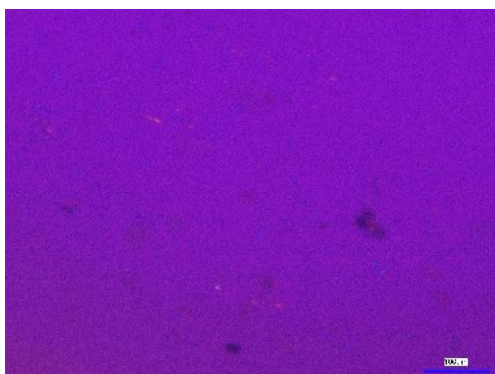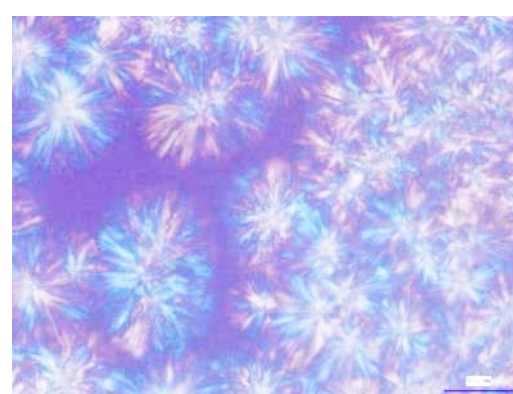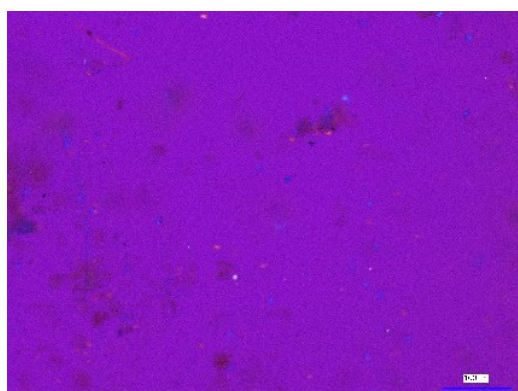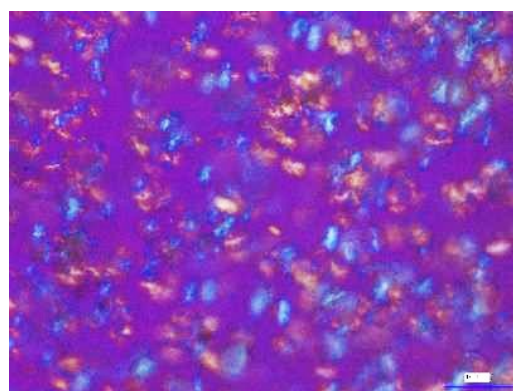

t=3s
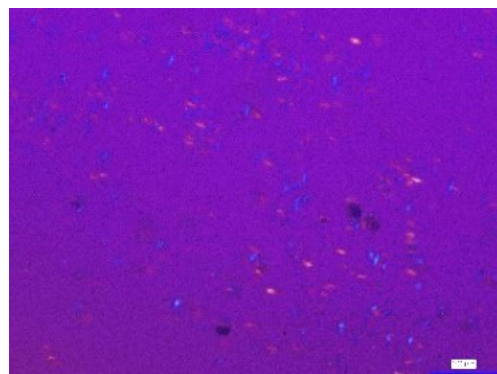
t=15s
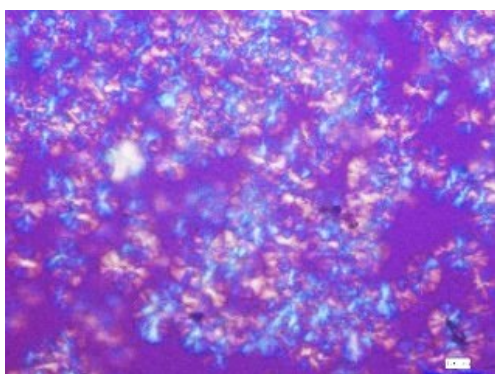
t=60s
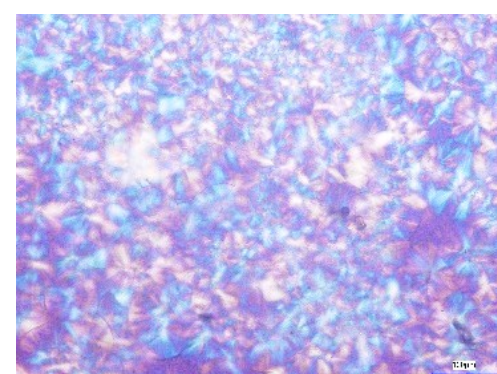
t=120s

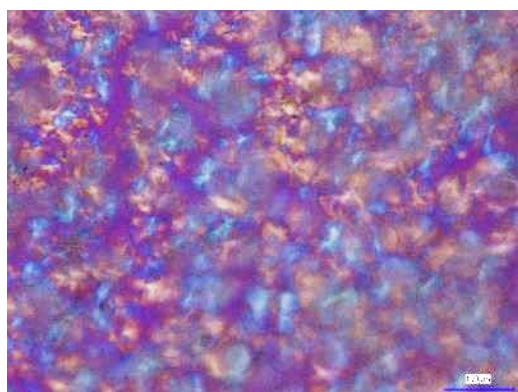**Fig. 5.6:** Growth of Spherulites of Homo PP observed under the Polarized Optical Microscope at specific intervals at 125°C
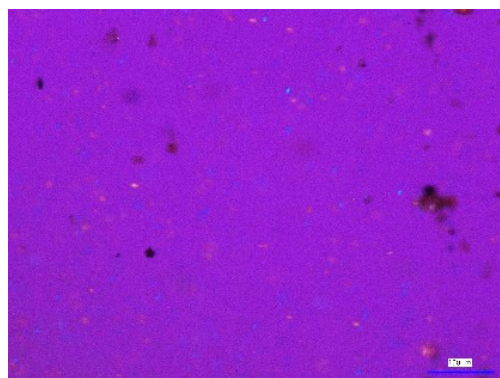
t=5s
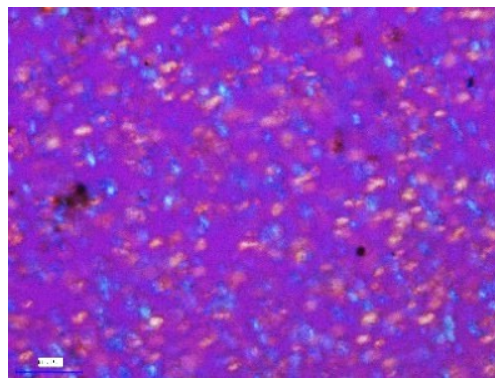
t=20s
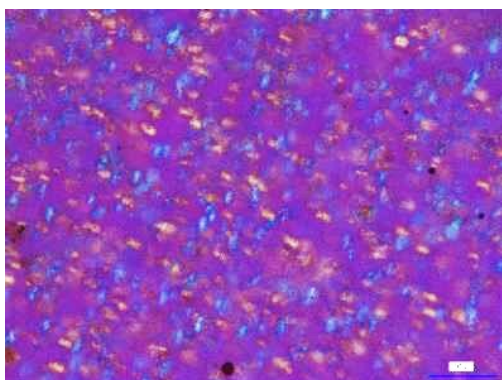
t=40s
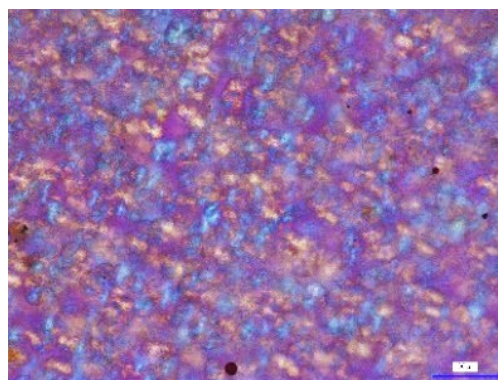
t=60s

Fig. 5.7: Growth of Spherulites of Block PP observed under the Polarized Optical Microscope at specific intervals at 130 °C
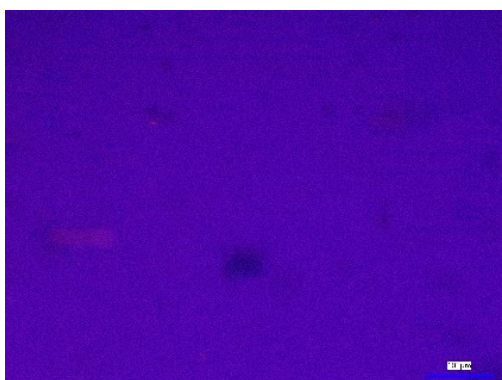
t=4s
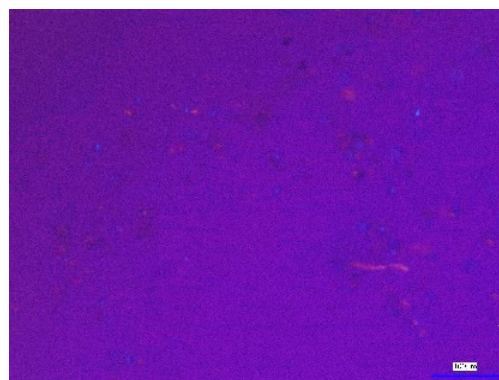
t=20s
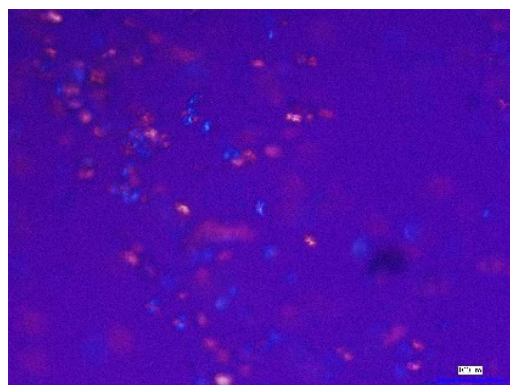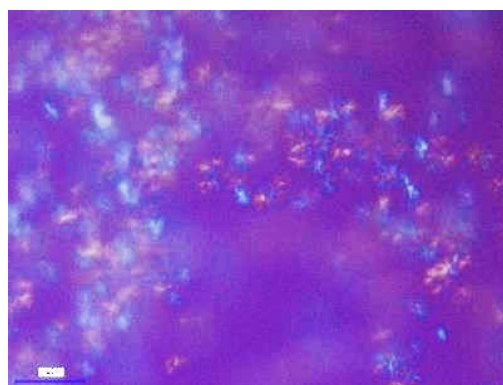
t=40s   t=60s
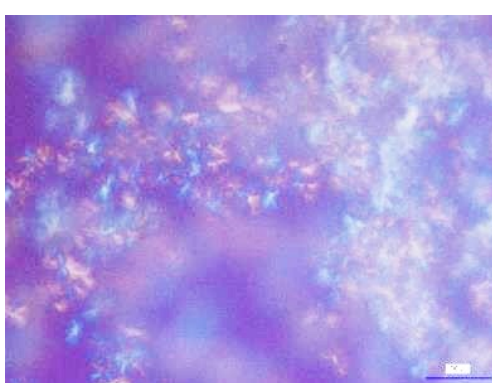
t=120s   t= 240s
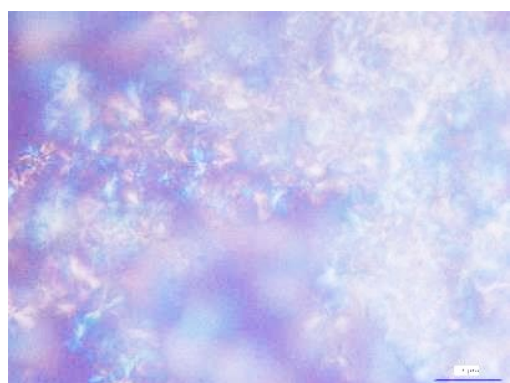
t=180s

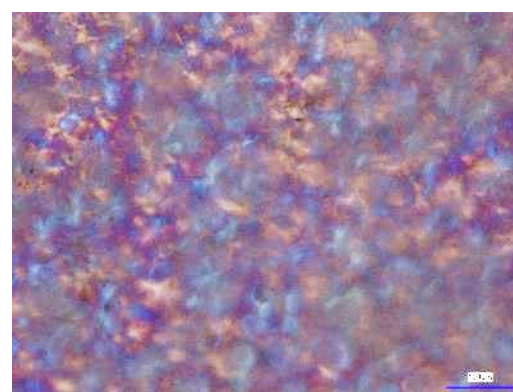**Fig. 5.8:** Growth of Spherulites of Homo PP observed under the Polarized Optical Microscope   at specific intervals at 130 ^{o}C

t=30s
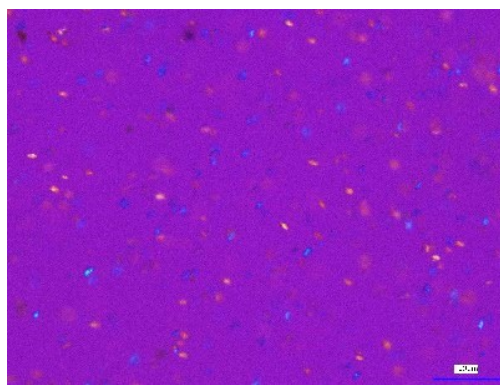
t= 120s
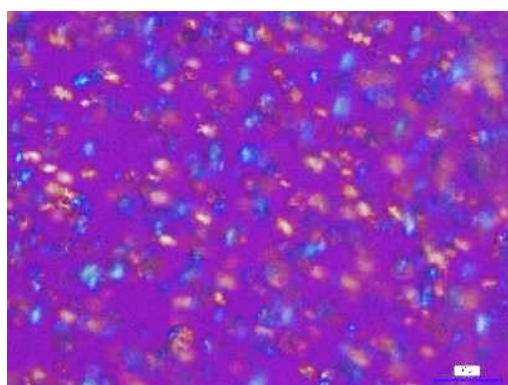
t=210s
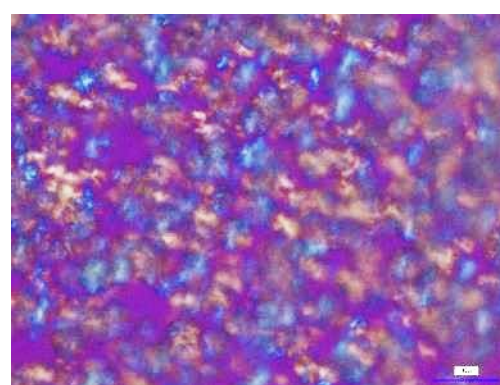
t=330s
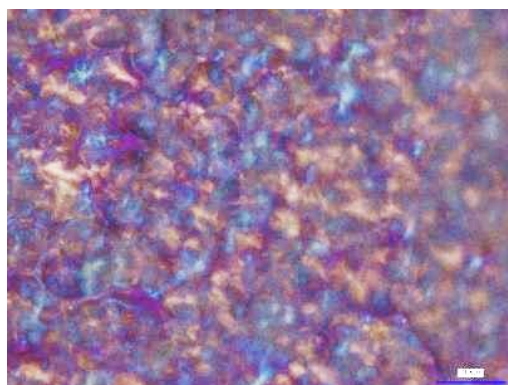
t=420s

Fig. 5.9: Growth of Spherulites of Block PP observed under the Polarized Optical Microscope at specific intervals at 135 °C

t=61s
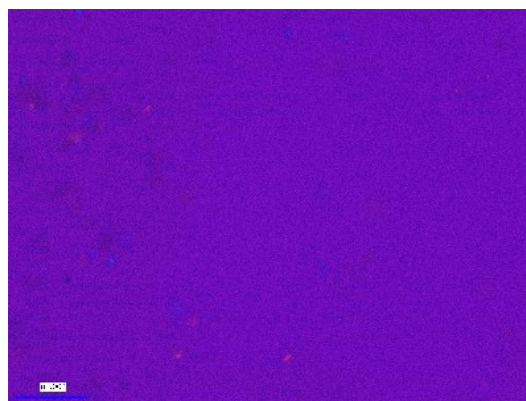
t=180s
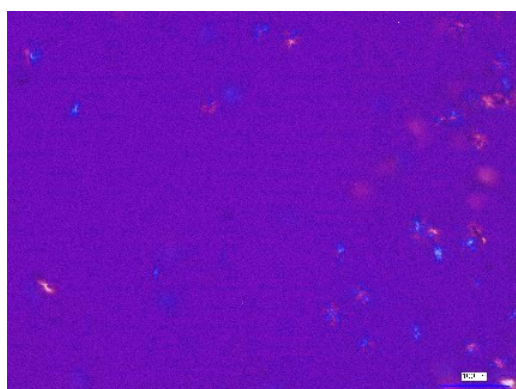
t=300s
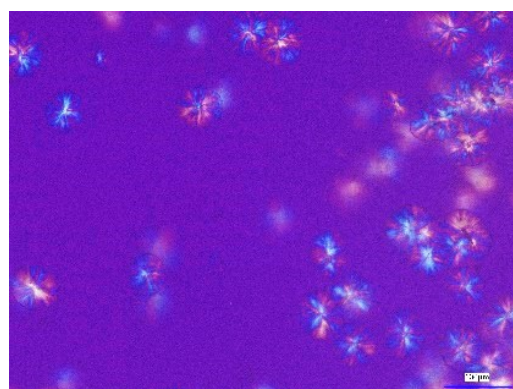
t=600s
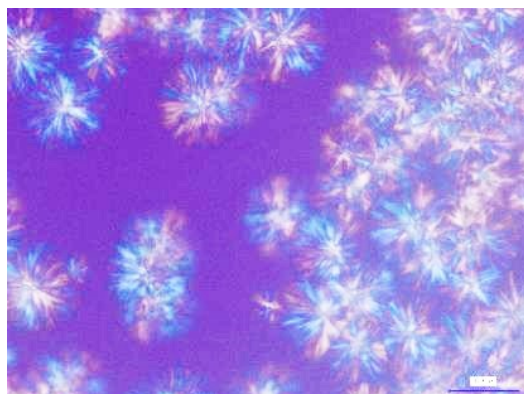
t=1200s

t=1800s

Fig. 5.10: Growth of Spherulites of Homo PP observed under the Polarized Optical Microscope at specific intervals at 135°C
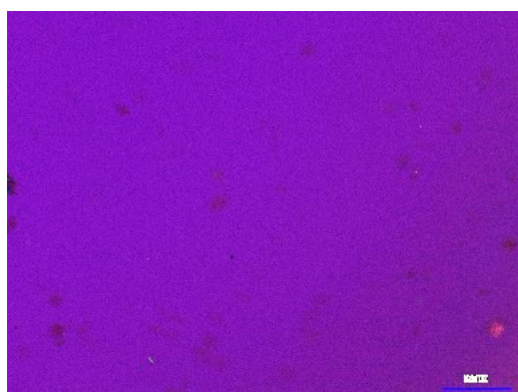
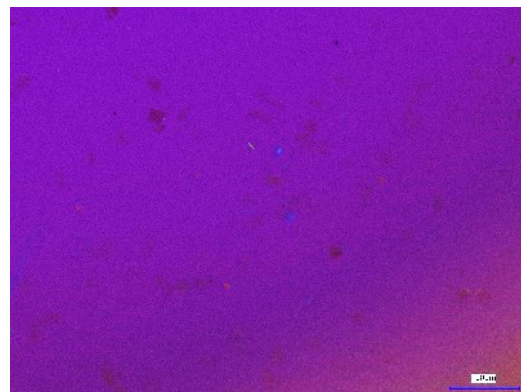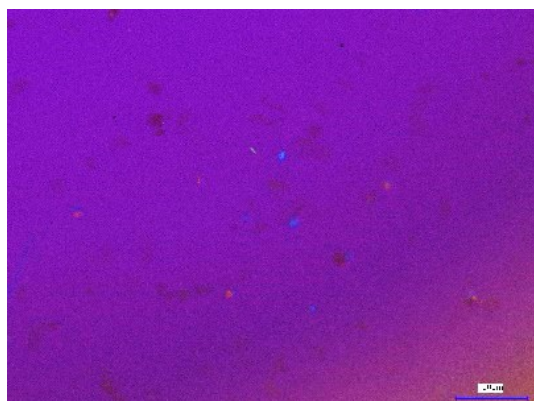t=169s

t=300s

t=480s

t=600s

Fig. 5.11: Growth of Spherulites of Block PP observed under the Polarized Optical Microscope at specific intervals at 140oC

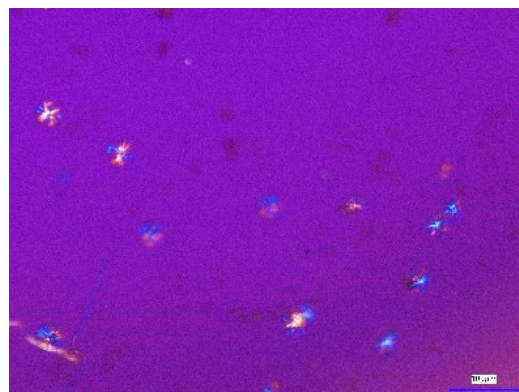t=180s

t=480s

t=600s   t=1200s

Fig. 5.12: Growth of Spherulites of Homo PP observed under the Polarized Optical Microscope at specific intervals at 140°C

Fig. 5. 13: Spherulites of Homo Random and Random Block PP respectively